

**VICTORIA
UNIVERSITY**

MELBOURNE AUSTRALIA

**MACHINE VISION CONTROL ALGORITHM DESIGN FOR
INDUSTRIAL PALLETIZING ROBO MACHINES TO INCREASE
THE DYNAMIC STABILITY BY REAL-TIME IMAGE
PROCESSING**

Muhammad Hassan Tabish

A thesis is submitted in fulfilment of the requirements for the degree of

DOCTOR OF PHILOSOPHY

Feb-2020

**Principal Supervisor: Prof. Akhtar Kalam
Associate Supervisor: Prof. Aladin Zayegh**

Institute for Sustainable Industries and Liveable Cities
College of Engineering and Science
Victoria University

Gratitude to my
teachers.....

**I have come to believe
that a great teacher is a
great artist who gives hard
time to favour you**

To my beloved father, Muhammad Usman, who work tirelessly to offer the best education, encouraged, assisted and never giving up on me to finish this thesis. To my family who have supported me during this entire journey. Thank you for your immense support and encouragement.

Muhammad Hassan Tabish

Abstract

The focus of the research is to palletise the laser cut irregular objects of metal, wood and marble. The large and heavy regular objects are very difficult to palletise by humans, even in the presence of manual palletisers. This becomes more complicated when the objects are of irregular shape. These objects are cut by precise laser into any shape, size and weight. Due to irregularity on the boundary and perforation inside the boundary makes it complicated for the Robots to palletise. Since palletising Robots are designed to grasp the objects from the fix spots and are preferred to be used for repeating jobs of same size and shape from same position. Therefore, Robot handling is also prohibited due to vast geometrical variation in objects.

This issue has been raised in manufacturing industries that uses CNC (Computer Numeric Control) machines to mill or laser cut of large sheets. These sheets are commercialised in variety of most known materials like wood, marble and steel. Initially, all sheets are of regular shape mostly a rectangle with standard size of 1220mm x 2440mm observed in the wood industry. Since this configuration favours the Robot to palletise from pre-defined spot to the machine bed and cuts off the material into different shapes using precise laser. Once the laser cutting process is completed, the shape and size of the sheets are unpredicted, and this configuration is beyond Robot limitations therefore human handling is required. To develop a fully automated system and avoid heavy manual lifting, the Robot is necessary to collaborate with the environment by real time feedback system and integrate a controller to understand and solve the complex irregularity problems. This way the Robot can be used for non-repetitive task at unknown predefined spots.

The Robot currently working on commercial scale uses the pneumatic grippers to palletise regular sheets. Some Robots have the capability to deal with irregular objects with limitations. These Robots pick the objects from COM (Centre of Mass) since they are very small in size and does not have sharp edges or perforation. The COM is a good technique for palletising only, if the objects are not too heavy or does not have much irregularities on the boundary. When a sheet is cut in a star shape with a hole at the centre or a grill type perforated having only 30 % of material after laser cutting, these scenarios are not yet been researched.

The research proposes a MV (Machine Vision) controller that is designed, simulated on MATLAB (Matrix Laboratory) software and validated by implementing on a Robot in real time. The Algorithm is developed to work in a loop that repeat its cycle until or unless a human intervention subroutine is requested. The software takes images of irregular objects after fixed interval of time and evaluate the features of the shape. The image is disintegrated into finite small regular polygons through real-time image processing to formulate the trajectory. This trajectory is further analysed to configure the spot where the object can be grasped. Once the calculation is completed the MATLAB Algorithm communicate with the Robot controller and shares the positional information to the Robot. Now the Robot controller check the possibility to reach all the position and postures of manipulator. Further, this information is sent to check the range of end effector and enable it to start the operation. The whole system is in a feedback loop, if the object is dropped between operation due to miscalculation or mishandling. The Robot will stop and ask the MATLAB to re-evaluate the position of dropped object. If MATLAB is unable to calculate the trajectory for this object, the whole system will shut down and wait for human assistance.

The robustness of the proposed method is evaluated through MATLAB simulations. To appreciate the validation of the Algorithm it is necessary to develop a prototype. Therefore, a 5-Axis Serial Robot (Mitsubishi RM-501) is used and the controller of this Robot is developed to read the information from MV system and integrate the pneumatic end effector with the Robot. F280049C Launchpad is used as main control unit of the Robot to control actuator, sensors and to communicate with MATLAB. MACH3 is also used as Robot interface software more details are available in chapter 5.

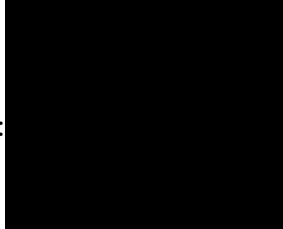
The research has also been integrated in a project at R&D Department of a medical device manufacturer in Australia. The research internship provided development of an AUWS to weld soft polymeric materials together. The main objective after developing the machine from scratch was to weld these medical devices of different size and shapes. Therefore, MV technique is used to generate the different regular and irregular bonding pattern that could results in strong weld joints. Furthermore, the position and torque of ultrasonic welding head were also controlled based on thickness. The project is working and producing the medical devices for research purpose.

Student Declaration

Doctor of Philosophy Declaration

“I, Muhammad Hassan Tabish, declare that the PhD thesis entitled **machine vision control Algorithm design for industrial palletising robo machines to increase the dynamic stability by real-time image processing**, is no more than 100,000 words in length including quotes and exclusive of tables, figures, appendices, bibliography, references and footnotes. This thesis contains no material that has been submitted previously, in whole or in part, for the award of any other academic degree or diploma. Except where otherwise indicated, this thesis is my own work”.

Signature:



Date 22-Feb-2020

Acknowledgement

My journey through PhD in Victoria University has given me a new way to think and I enjoyed this transition period in my life. Completion of the thesis has enlightened my life and is one of my biggest achievement. This journey would not be complete without incredible tremendous support and encouragements given to me by many great people around me. Hence, it is my pleasure to express my gratitude and acknowledgment to all of them.

First and foremost, I would like to express my sincere thanks to **Professor Akhtar Kalam** for his persistent extensive kind support, valuable comments, unique suggestions and words of wisdom are my primary source of inspiration throughout this journey. I would like to dedicate my heartfelt appreciation for my co-supervisor, Professor **Aladin Zayegh**, for his intellectual input, great concern, thoughtfulness and mostly his unique kindness helped me to raise in the entire process.

I would like to convey my heartfelt thanks to provide me D532 lab for the Robots experiments and a Robot Mitsubishi RM-501. This lab is my most memorable place where I spent most of my doctorate period. Sometimes here I felt like my second home.

Specifically, I am very honoured to give special thanks to Dr Bruce Verity and Jiamin Aw for the Research Internship. **Bruce Verity** is Research Manager at PolyNovo Biomaterials and my industrial supervisor. He is an inspiration to me as my whole internship time was a great learning curve where I learnt about project management, specially the URS (User Requirement Specification) and VP (Validation Protocol). I also understood the medical device standards and safety parameters to work in such industries. The internship could have never been successful without his unflinching support, as he was always standing by my side in this great Endeavor.

Furthermore, this Research Internship is very effective experience during the journey of PhD as I worked close to the R&D team and learnt a lot about how the application research is conducted and documented in a commercial environment, particularly with regard to Good Manufacturing Practices such as calibration and validation. This internship has also opened the ways to think differently for a given problem. The personal experience and employability are also enhanced by experiencing the application of

automation in development of commercial medical devices. This is a really very big add on to my qualification and the industrial contacts will help in career pathways.

I am grateful to my parents for their tender heart, sincere prayers, love, kindness and patience. My heartfelt thanks to my parents and siblings their unconditional support encouragement and exceptional care I owe a huge debt of gratitude to them.

Furthermore, and most importantly, I would like to acknowledge the help and support I received from my friends and colleagues. My special thanks to Pejman Peidee for providing me guidance during the servo controller development. His support I shall ever owe. Deeply grateful to Piyali Ganguly for helping me during the conference by providing Endeavor support about campus travel and things to remember. Last but not the least thanks to Ujjwal Dutta for his sincere help in setting up Robot and transferring his knowledge in power system. The friends and colleagues helped me in this journey that is totally unforgettable.

I appreciate the efforts of academic, administration and international enrolment staff members at Victoria University Footscray Park campus, including Elizabeth Smith, Michael Agrotis, Joyce Nastasi, Meika Scholz, Abdulrahman Hadbah and Palmina Fichera for all their incredible extraordinary support and guidance. I convey sincere thanks to all of them.

I am indebted to Almighty Allah for granting me courage, wisdom and blessing to walk through this demanding journey.

Table of Contents

Contents

Table of Contents	ix
Abstract	iv
Student Declaration	vi
Acknowledgement	vii
List of Figures	xiv
List of Abbreviations	xviii
Chapter # 1 Thesis Overview	1
1.1 Introduction	2
1.2 Research Aims and Objective.....	2
1.3 Contribution to Knowledge	3
1.4 Statement of Significance.....	4
1.5 Methodology and Conceptual Framework	7
1.6 Analysis of Irregular Polygonal Objects using MV	10
1.7 Thesis Organisation	12
1.8 Summary.....	15
Chapter # 2 Literature Review	16
2.1 Introduction	17
2.2 Calculations of Regular and Irregular Polygons.....	18
2.2.1 Calculation of Polygons Case Studies.....	19
2.3 Meshing Techniques of Irregular Polygons	21
2.4 Numerical Methods to Formulate Irregular Polygons.....	23
2.5 Robot and MV	26
2.6 Camera and MV	29

2.7	CPU, GPU and FPGA based Accelerating Hardware	33
2.8	CUDA Programming and Image Processing.....	35
2.9	Shortcomings in the Literature Survey and Contributions from this Research Work	38
2.10	Summary.....	39
Chapter # 3 Irregular Polygons Feature Extraction by Analytical and Numerical Method		40
3.1	Introduction	41
3.2	Shape Descriptor and Feature.....	41
3.3	Analytical Method Formulation	43
3.4	Numerical Method Algorithm	60
3.5	Summary.....	71
Chapter # 4 Trajectory Development of Irregular Polygons in MATLAB...72		
4.1	Introduction	73
4.2	Study of MATLAB Software and Image Processing.....	73
4.2.1	MATLAB Toolboxes	75
4.2.2	MATLAB Image Processing.....	77
4.2.3	SIMULINK and Image Processing	79
4.3	Shape Recognition of Polygons.....	79
4.3.1	Codes to Call the Original Image into MATLAB.....	80
4.3.2	Codes to Convert Image from RGB to GRAY	81
4.3.3	Invert the Binary Image and Morphological Operation.....	82
4.3.4	Coding for Polygons Recognition and Calculation.....	83
4.3.5	Results Generated from Algorithm	89
4.4	Methodology to Develop Trajectory	95
4.4.1	Get the Original Image into MATLAB.....	95

4.4.2	Disintegrate the Irregular Polygons into Small Regular Polygons ...	97
4.4.3	One Red Star Symbol ‘*’ in the Centre of Every 5 Boxes.....	99
4.4.4	Remove All the Boxes That Are Outside the Boundary	100
4.4.5	Remove the Sharp Edges from the Boundary	101
4.4.6	Remove All the ‘*’ that Are Touching or Outside the Boundary ...	102
4.4.7	Remove All the Boxes Inside the Shape	103
4.5	Robot Coordinates and Communication	104
4.5.1	Distance in Cartesian Coordinates with Respect to Origin	105
4.5.2	Cartesian Coordinates of Trajectory	106
4.6	Summary.....	108
Chapter # 5 Developing a Prototype to Test the Algorithm Experimentally		
	109
5.1	Introduction	110
5.2	Development of Robot Control Unit	110
5.2.1	RCU Part-1 F280049C DSP Micro-Controller	112
5.2.2	RCU Part-2 DCM50202 DC Servo Motor.....	115
5.2.3	RCU Part-3 MDD10A CYTRON Actuator	116
5.2.4	MATLAB Support Package for F280049C	118
5.2.5	Parameter Estimation for DCM50202.....	121
5.2.6	Algorithm Development for RCU.....	124
5.3	MACH3 Configuration and Robot Programming.....	127
5.3.1	MACH3 Hardware Configuration for Robot	129
5.3.2	MACH3 Software Configuration for Robot.....	132
5.3.3	Robot Programming by ‘G’ codes	134
5.4	Preliminary Study of Robot Motion.....	138
5.5	Experiments on Irregular Shapes.....	139

5.6	Overall Performance of MV System	140
5.7	Summary.....	140
Chapter # 6 Industrial Application of Research		141
6.1	Introduction	142
6.2	PolyNovo Requirements for AUWS	144
6.3	Construction of 3-Axis Cartesian Robot	147
6.3.1	CAD Model of 3-Axis Cartesian Robot.....	147
6.3.2	Linear Actuator Installation	149
6.3.3	Electrical Panel Box Design and Installation.....	151
6.3.4	Panasonic Servo System.....	151
6.3.5	Beckhoff I/O.....	151
6.3.6	Safety Devices.....	153
6.3.7	Integration of Ultrasonic Welder.....	155
6.4	Parameterization of Panasonic AC Servo System.....	156
6.4.1	EtherCAT Process Data Communication - PDO and SDO.....	157
6.4.2	Position Control.....	158
6.4.3	Velocity Control.....	158
6.4.4	Torque Control	158
6.5	Programming of Daincube Robot Controller	159
6.6	Repeatability Test of Robot.....	167
6.7	Welding Test on Soft Material based Medical Devices	168
6.8	Welding Test on Irregular Shapes by MV Algorithm	169
6.9	Algorithm to Generate Different Bonding Pattern	169
6.10	Summary.....	169
Chapter # 7 Conclusion and Future Work.....		170
7.1	Conclusion.....	171

7.2	Future Scope.....	175
References	177
Appendix 1: Authorship Declaration: Co-Authored Publications	187
Appendix 2: Doctorate Industrial Research Internship	188
Appendix 3: International Robotics Competition NIARC	189
Appendix 4: Articulated Robot based Research Project	192

List of Figures

Figure 1. 1	In the Human Era, jobs were tiring and hard	5
Figure 1. 2	In the Robot Era, regular sheets are moved	6
Figure 1. 3	In the Current Era, Irregular shapes are the problem	6
Figure 1. 4	Robot end effector activated in L shape.....	7
Figure 1. 5	Method 1, Grasping spots along the curve.....	8
Figure 1. 6	Method 2, Grasping spots around four different COM.....	8
Figure 1. 7	Method 3, Grasping points around COM.....	9
Figure 1. 8	Regular Polygonal Objects.....	10
Figure 1. 9	Irregular Polygonal Objects	10
Figure 1. 10	Irregular Polygon Analysis using Machine Vison	11
Figure 1. 11	Thesis Organisation.....	15
Figure 2. 1	Meshing of different sizes.....	22
Figure 2. 2	Demonstration of COM for Amoeba	25
Figure 2. 3	Frame Grabber used in MV application.....	31
Figure 2. 4	CMOS Camera Function.....	32
Figure 3. 1	High and Low Elongation.....	47
Figure 3. 2	High and Low Eccentricity	48
Figure 3. 3	Bounding Box	53
Figure 3. 4	Signature Analysis	59
Figure 3. 5	Original Image	61
Figure 3. 6	Convex Hull	64
Figure 3. 7	Bounding Box	65
Figure 3. 8	Signature Analysis	69
Figure 3. 9	Hough Transform.....	71
Figure 4. 1	MATLAB Software Environment.....	75
Figure 4. 2	MATLAB Toolboxes.....	75
Figure 4. 3	MATLAB Image Processing Toolbox.....	76
Figure 4. 4	Image Processing Techniques.....	77
Figure 4. 5	SIMULINK Software Environment.....	78
Figure 4. 6	SIMULINK Library	79

Figure 4. 7	Original Image	80
Figure 4. 8	Binary Image.....	81
Figure 4. 9	Processed Image.....	82
Figure 4. 10	Triangle	90
Figure 4. 11	Pentagon.....	90
Figure 4. 12	Hexagon	91
Figure 4. 13	Quadrilateral.....	91
Figure 4. 14	Octagon	92
Figure 4. 15	Triangle	92
Figure 4. 16	Pentagon.....	93
Figure 4. 17	Octagon	93
Figure 4. 18	Hexagon	94
Figure 4. 19	Octagon	94
Figure 4. 20	Original Shape.....	96
Figure 4. 21	Disintegrated Irregular Polygon.....	98
Figure 4. 22	Mark the targets at specific sequence	99
Figure 4. 23	Irregular Polygon with Clean Boundary	100
Figure 4. 24	Irregular Polygon without Sharp Edges	101
Figure 4. 25	Final image including boxes	102
Figure 4. 26	The final trajectory of the polygon to grasp the object	103
Figure 4. 27	Robot Coordinates of trajectory	104
Figure 5. 1	Robot Control Unit.....	111
Figure 5. 2	Mitsubishi RM 501 5-Axis Serial Robot	111
Figure 5. 3	DC Servo Motor Parameters List.....	117
Figure 5. 4	Parameter Estimation in MATLAB.....	123
Figure 5. 5	DC Servo Motor Real Time Data Collection DSP F280049C.....	124
Figure 5. 6	Speed data in real time (Input is 0 and 1)	125
Figure 5. 7	Speed data in real time input is (0, 25, 75, 100)	125
Figure 5. 8	RCU Control Algorithm.....	126
Figure 5. 9	Test results of the designed controller	127
Figure 5. 10	System Specification for MACH3 Software.....	128
Figure 5. 11	Flow of information from ‘G’ codes to the Actuators	128

Figure 5. 12	MACH3 Hardware or Break Out Board	129
Figure 5. 13	MACH3 Board Electrical Properties	130
Figure 5. 14	MACH3 Software Interface	132
Figure 5. 15	MACH3 ‘G’ codes Programming in Teach Mode.....	135
Figure 5. 16	Reference Table A	136
Figure 5. 17	Reference Table B.....	137
Figure 5. 18	Reference Table C.....	137
Figure 5. 19	3-Point and 5 Point tool coordinate system	138
Figure 5. 20	Irregular shapes	139
Figure 6. 1	Automated Ultrasonic Welding System.....	143
Figure 6. 2	3-Axis Robot Control Unit.....	143
Figure 6. 3	Top view of the 3d CAD Model	148
Figure 6. 4	Front view of the 3d CAD Model	148
Figure 6. 5	Linear Guide for X and Y Axes	150
Figure 6. 6	Linear Guide for Z-Axis	150
Figure 6. 7	Panasonic Servo System	151
Figure 6. 8	Beckhoff Digital I/O	152
Figure 6. 9	Safety Devices.....	153
Figure 6. 10	Tool Installation	155
Figure 6. 11	DainCube Robot Controller	160
Figure 6. 12	Select Switch.....	162
Figure 6. 13	Detailed Teach Pendant	162
Figure 6. 14	Main Menu and Sub Menu.....	163
Figure 6. 15	Jog Buttons.....	164
Figure 6. 16	Inching Control	164
Figure 6. 17	Speed Control.....	165
Figure 6. 18	Run Menu.....	165
Figure 6. 19	OFF Position and ON Position.....	166
Figure 6. 20	Repeatability test using dial indicator.....	167
Figure 6. 21	Welding test of plastic materials.....	168
Figure A. 1	Automated Ultrasonic Welding System 2019.....	188
Figure A. 2	The Robot breakdown	189

Figure A. 3	CAD Model of the Robot.....	190
Figure A. 4	NIARC 2018 Robot, team (VU Robots).....	191
Figure A. 5	DC Motor Test Bench	192

List of Abbreviations

ADC	Analog to Digital Converter
API	Application Interface
APR. Int.	Australian Postgraduate Research Intern
AUWS	Automated Ultrasonic Welding System
BOB	Break Out Board
CAD	Computer Aided Design
CAM	Computer Aided Manufacturing
CAN	Controller Area Network
CFD	Cumulative Density Function
CLB	Configurable Logic Block
CNC	Computer Numeric Control
COM	Centre of Mass
CPU	Central Processing Unit
CUDA	Compute Unified Device Architecture
CW	Clockwise
CCW	Counter-Clockwise
DC	Direct Current
DFT	Discrete Fourier Transform
DSP	Digital Signal Processor
EMC2	Enhanced Machine Controller
eQEP	Enhanced Quadrature Encoder Pulse
ESC	EtherCAT Slave Controller
FOC	Field Oriented Control
FPS	Frames Per Second
FPGA	Field Programable Gate Array
GHz	Gigahertz
GND	Ground

GPU	Graphic Processing Unit
GPIO	General Purpose Input Output
HDMI	High Definition Multimedia Interface
HMI	Human Machine Interface
IO	Input Output
IPPro	Image Processing Processor
IR	Infrared Radiation
KHz	Kilohertz
MAC	Media Access Controller
MATLAB	Matrix Laboratory
MBR	Minimum Boundary Rectangle
MC	Magnetic Contactor
MCB	Mini Circuit Breaker
MCU	Microcontroller
MHz	Mega Hertz
mm	Millimetre
MPG	Manual Pulse Generator
MV	Machine Vision
NIARC	National Instruments Autonomous Robotics Competition
NTSC	National Television System Committee
OHS	Occupational Health and Safety
PC	Personal Computer
PCI	Peripheral Component Interconnect
PID	Proportional Integral Derivative
PIL	Processor in the Loop
PLC	Programmable Logic Controller
PMSM	Permanent Magnet Synchronous Machine
PWM	Pulse Width Modulation
RCD	Residual Current Device

RCU	Robot Control Unit
RGB	Red Green Blue
SCI	Sequential Communications Interface
SIMD	Single Instruction, Multiple Data
TCP	Tool Control Point
TI	Texas Instruments
TTL	Transistor-Transistor Logic
UART	Universal Asynchronous Receiver-Transmitter
URS	User Requirement Specification
USB	Universal Serial Bus
V	Voltage
VCP	Virtual COM Port
VP	Validation Protocol

Chapter 1

Chapter # 1 Thesis Overview

- 1.1 Introduction
- 1.2 Research Aims and Objective
- 1.3 Contribution to knowledge
- 1.4 Statement of Significance
- 1.5 Methodology and Conceptual Framework
- 1.6 Analysis of Irregular Polygonal Objects using MV
- 1.7 Thesis Organisation
- 1.8 Summary

1.1 Introduction

This chapter describes the significance of research along with key contribution in integrated MV system for grasping irregular polygons. It showcases the motivation behind the research and methodologies applied to achieve the research goals and objectives. This chapter also highlights the justification of research study conducted during experimental work. Furthermore, the brief description of each chapter and its organisation is provided.

1.2 Research Aims and Objective

The Robotics palletising of large and heavy irregular polygonal object creates additional dynamics stability concerns when it is not constrained by same shape, weight and size. Palletising the irregular objects is the main aim of this research, that is achieved by the integration of MV system under typical conditions with the Robot controller. One such industrial application domain is the handling of irregular plane objects in wood, metal and stone industries.

The research project has following milestones.

- ❖ Review the literature concerning the Robot palletising that are integrated with MV systems.
- ❖ Investigate perceptions and attitudes towards irregular polygonal objects that process in the industries.
- ❖ Identify the improvements in the design of Robot end effector control Algorithm to grasp continuously varying object.
- ❖ Develop Algorithm to analyse the features of irregular polygons by disintegrating these polygons into finite small regular polygons through real-time image processing and formulating the trajectory to control Robot position.
- ❖ ‘G’ codes generation for the trajectories to move the Robot on designated position.
- ❖ Develop RCU (Robot Control Unit) to communicate between MATLAB Algorithm and Robot for the transmission of positional information.
- ❖ Compare the Algorithm results among different irregular shapes in real time using Robot.

1.3 Contribution to Knowledge

There has been a significant amount of discussion about grasping the irregular polygonal object using Robot with integrated MV system. Many formulae and methods are available in literature to find the COM, but they are restricted to regular polygons. Any object can be grasped from its COM, only if the object does not have sharp corners or perforation. When the object shape is perforated more than 50% with irregular long corners the COM theory does not apply to grasp objects through Robot. Furthermore, the Robot end effector does not have tremendous opportunity to deal with large variations, because it is only programmed to grasp from specific locations. If the object shapes continuously change, the Robot needs to replace the end effector every time to grasp a new shape and that is not productive even in such scenario humans can work faster than Robots due to limitations.

The research has adopted very different approach to find the grasping trajectory of irregular and perforated shaped objects made of steel, wood and marble using CNC mill or CNC laser cutter. The development of trajectory using MV techniques begins with the disintegration of digitalized image of irregular polygonal object into small regular polygons, this process is also known as meshing. Once the meshing process is completed, the extra traces of mesh is removed that are outside the shape. The next process in the development of trajectory is to formulate the predefined statements (subroutine programs) to avoid the sharp edges in the image that are very small in width and cannot be picked by the Robot end effector hence these edges are also removed. Now define each disintegrated regular polygon on the processed image by asterisk sign “*” and remove the asterisk that lies on the perforation area as the Robot cannot grasp from perforated zones. Final process in the development of the trajectory is to calculate the total points against the load grasped. If there are any other limitations or addition of more spots will be resolved at this stage. The trajectory is now developed using the remaining asterisk on the image. As yet, this technique of developing the trajectory for the Robot has not been used in any palletising system and is the main contribution of research.

Further the trajectory is analysed to transfer into positional information of ‘G’ codes, the language that Robot understands. These codes are then communicated with Robot controller to follow the pattern. Hence, the Robot will do as directed and pick the object using a specific trajectory of its end effector. This process will continue and for next cycle, which can be totally different from another and so on. This Algorithm will continue to work until the object is not bigger than the end effector or smaller than its limitations.

This work also includes specific artificial intelligence process, as the controller takes the decision itself. If the Robot palletises an object and it drops down before completing the cycle, the Robot will stop as continuously feedback system is attached in terms of MV system and take the decision that should it start another cycle or find the object which was dropped. The Robot will start searching, if the object is in the range. The Robot will start a subroutine which is pre-programmed and grasp the object to complete the task and if it is not in the range then either Robot will stop for human assistance or start another cycle.

1.4 Statement of Significance

The Palletising Robots has been used for many years in the manufacturing industries, but these Robots have limitation with respect to shape, size and weight of the object. For a variety of products, the end effector of the manipulator must be changed according to each product variables. The research has brought new methodology using the MV System where the end effector is capable enough to deal with continuously varying shape and size.

Human Era: The companies made use of the humans to pick and place the objects that is always very hard and tiring job as shown in Figure 1.1. Some application domains are the Wood, Metal and Stone where these heavy objects are cut by cutters in different shape and sizes. This was one of the main causes for human with back pain problems in their early ages and was also caused the violation of OHS (Occupational Health and Safety) reputations.

Robot Era: With the change in time and technological advancement, the human handling is reduced on a large scale by using machines and Robots for repetitive works. Therefore, much of human problem is resolved. The industries started using Robots to pick and place the objects as shown in Figure 1.2 Everything was going good as long as the objects were being built by regular polygons.

Current Era: Since humans are now demanding more luxurious design, which compels architectures to build more beautiful objects with smooth curves and shapes as shown in Figure 1.3 and that is not a regular polygon and most of the time every object is different from other when it is made to order.

Now the problem again started with the Robots as they are only designed for either grasping regular polygonal objects or fixed shapes irregular polygonal objects. Because of advancement, every design is different from other. Hence, it is not feasible to design and fabricate a gripper for each part and then Robot change its holder on every cycle. This way the productivity is compromised, and the use of humans is considered again.

The current research on Robots has extended to the new stage of irregular polygonal objects and therefore this research is developing an end effector trajectory to resolve this issue. The research mainly has three very precise benefits:

- ❖ Grasp the irregular objects which has started being pelletised by humans,
- ❖ Help the companies to stop avoiding OHS rules by adopting new technologies and
- ❖ Enhance the productivity using Robots.



Figure 1.1 In the Human Era, jobs were tiring and hard



Figure 1.2 In the Robot Era, regular sheets are moved



Figure 1.3 In the Current Era, Irregular shapes are the problem

1.5 Methodology and Conceptual Framework

There are three possible **methods** at this stage available which can be used for finding Trajectory around COM. These methods will be used during the research practice. Before explaining the methods, limitations of Robot end effector are very important. End effector contains small vacuum nozzles at 50 mm from each other as shown in Figure 1.4. Every nozzle is controlled by solenoids. This unit is attached with the Robot under the direct supervision of MV system that provides feedback and the positional information back to the controller. The end effector operation is very easy, as it receives the information about which pressure point should be activated as every pressure point has an address. The red colour pressure points in Figure 1.4 is forms a trajectory of L type shaped, this information is calculated in the research with different methods.

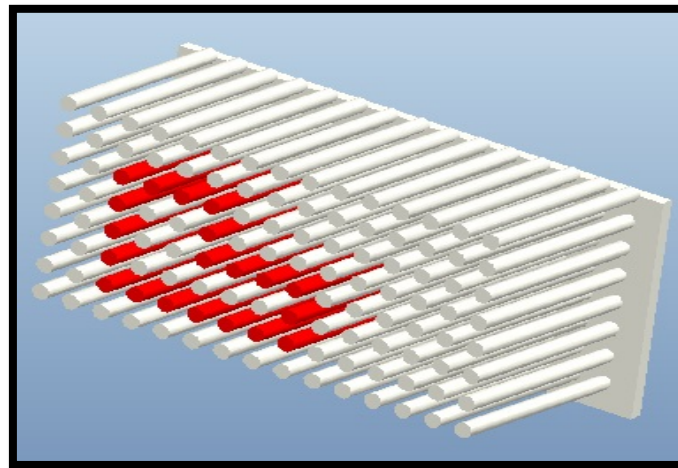


Figure 1. 4 Robot end effector activated in L shape

The first method is designing the trajectory near the far edge of the shape of irregular object and sends the addresses about these points to the Robot. The grasping points near the wall of the irregular object is activated and grasped as seen in Figure 1.5. However, there is one issue with this method and that is, if the object is symmetrically divided, the dynamic stability will be high, but if the object shape is unevenly divided like $\frac{3}{4}$ weight lies at one side and $\frac{1}{4}$ weight lies on other side then the object could drop during the operation. Further investigation is taken into consideration during the research work.

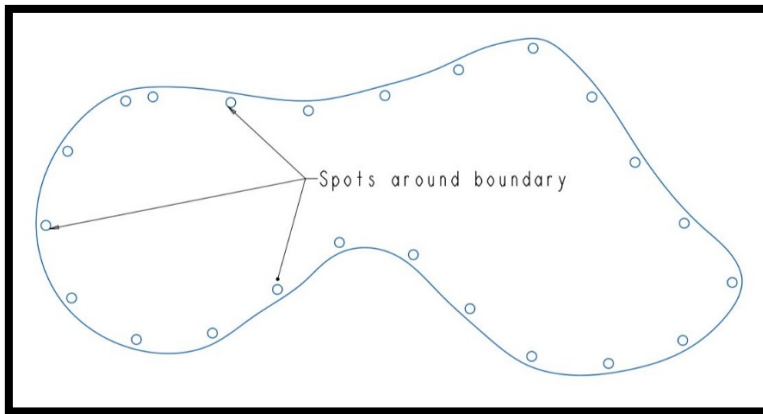


Figure 1.5 Method 1, Grasping spots along the curve

The second method is dividing the shape into equal area. The object is divided into sections and again follow the trajectory in each section to grasp the object around different COMs as shown in Figure 1.6. This approach could cause too many grasping points required for each section as well as when the COM does not on the object due to shape variations. Detailed study of this hypothesis is conducted during the MATLAB simulation.

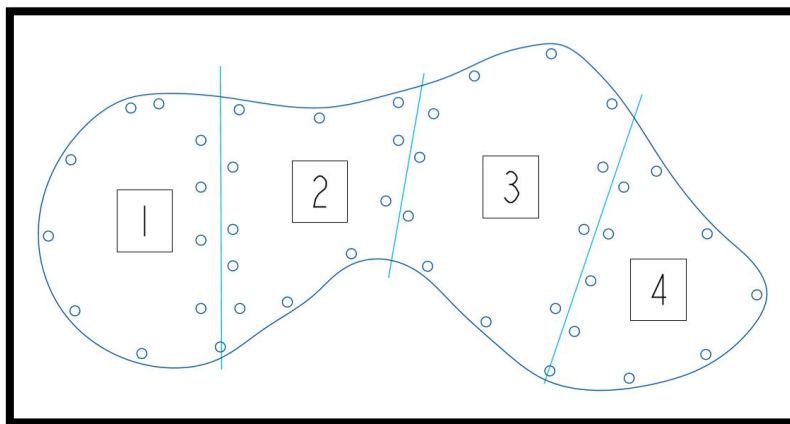


Figure 1.6 Method 2, Grasping spots around four different COM

The third method is very efficient from the other two methods, as it does not use too many pressure points to grasp the object. This method uses the COM coordinates and develop a very small possible trajectory to grasp the object as shown in Figure 1.7. When the sheet is perforated, fragile or very thin, then instability concerns occur. There can be many scenarios that is tested to achieve optimised result during the research.

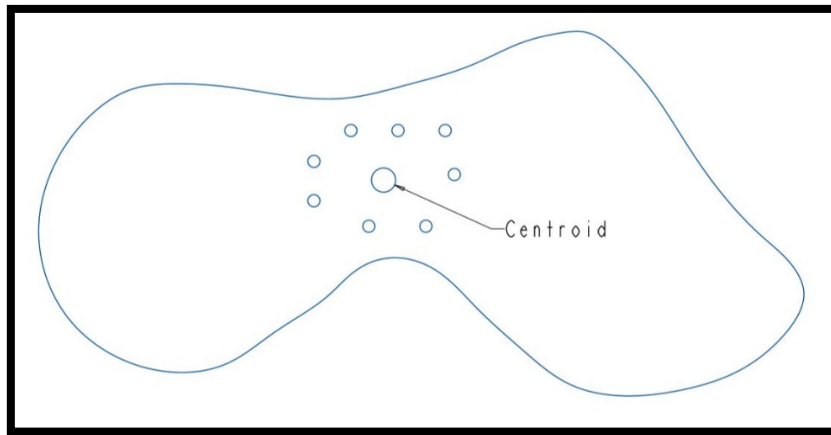


Figure 1.7 Method 3, Grasping points around COM

The **conceptual framework** of the research has three phases:

1. The development of MV Algorithm and techniques to find the grasping points as discussed;
2. The simulation of the findings in MATLAB using irregular polygons; and
3. The verification of the finding in real world using Robot.

The MV system uses a Camera, Lenses, Light for image processing and feedback purpose. The image taken by the camera is in JPEG format and the camera output is TTL (Transistor-Transistor Logic). The camera is connected to the computer through the serial connection and transfers all data. This data is sent into the MATLAB program and start image processing where different parameters are calculated which include the edge detection, measuring the size of the object, shape of the object, position of the object and calculating its COM to formulate the trajectory. This trajectory calculation is very important because if the errors exists in the calculations, the Robot can become hazardous, the object might drop during the cycle and can cause severe human injuries.

The last phase is the development of RCU to communicate with the MATLAB Algorithm to verify the findings. The DSP (Digital Signal Processor) is capable of fast mathematical calculations and the selection of F280049C processor is based on its capabilities, like high resolution 24-bit position counters, two independent channels for interfacing the incremental encoders and ten PWM (Pulse Width Modulation). The board connects with MATLAB environment and can run all simulation in real time through its add on software.

1.6 Analysis of Irregular Polygonal Objects using MV

The regular objects formulae are available which helps the MV system to calculate the COM very easily that is why dealing with regular polygonal object is very common and Robots are used worldwide. The regular polygonal object has pre-defined positions as shown in Figure 1.8. For example: Triangular through $1/3^{\text{rd}}$ distance from the base, Square can be picked by the four corners positions and similarly circular one from Centre.

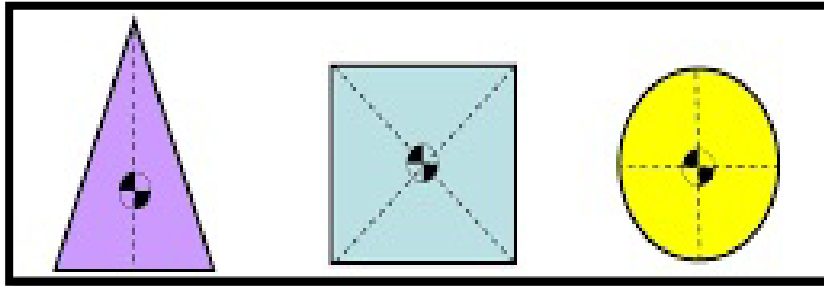


Figure 1.8 Regular Polygonal Objects

The irregular objects shown in Figure 1.9 do not have specific shape like square or triangle that is why this is referred as irregular polygonal objects, thus they neither have a formula nor it can be pre-defined (Controller do not have the image to compare as they are continuously varying, each object is partially or completely different from the previous one, even some object is only used once).

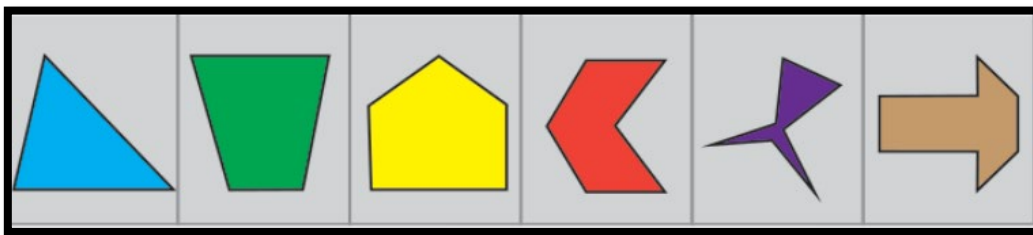


Figure 1.9 Irregular Polygonal Objects

Several case studies in the Automation and Control industries deals with irregular polygonal objects. This study aims at grasping the objects using numerical analysis of images. The Figure 1.10 describes the step by step procedure involved in this study.

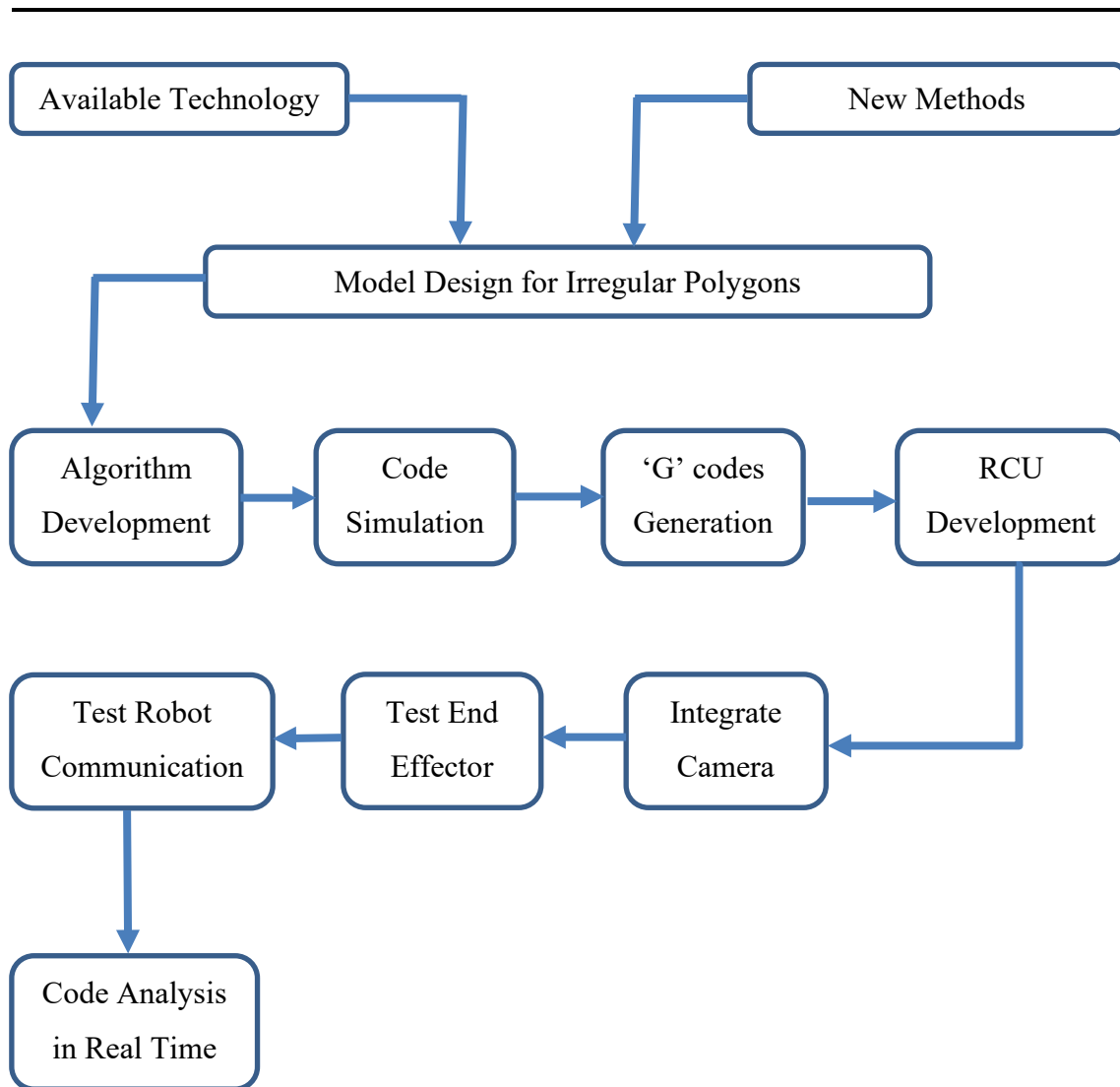


Figure 1. 10 Irregular Polygon Analysis using Machine Vision

Furthermore, RCU is developed to communicate the Robot with the MATLAB program in order to verify the Algorithm results. This is the main control unit of the Robot. All other calculations regarding MV takes place in the MATLAB environment. MV is basically the integration of Algorithm, GPU (Graphic Processing Unit), Camera and Robot. When these units work simultaneously it forms a hardware and software in loop that provide a real time feedback system. Code analysis takes place using an A4 white board and a black marker by drawing different Polygonal Objects. Once the shape is drawn, camera takes image at constant interval of time and if any difference is found from the previous image it starts processing the image and follow the pre-defined procedure.

1.7 Thesis Organisation

Chapter 1 – Thesis Overview

This chapter provides the synopsis of the research along with the key contribution in integrated MV system for grasping irregular polygons is defined. Furthermore, the original contribution and significance of research is described in detail. A brief discussion of each chapter is highlighted, and organisation of the thesis is also provided.

Chapter 2 – Literature Review

This chapter highlights the works which has been developed in academic research and industries showcasing the role and importance of MV applications in irregular polygons. The challenges involved in MV technology and contextual studies from the literature are studied to solve the irregular shape complex behaviour. Understanding the industrial case studies of MV in the field of irregular shapes has been explored in detail. The cabinet manufacturing industries are also visited to better understand the requirements for palletising the sharp and perforated objects. The shortcomings of the study undertaken in the literature survey conducted has been summarised and the contribution of the research to overcome these shortcomings are highlighted.

Chapter 3 - Irregular Polygons Feature Extraction by Analytical and Numerical Method

This chapter gives an insight into feature extraction by MV using MATLAB. It also illuminates how the Analytical methods formulae and Numerical methods Algorithm deals with different irregular polygons. A shape can be defined using different methods. This chapter instigates twenty-five geometrical characteristics by both the methods numerically and analytically. Different MATLAB Algorithms are used and explained in detail to understand complex shape and their features even if they are not possible analytically. Thus, these methods would not only have a substantial impact on the industrial palletising of irregular shapes but also provide detail information to Robot controller to enhance the dynamic stability for grasping the shapes.

Chapter 4 - Trajectory Development of Irregular Polygons in MATLAB

This chapter summarises the research conducted in this thesis and the achievements of the aims by the development of Robot end effector trajectory. The coordinates found is further processed in the next chapter. Different MATLAB tools has been used to design these Algorithms. Nonetheless, there are many studies on MATLAB software which is considered more reliable by many MV technology providers in Australia. Not many other software packages have been explored other than MATLAB. The current study aims at exploring further MATLAB image processing tools and techniques to understand the MV for irregular shapes. As discussed earlier, the objective of the software analysis is to reduce the processing time using numerical methods. However, the analysis made by MATLAB is the best method of evaluating all the possible combinations to test and deploy them on the hardware in real time.

Chapter 5 - Developing a Prototype System to Test the Algorithm Experimentally at the Victoria University Footscray Campus Lab

This chapter is the continuation of chapter 4. The Robot used in this experiment is Mitsubishi RM-501 5-Axis Serial Robot to validate the findings in real world. The control unit of the Robot is replaced by the new state of the art DSP controller F280049C. This controller is configured in MATLAB software to use as a DC (Direct Current) servo driver and integrated with CYTRON MDD10A board. Furthermore, the ‘G’ codes are generated and tested using MACH3 software. There are various experiments conducted to validate the Algorithm. Initial test was to check the Robot accuracies and kinematics to make sure that it is working in tolerances. Afterwards the different irregular polygonal shapes are placed under the camera and the Robot moves on the designated trajectory points for verification.

Chapter 6 - Industrial Application of Research (APR Research Internship at PolyNovo Biomaterials Port Melbourne)

This chapter describes the significance of the research and one of its application domains in medical industry. PolyNovo Biomaterials offered the research internship to Research and Development of an AUWS (Automated Ultrasonic Welding System).

PolyNovo is a manufacturer of novel medical devices based on proprietary biodegradable polymers. The project requires the intern to develop an automated machine or mechanical arm that moves the existing point-bonding tool across the surface of the sheets of material that need to be bonded. The tool needs to move in both the X-Axis and Y-Axis directions to create a matrix of bond points, with control of the depth in the Z-axis. The project needs to provide flexibility for the company to be able to test the effectiveness of different bonding patterns for the performance of their developmental products. The contribution in the research is the welding of different shapes of medical devices and development of Algorithm to allow generation of different bonding patterns to achieve 100% strong weld between the plastic materials.

Chapter 7 - Conclusion and Future work

This chapter summarises the research conducted in this thesis and the achievements of the aims. Furthermore, it explores the benefits of the Algorithms developed for irregular polygons and opens a wide range of application in many industries. Now the irregular objects can be grasped provided the sharp edges and perforation. The validation on the Robot using A4 white board proved that the research could deal with any irregular shape to utilise in MV applications. This chapter also focuses on the possible future scope along with the research internship.

The thesis organisation is also demonstrated in the following flow chart of Figure 1.11 to understand the relations between the chapters.

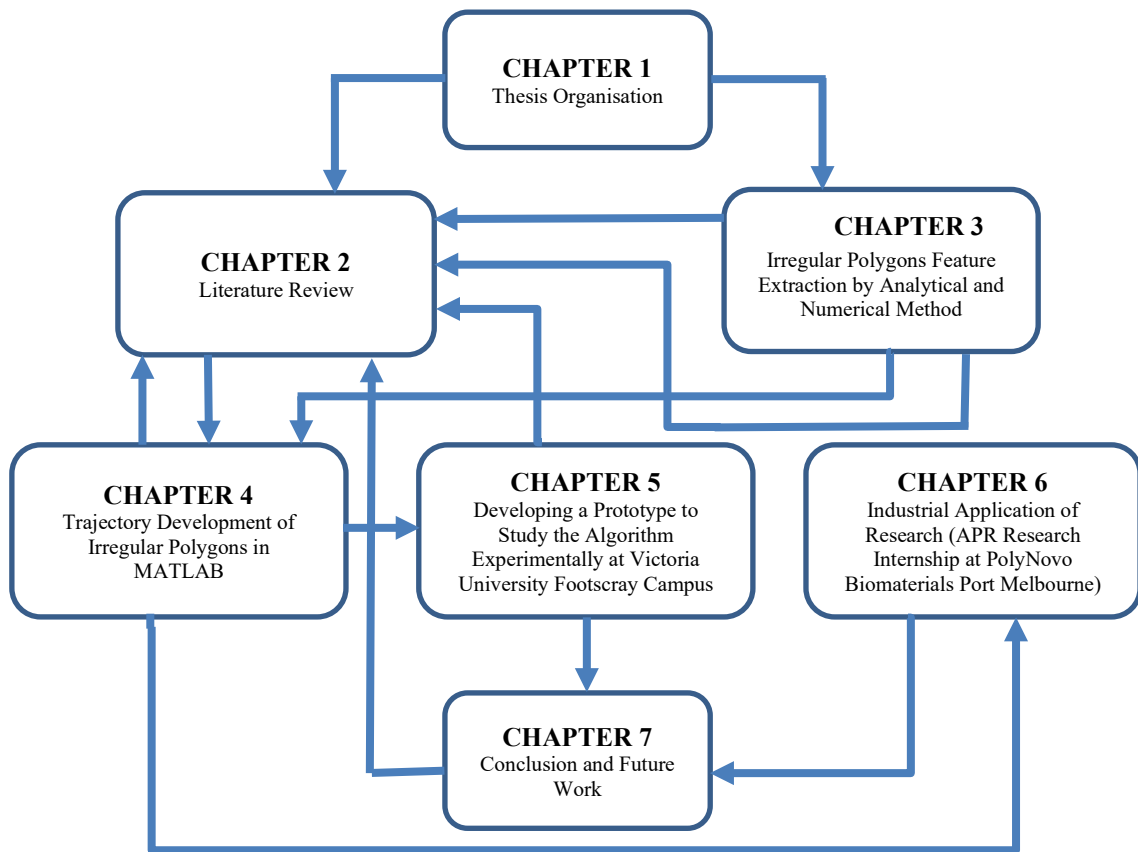


Figure 1. 11 Thesis Organisation

1.8 Summary

Cabinet making is one of the growing industries in Australia. BIESSE is one of the largest suppliers of wood CNC machine. These machines are very high tech that feed in the big sheets on the CNC table automatically and run a series of procedures to complete the product without human interventions. But the method used to unload the wood sheets from machine bed to edge bender is very slow and most of the time, operator intervention is required when the sheets are very perforated, fragile or thin because the roller system is used to move the sheets from one station to another. The research turns the way of feeding the irregular shape objects on to different stations by means of Robot that is fast, accurate and artificially intelligent to take decisions on its own that contributes to the focus of unmanned factories. Furthermore, Mitsubishi RM-501 5-Axis Serial Robot is used as a prototype to verify the findings in real world. This research is also applied in the medical device industry at PolyNovo Biomaterials by dealing with ultrasonic welding of sheets of proprietary biodegradable materials.

Chapter 2

Chapter # 2 Literature Review

- 2.1 Introduction
- 2.2 Calculation of Regular and Irregular Polygons
- 2.3 Meshing Techniques of Irregular Polygon
- 2.4 Numerical Methods to Formulate Irregular Polygons
- 2.5 Robot and MV
- 2.6 Camera and MV
- 2.7 CPU, GPU and FPGA based Accelerating Hardware
- 2.8 CUDA Programming and Image Processing
- 2.9 Shortcomings in the Literature Survey and Contributions from this Research Work
- 2.10 Summary

2.1 Introduction

The measurement of irregular objects through formulation is almost an impossible task. This problem is solved by the image processing techniques that introduces different methods to deal with 3-D, Novel and Irregular planar objects. Calculation to such objects are now possible by the processing of images. In image processing, the image of the object is taken with the help of a camera and later this raw data is sent for further processing to collect valuable information. This information is then used by different Robots or automatic system to perform their scheduled tasks. This overall system is called MV, where the camera is integrated with the Robot or Machine to communicate with the control unit in terms of sharing the images. There are many case studies discussed where irregular objects are measured and utilised to achieve different objectives. To run and test these Algorithms is very time consuming in terms of processing as these images are supposed to process in seconds. Therefore, there are multiple accelerating hardware available like CPU (Central Processing Unit), GPU and FPGA (Field Programable Gate Array) to debug the Algorithm on the external board for the validation of results in real world scenarios. This chapter also elucidates the state of art study in the integration of MV systems on Robots and develop different trajectories to deal with a variety of irregular objects.

MV is creating high impact in the manufacturing industries by reducing the labour cost and enhancing the productivity with quality. Now Robots are not bounded to do the repetitive tasks only. The MV system unleashed the Robots to achieve the rear tasks that might occur only once in the whole tenure of Robot life. Today's Robot can think, learn and take decisions to deal with multiple scenarios using artificial intelligence and machine learning. The MV industry application is rising in almost every field such as food processing, palatizing, welding, medical imaging, traffic management and so on. MV global market is expected to hit billions dollar by 2025. This thesis also contributes in the global market of Cabinet manufacturer, Laser cutting and Marble machining because the objects turns into different irregular shapes of unknown size and perforation after operations.

2.2 Calculations of Regular and Irregular Polygons

Polygons are the basic differential terminology that defines the simple mathematical structure of the object. If observed over a descriptive range, this object constitutes the polygonal structure over a large scale. The starting point of the well-known problem i.e. the calculation of these polygons is the evaluation of their angle ' Θ ' with the help of pure elementary geometry. The basic laws of geometry dates back to the 9th Century and beyond which have eventually led the world towards complex and advanced calculations, carried and investigated geometrically.

The concerns related to the calculations of polygons have focused over the calculations of all concurrent chords of the regular polygons. It has been observed that either way, calculations can be focused towards a much wider goal by evaluating the quadrangles within the polygon. The quadrangles partake the angles between every pair of the six sides as an integral multiple of π/n radians, in theory [1]. The advancements within the calculation of regular polygons continued towards the classification and generation of symmetric integration formulas. These formulations were carried with the help of the theories defining the interpolator integration formulas in n-dimensions, which were combined with the group theory. The points that have been evaluated are computed as the common zeros over a set of polynomials that set a canonical basis for the real part within the formula. To get a symmetrical formula, the values are derived as a span in representation of the symmetry group. It should be kept in mind that the canonical basis does not provide with the complete symmetry and degree, yet they do help keep a general basis of suitability [2]. Research over the calculations of regular polygons has led towards far more advanced structure than imagined. The mathematical representation of the regular polygon's chord length distribution utilized the δ -formalism in Pleijel identity. This has been tested as separate studies over 3-sided, 4-sided, 5-sided and 7-sided polygons. This research helped researches constitute the chord length density function for regular polygons [3]. Research over the regular polygons has been computed with the exact CFD (Cumulative Density Function) value which for some cases was covered from a node to an arbitrary reference point within an n-sided polygon [4].

It should be seen that these researches have continued leading to more contemporary methods and conceptual understanding. The research then moved their focus on discussing outer billiard maps from the restrictions of regular polygons and puts convex

polygons into the spotlight. They analyse the symbolic dynamics connected with this map. The case studies involved the polygons having three, four, five, six or ten sides which were provided with a complete description of the constituted dynamics with the characterization of the related languages and the global complexity functions. To understand the properties of the dynamical system to a greater extent, the methods involving combinatorics and geometry redeems usefulness. The symbolic dynamics and complexity of the language are computed conclusively [5]. Further investigation describes the outer billiards with contraction. The study maintains a conceptual understanding of 3, 4, 5, 6, 8 and 12-gon protruding a contraction rate approaching to 1 with a converging nature of the system dynamics. It was kept majorly in comparison of the usual outer billiards map. This was, for values of n greater than three with a subtle condition of equation (2.1). The study also emphasized on the reasoning over the failure of evaluating convergence in the case of n equalling 7 [6].

$$[Q(e^{2\pi i/n}): Q] \leq 2. \quad (2.1)$$

The study then utilizes the regular polygons and their relationship with the golden section. They undertake an isosceles triangle and its constituted circumcircle, on which a chord parallel to its base is formed into the golden ratio. The results of equilateral triangle determined by the authors and for a half-square by other authors generalized with this hypothesis. The research hypotheses are also applied onto an isosceles triangle formed by two adjacent sides of a regular n -gon [7].

2.2.1 Calculation of Polygons Case Studies

Case Study 1

Steiner minimal trees [8] have gained importance whilst being conjoined with the regular polygons and their geometric evaluations. Five decades ago, it was displayed that a Steiner minimal tree for the pinnacles of an n -sided polygon containing Steiner points between the values of 3 and 5, whereas it displayed no Steiner point at the value of 6 and values greater than 13. This paper further evaluates the Steiner point for the values between 7 and 12. It was observed in the case of equation (2.2) yielding similar results as equation (2.3). The paper demonstrates that collections of numerous equally distanced points provide the lengthiest Steiner minimal tree among the n number of co-circular points [8].

$$7 \leq n \leq 12 \quad (2.2)$$

$$n \geq 13 \quad (2.3)$$

Case Study 2

As regards of regular polygons in Euclidean space, a mathematical appraisal has been designed for their calculation. The solutions of these problems reside over a sphere, whose centre of gravity on observance evaluates the centroid of all the points. This approach also led towards the evaluation of a newer concept of triangular coordinates as points of the interior section of triangle that combined the relation with the regular hexagons of the 5th dimension. The results that led towards the testing of this approach was evident amongst the two of the three points of the regular triangle that connected the 3-D regular hexagons whilst the remaining interval of the three points directed towards the 4-D hexagons [9].

Case Study 3

Garza-Hume, et al. analysed and evaluated, the feasible shapes and areas for the planar space of irregular polygons explained through side-lengths [10]. The cyclic configuration has been devised with the help of computer programs and written Algorithms which are correlated with the circum-circle. This was proposed for the calculation of the maximum possible area. Quadrilaterals with their specific intersection are studied in this paper and it has been proved that minimizers are not a cyclic coherence in this method. The quadrilaterals were classified according to their reversing orientations and every possible shape with side-lengths and areas were considered during analysis.

Case Study 4

A problem related to the industry is in the allotment of the 2-D irregular shapes onto a pile of planar sheets with finite lengths and breadths. The specifications are deliberated towards minimizing the area of the amount wasted. This problem was observed for practical applications like shipbuilding, clothing manufacturing or cutting of leather. The solution to this issue was achieved through the method of Heuristic Search inclined towards the dynamics of artificial intelligence. This framework not only allows a simple formulation of the solution but represents an effective technique to obtain solutions competitive with the ones produced by hand [11].

2.3 Meshing Techniques of Irregular Polygons

Where the world is a commemoration of regular polygonal structures, there remains a major chunk of the object belonging to the irregular structures, referred as irregular polygons. In basic geometry, it is believed that the irregular polygonal structures are either difficult, impossible in most cases, to be measured and evaluated accurately. Hence, in the earlier stages of evaluating irregular polygons, it was either estimated or closely calculated by researchers and scientists but with progressing time and technology, the knowledge related to its measurements enhanced thus providing the world with different meshing techniques. It is seen that a wide range of techniques refer to Figure 2.1, help create regular polygonal structures out of it or would help with the irregular structure that can be evaluated easily.

A mesh generator is designed for subdividing irregular polygons into quadrilaterals of regular structure. It is believed that this method is applicable over any irregular arbitrarily sided polygon. This method, if briefly described moves in the direction of referencing the polygon with coordinates of a commemoration of primary nodes. The sides of the polygons would be referred to as lines that are connectors of the nodes acting as straight or curved lines, allowing their advanced segmentation into more lengths. This allows the interior to be converted into a quadrilateral by itself [12]. The abnormal polygons have been focused with a vast range of meshing techniques, amongst which another method was proposed of rotationally placing the polygons over such dimensions that fixates the overall figure. This technique used two basic methods of simulated annealing and no-fit polygon. This work was rather objectified as a solution to the wastage of different bi-dimensional substances within an object [13].

Algebra and geometry always remained an integral part of the research over polygons. Research conducted on the assessment of the maximum number of symmetry lines during their sinter-forging related with the irregular polygon utilized the similar concepts. It was evaluated that the maximum number of lines equals the lengthiest proper divisor of the number of sides of the irregular polygon [14]. There has been different Algorithm that had a specific approach over the use of irregular polygons and their fitting into the calculations that provided a cognitive result with minimal errors. A hybrid Algorithm was devised in the case of a 2-D layout issues, in the case studies of regular and irregular shapes. This mechanism comprises of the process of calculating the smallest

length layout in the case of both the consistent and unbalanced shapes surfaced on a set of sheets [15].

The calculations of regular polygons yielded different questions, which led towards newer approaches. Over the question of the dissection of balanced polygons turned as triangles of same areas. The paper evaluates the question of an n -sided polygon dissected into m -triangles which results as values of m to be a multiple of n . The stated hypothesis was negated for the values of 3 and 4-sided polygon where it was stated that a square has not the capacity to be disjointed into odd number of triangles. With the adopted techniques along with the utilization of Sperner's lemma, a conclusive approach for evaluating the basic question of dissecting polygons into equally sectioned triangles [16]. Cureton et al. [17] uses the regular polygons and dissected polygons, which provided eigenvalues of the Laplacian. The research discusses the problem related to the eigenvalues, which is considered for Laplacian on regular polygons; this was based on Neumann's boundary conditions which were presented to the unit circle with a relation of conformal mapping. The upper bounds evaluated are the products of Bessel and trigonometric functions which evaluates a new recursion formula for the generation of new Bessel function integrals. The symmetry classes were efficient for a range of polygons, with aid from previous researches.

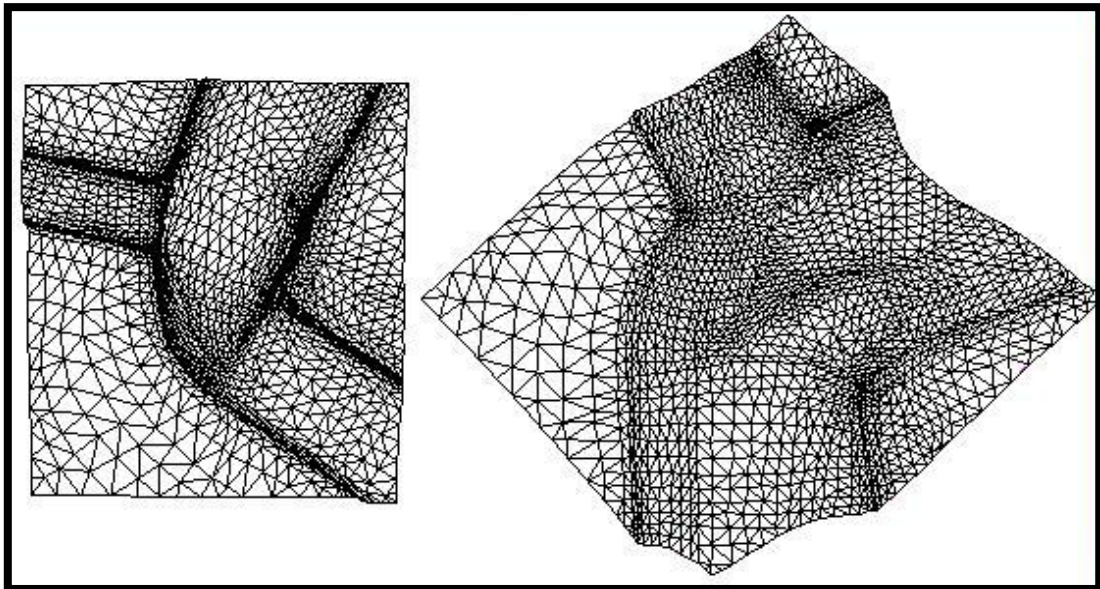


Figure 2.1 Meshing of different sizes

2.4 Numerical Methods to Formulate Irregular Polygons

As it has been observed in the previous sections that there are different meshing techniques that have been designed to evaluate the irregular polygonal structures, science and mathematical evaluation never remained at a single direction. There are different numerical methods that have been devised for the calculation of the irregular polygons which includes a variety of methods and evaluation techniques that have proved advantageous in designing a clear gateway of solution for the polygons.

Amongst such accurate and coherent methods, one such method evaluates the irregular convex polygons and polyhedrons whose numerical integration was devised of their polynomials and relative discontinuous functions. For this, effective quadraturism has been utilized based on the moment fitting equations. Yet this scheme calculates the commemoration of monomial basis function with a set of linear equations as a solution of the mathematical modelling. This involves the building of homogeneous quadrature which is based on the Lasserre's methodologies for polytopes [18]. Another approach was formulated which analysed and evaluated the feasible shapes and areas for the planar space of irregular polygons explained through side-lengths. The cyclic configuration has been devised with the help of computer programs and written Algorithms which are correlated with the circum-circle. This was proposed for the calculation of the maximum possible area. Quadrilaterals with their specific intersection were studied and it has been proved that minimizers are not a cyclic coherence in this method. The quadrilaterals were classified according to their reversing orientations and every possible shape with side-lengths and areas were put into consideration during analysis [19].

It should be seen that such numerical methods evolved into much simpler and feasible cases that allowed the calculations of different parameters of irregular polygon at ease. Another basic approach designed a framework for evaluating the time taken for freezing or thawing submissive of multi-dimensional irregular shapes with the help of simple formulae. Different hypothesized and calculated data was mirrored to different methodologies which comprised of the measurement of the effects in the shape in different time predictions. With the help of actual experimentation, the empirical formulae for the factors were proposed and implemented giving an accurate result for all 2-D shapes along with most 3-D shapes [20]. As the research levels towards more advancements and technicalities, a method uses an irregular shape to observe the 3-D

scattering of the guided waves with the flat-bottomed cavities. The scattering and standing fields were dissected over the utilization of waves with the inclusion of propagating and non-propagating modes. The nullity of the total stress at the cavity's boundaries is jotted down for the calculation of the amplitudes [21].

Different past mathematical methodologies have been utilized in the evaluation of the irregular polygonal structures. A research considered the Wilhelmy plate methodology as the most accurate measurement for the evaluation of the dynamic contact angle of the liquid states placed over solid surfaces. The study focusses on the Wettability measurements for the irregular shapes with the utilization of the Wilhelmy plate methodology. The researchers devised a contemporary formulation for the determination of the contact angle for the samplings of irregular shapes which was based on the Wilhelmy force balance equation. The raw force measurements from the force tensiometer were calculated with the profile plotting and the Wilhelmy equation [22]. It is seen that different methods that are relatively easier and efficient in procedure are based on the finite difference methodology for the evaluation of partial differential equations on the systems of irregular polygons [23]. There exist several methods that account for devising solutions that are utilized in the discontinuous numerical methods. Therefore, the use of such methods for the computation of volume and centroid of the irregular blocks with the help of simplex integration and 3-D simplex integration have been recorded [24].

Different studies have put their focus towards a more logical and advanced approach resulting into simpler models of calculation. Over the prediction of overall elastic properties of solids in terms of irregular shaped pores, the approach proposed used the Mori-Tanaka and Maxwell's micromechanical model with an H-tensor mechanism. Effects because of pore shape and matrix Poisson's ratio were discussed [25]. Experimental studies have also been designed for the numerical modelling of biomass micro size particles which are anisotropic and irregular in shape [26]. This clearly shows the advancements that the numerical calculations of irregular shapes have covered.

In physics, it is always beneficial to imagine the mass of the body as projected towards one Centre point which is commonly known as COM. Fitzpatrick [27], describes the calculation of COM for regular polygonal objects. He formulated an equation which illustrates that the COM of the extended objects is the mass weighted averages of the coordinates of the element. The importance of COM for the research project is because the RCU is programmed in such a way that it picks up the object from the COM or trajectory, described in methodology section to balance its weight from all sides to enhance the stability. The COM for regularly polygonal objects has been known for many decades but very few successes are observed in determining the COM for irregular polygonal structures. It has been found that an amoeba or any irregular polygon can be suspended through numerous points from its edges with a plumb line, as a result it will give a straight line through the COM as shown in Figure 2.2. Thus, by drawing two or more lines on this object COM can be found for irregular polygonal objects.

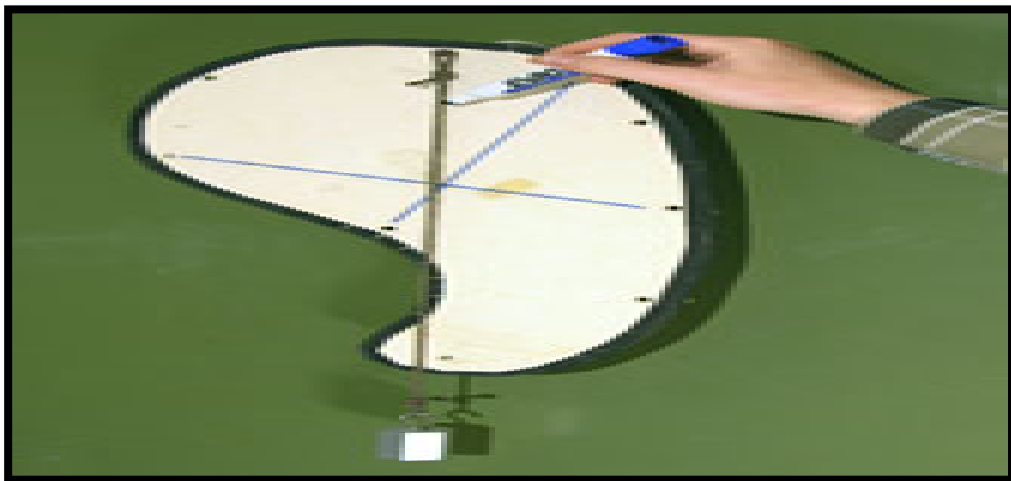


Figure 2. 2 Demonstration of COM for Amoeba

Maus et al. [28] research article hereby refers to the calculation of COM either from the force data (dynamic method) or motion capture data (kinematic method). Both the approaches depend upon the quality of signal received, where inaccuracies depend on the parts of the Fourier spectrum. The researchers represent a new methodology to find out the COM motion through trustworthy frequency range and kinematic measurements of the body which therefore resulted in the establishment of COM trajectory.

2.5 Robot and MV

This section describes the detailed literature available for dealing with regular and irregular objects by image processing technique using Serial Robot.

Sang [29] research shows that, the orientation of the camera relative to the platform can be solved using 3 pure translational motions. If the intrinsic parameters are unknown, then two sequences of motion, each consisting of three orthogonal translations, are necessary to determine the camera orientation and intrinsic parameters. Once the camera orientation and intrinsic parameters are determined, the position of the camera relative to the platform can be computed from an arbitrary non-translational motion of the platform. Harada [30] validates the object placement manner for pick and place of Robot. He suggested a polygon model of the environment which has been established by the conversion of point cloud. The tests are taken out in three categories as convexity test, contact test and stability test. Museros et al. [31] illustrates the 2-D matching of qualitative shapes for the assembly of mosaic designing industry. The research explains the shape recognition of 2-D objects and their usage in the industry of ceramic designing and manufacturing. The theory depends on the qualitative characteristics of objects such as angles, relative lengths, concavity, complexity and curvature. However, it further deals with the matching of various shapes whether they are regular or irregular polygonal objects or closed curvilinear shapes.

A research conducted in 2016 [32] focuses on Object sorting by Robotic Arm using Image Processing that fulfills the requirement of efficient production by speeding up the manufacturing process. In the research, Computer vision is carried out with assistance of open CV software and articulated Robotic arm. The system is based on MCU (Microcontroller). With the help of programming, different Algorithms are carried out which enables the Robotic arm to either sort the objects based on faults like missing holes, irregularity in shapes or other faults. This work is based on the study for automation of container unloading at Elgiganten's Central warehouse in 2012 [33]. Here, container unloading is accomplished by Robotic palletising. The vital topic of the research is to effectively increase the automation of distribution centres and warehouses. This involves the evaluation of a software named Palletising Power Pac, which is specially made to deal with palletising procedures. For the large variety of cartons present at Elgiganten, a suitable gripper has been selected and by practically using it, it has been found that cartons

which are 60 mm or less in length and weighs less than 30 kg are more accurately carried out by the gripper. Control configuration of newly developed Robotized palletiser which runs on a graphical application through HMI (Human Machine Interface) touch screens. PLC (Programmable Logic Controller) program and Servo system parameterisation were used to reconfigure Robotic palletiser function to make it capable for high speed mechanical applications. In the past, Robotic palletising was carried out with many limitations like long cycle times between pick/place actions. These Robots had the requirement to decrease the manipulation speed because the inertia makes product retention in the gripper that creates difficulties during the acceleration/deacceleration, and human involvement was compulsory to place the objects before Robot grips them. To resolve these issues, a project was developed that is a combination of HMI design and PLC programming, continuous infeed of Robot design, design of Robot gripper and servo motors, which are used to perform fast and accurate machine automation. The research has successfully achieved to design and built a Robotic Palletiser which achieved palletising speeds comparable to dedicated mechanical palletiser and have also successfully maintained high flexibility, short set up times and ease of operation [34].

An introduction of using various image processing methods on a Raspberry Pi Platform by employing SIMULINK and MATLAB was introduced in [35]. The real-time image processing is achieved by developing a cheap framework, which includes all feature extractions of objects and image transformations methods. MV is the most expensive and crucial part in mobile Robot systems, which has become highly inconvenient to be used by researchers and students. Therefore, a cheap and universal mobile Robotic platform was created, named Cube. The horizontal dimensions of cube are approx. 150 mm. A small cube shaped Robot was created by using a low cost 3-D printer equipped with Raspberry Pi 2 platform. The native camera boards are also used for visibility by combined visible and IR (Infrared Radiation) light. Now, for image detection methods, the researchers decided to implement various geometric based feature detection ways which are very commonly used in environment detection and object recognition. To achieve this task, three Algorithms for edge, corner and line detections have been selected and discussed. The implementations of these Algorithms are done in SIMULINK and performance are measured in Raspberry Pi 2 platform. The researchers have used Edge detection by Sobel Operator, Corner detection by Harris Operator and

Line detection by Hough Transform. Models for each kind of detection are accomplished in SIMULINK and at a testing stage each model is connected to Raspberry Pi 2 platform by an Ethernet cable. It has experimented on various frames and as a result it was found that measured FPS (Frames Per Second) values is quite good and Raspberry Pi 2 platform is very handy for normal Robotic tasks where optimization via the SIMULINK schemes and target code (C/C++) are carried out.

Xu et al. [36] introduced a contemporary methodology for the computer-aided reassembling of the polygon imaging fragments. This is supposedly a faster reassembly methodology for ranges of polygons. Polygon image fragments have a settled category of having corners, which is taken and detected through the Hough transformation and fuzzy reasoning methodology. This method evaluates the value for each side, compare the lengths and determine the sides that are equal to the length in the different fragments that are being considered a part of the method. An effective and efficient result has been delivered with the help of the methodology in [36]. Meng et al. [37] developed a contemporary approach for the camera-inclusive Robot manipulators. This approach provides a self-calibration of the manipulator where the Robot develops a complete system of measurement of its geometric parameters without an inclusion of external measurements. This led to the evaluation of the rotational parameters along with a complete set of translational properties without any input. With a settled measurement factor along with a measured trajectory, the poses are measured for the set of such values without any constraint along with the scale factors. With different view angles, scale factor was evaluated.

Vischer et al. [38] dealt with the kinematic calibration of a Delta Robot. For this, two methods of calibration were devised. The differences of all the mechanical parts in the Robot except for the spherical joints which are supposedly considered to be ideal is the first technique of evaluation. Furthermore, the second method accounts for the deviations that have an effect over the position of the end-effector, yet its orientation remains same where it is assumed for the model that the spatial parallelogram is constant. The set-up then helps figure out all the parameters with respect to the base.

2.6 Camera and MV

MV equipment's are used to perform complicated and tough tasks by replacing human vision during the automatic processes where Robots and CNC machines are supposed to work unsupervised. They are used to make the existing Robotic parts smarter and plays major role in moving forward one step to the unmanned factory of the future. Following are the few companies that enable industrial Robots to see:

Aquifi merge 3D Data and 3D deep learning with 3D sensors to create low cost and high-performance 3D fluid vision that helps devices to solve the obstacles in industrial automation, logistics, quality control and inspection. Aquifi is famous for their mobile hand-held 3D vision sensors.

Industrial Vision is known for producing MV cameras, equipment for the production sector to bring the improvements in the quality and delivery of superior products to customers. Industrial vision helps to reduce the defected products and increase the production speed.

Pick-It 3D is known for easy installing MV solution that guides Robots to pick and place wide range of products in different applications. There 3-D camera spots the dimensions and position of products. That is why the performance of the Robotic gripping system enhances by absorbing the irregularities of the environment.

Daitron has a wide and diverse collection of cameras including medical cameras, MV cameras, security cameras and others. They have several diverse options such as high-speed Analog cameras, HDMI (High Definition Multimedia Interface) and high-resolution cameras with colour progressive output.

HTE Automation's offers wide selection of MV solutions such as vision sensors, MV cameras and ID readers. There industrial vision systems are used to actively and rapidly spot defective parts and verify assembling of products in automated manufacturing. They also help for installation, system design assistance, training, maintenance and support.

The most critical part of achieving the desired imaging performance of high-speed MV imaging application is to find and select right camera interface. It can be difficult to find and select the right interface because there are so many interfaces are available. USB (Universal Serial Bus) 3.2, Camera Link HS, Thunderbolt3. 10 Gigabit Ethernet and Coax press 2.0 are all the most common interfaces of high-speed applications. The performance and potential of each camera interface differ from each other.

Following are the few pros and cons of each high-speed camera interface:

USB 3.2: The adoption of this camera interface is limited because of short cable length. If the camera needs to be hard wired, this interface cannot be used due to its quality over length and high cost. However, it is beneficial because it is 2 times faster than USB 3.1 provided that the long length is not the basic requirement.

Camera Link HS: The camera interface come with several cable options and it features error correction for reliability, but at same point the speed of this camera interface decreases as the length of the cable increases somehow like USB 3.2.

Thunderbolt3: This interface is used for the transfer of extremely high speed of 40 Gigabit/second. Its major drawback is its length that is of 0.5 meters for passive copper cables.

10 Gigabit Ethernet: These interfaces are perfect for industrial applications because of their long cables and reliable transfer. However, low throughput limits their ability in many high-speed applications.

CoaXpress 2.0: This camera interface gives permission for 4K60 video through a single cable with triggering rates over 500 KHz (Kilohertz), but it is expensive, and it needs a frame grabber.

The MV system contains camera, computer, sensor and software whereas, there is another important component named “the frame grabber board” as shown in Figure 2.3. The Frame Grabber needs some attention in MV applications. The frame grabber board plugs into a computer and connects one or more cameras to the computer. Frame grabber board is also known as frame grabber and it is available in several varieties. MV software process when frame grabber transforms Analog signals into digital information. This board plays an important role in ensuring a MV system receives quality data.

For obtaining image data, this board also provides some other input and output functions such as communicating with PLCs, triggering of camera and turning lights on and off. Its main function is to transform an image into digital data.

Monochrome cameras are used in most of the area and their main function is to use with MV applications. The Analog NTSC (National Television System Committee) signals are put into it by those applications to connect frame grabber directly. Extraneous information is filtered out by using frame grabber so that it can easily separate video signals from timing signals, one of those timing signals is also known as horizontal sync. Their main function is to work with Phase locked loop. An accurate pixel clock is on board and recreated by phase locked loop. An accurate pixel clock connects with frame grabber’s operations and with the video data that is receiving from the camera. This clock further explains the digitization of the video portion when grabber’s Analog to digital function is converted. To get the correct timing for ADC (Analog to Digital Converter) the circuit can setup for special type of camera. Digital value is created by every Analog to digital conversion in the received image.



Figure 2.3 Frame Grabber used in MV application

Imaging devices and image sensor in Figure 2.4 are used in the camera to capture images. In most of the imaging devices, light enters from an aperture from one end of the imaging device after that it passes through an optical element such as lens and finally it transfers to an image sensor. In typical imaging devices, there are more than one layers of optical elements are placed between the image sensor and opening (aperture) to focus light onto the image sensor. Image sensor contains pixels that transmits signals when light enters through an optical element. It is amazing thing to know that image sensors have array of pixels, there are millions of them. It can also be measured that how much light enters each pixel and transmit the data to every pixel thousands of time per second. There data rates are huge. Image sensor contains one or more ADCs, which helps the photonic charge during the exposure period and transforms it into a number from 0 to maximum. Every pixel is read by ADC in sequence and then it sends the reading out to the serial data connection. Now it depends upon the application that how to utilize this data. The silicon chip can be designed or have another common approach known as FPGA, which is ideal for doing several things, such as getting all high-speed serial connections, and collecting them back in to recognizable 2D data map like Xilinx FPGA.

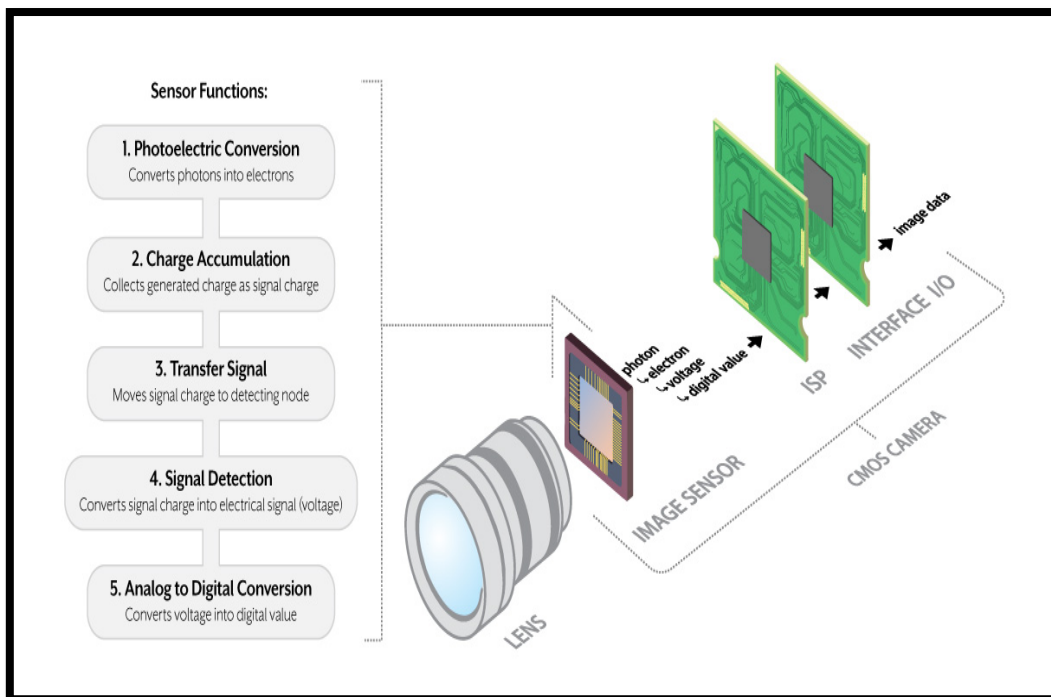


Figure 2.4 CMOS Camera Function

2.7 CPU, GPU and FPGA based Accelerating Hardware

Systems of image processing that are embedded with FPGA provide computing resources, but it comes with challenges in comparison to the systems of software. FPGA-based IPPro (Image Processing Processor) gives information on the programming of data flow. When this concept is applied in a k-means-clustering operation's application by the recognition of a traffic sign application several dataflows that are parallel with their mapping options were identified that speed-up 8 times. Because the k-means-clustering uses 16 processor cores, and a speed increase of 9.6 times for the filter morphology operation application of the recognition of traffic sign using 16 processors cores in comparison to software ARM. In k-means-clustering, the 16 processor cores implementation is 57, 28 and 1.7 x times more efficient in as compared to CPU [39].

In applications of real-time image processing its use in inspection of defects like scratches, dents, wrinkles on the metallic surface and moving cylindrical objects, the images are used to inspect the faults in real-time by the image processing technique using the CPUs and GPUs. A multicore CPU and GPU are used to implement the thresholding of military objects using about 8 real images. CPU showed that by increasing the size of the chunk, decreases approximately four times of the execution time in comparison with serial computing. while when speed up serial computing implementation results were compared. It showed that a GPU has a large capacity to enhance the performance of real-time applications [40]. Various benchmarks of the vision kernels run-time performance and the energy efficiency of kernels experiment on the embedded platforms like CPU, FPGA and GPU. The trend from simple to complex kernels illustrates the FPGA and CPU performance in contrast to the CPU, improves as the complexity of kernel increases. For simple kernels like the processing input and the image arithmetic, the GPU demonstrate the increased performance and efficiency in energy, while for more complex kernels such as the image filters, analysis and transform geometric, the FPGA shows the enhanced performance and the energy efficiency. As the nature of the kernel complexity of ascends, the FPGA shows more efficiency in energy than the CPU and GPU. This occurs because of more complicated Algorithms occupy more of the resources naturally on the logics that are programmed [41].

FPGAs have demonstrated high performance despite their low and less operational frequency in image processing that comes from high parallelism, Height ratio

operations of 8 bit and internal memory banks. When the performance of the processor is compared with that of FPGA, SIMD (Single Instruction, Multiple Data) and multicore processors using image processing simple problems like 2-D filters, k-means clustering and stereo vision the performance of FPGA are limited and restricted by size and the bandwidth memory. So, twice the performance is required twice memory throughput. The performance of quad cores processors is very much faster for real-time processing like above 30 FPS, when the size of the image is smaller. FPGA is needed for practical real-time applications [42].

Image processing requires more time to perform the image convolution when filtering is conducted on CPU because of the high image filtering computation demand. GPU is a good way to accelerate image processing in contrast to CPU. It can be concluded that GPU is more appropriate convenient embedded platform for processing large data parallel load of high-density computing, through experimentation and analysis. The execution on GPU can get a 61% speedup in comparison to CPU with the filtering implementation. CUDA (Compute Unified Device Architecture) programming on GPU performs image filtering and processing more efficiently. This is because of the reason that the computations are conducted at the same time in parallel by fully utilizing the available processing resources so that speedup can be increased [43]. GPU has the spark for acquiring the same performance as with the FPGA embedded platform in processing of image. Considering the lower operating frequency of GPU, and the parallelism in FPGA, this seems to be a natural result. The performance of CPU is less than FPGA, which represents that that CPU with its quad-cores can executes about 1/10 of FPGA operations in a unit time with the execution of the same Algorithm. The FPGA performance is restricted by the FPGA size and bandwidth memory. The latest and larger FPGA board can possibly give double performance by processing double image pixels numbers during image processing in parallel. [44]. CPU are for sequential processing which means that they do not support parallelism and are limited in their capabilities for conducting high-speed processing. FPGA also has challenges like complex programming. FPGAs work well in parallel in contrast to CPU and tend to be more energy efficient.

2.8 CUDA Programming and Image Processing

CUDA is a parallel computing platform and programming model developed by NVIDIA for general computing on GPU. With CUDA, developers can dramatically speed up computing applications by harnessing the power of GPUs. In GPU-accelerated applications, the sequential part of the workload runs on the CPU which is optimized for single-threaded performance while the compute intensive portion of the application runs on thousands of GPU cores in parallel. When using CUDA, developers' program in popular languages such as C, C++, Fortran, Python and MATLAB and express parallelism through extensions in the form of a few basic keywords.

The stream processing required more specific CUDA cores as compare to CPU which are more generalized that is why more CUDA cores can be fit onto a GPU. CUDA's provide GPU to work for more generalized works like video encoding process, or even video acceleration for decoding by using hardware. GPU clocks and memory bandwidth are required for gaming as CUDA provide massive power for computing. CUDA is useful for parallel Algorithms, good for number crunching and well for large datasets. CUDA is meant to run on NVIDIA's card but it can also run on any CPU. GPU can accelerate many video decoding processes [45]. There are many factors on which the GPU image processing acceleration depends that may include the Algorithm for the optimization, properties of the image, format of an image, the hardware used and the parameters of filters. That is why the performance is different and unpredictable in all systems. New GPU offers many features like managing the capabilities of the hardware, synchronization of the data, GLSL and CUDA support, benchmarking and the mechanism for switching the various set of operators for image acceleration with GPU. It is a dynamic mechanism that determines the efficacy of GPU in implementation and reducing its use penalties in image process acceleration [46]. GPU are SMID device that is data-parallel inherently. By utilizing CUDA, the Algorithm computation of image processing can be accelerated. Computer vision Algorithms map in applications of RGB (Red Green Blue) to grey transformation, morphological applications and integral images are ready to CUDA with significant gain its performance. Specifically, the efficiency of optimization and parallelization of image processing, morphology applications and image integral. Different computational applications have different needs that can carter with GPU like the stimulation of simple image processing, the adaptation of GPU in morphological

Algorithm and in integral images. The speedup can be achieved with GPU in image acceleration in its processing [47].

GPU with CUDA for images with small pixels can obtain a 30 Hz frame rate that represents the Algorithm utilization in processing real-time video processing. Using GPU parallel architecture, the processing times obtained are sufficient for their real-time application. Images of larger pixels, the Algorithm can be demonstrated for processing procedures in real-time and of the image size of much larger pixel area far closer to applications in real-time. The Algorithm has been used to adjust the parallel architecture of GPU. Algorithm performs better for larger segments than for small segments of the image. The segmentation of colour also works better for regions with large uniform areas in image. In the case of textured areas of the image, the performance of Algorithm declines as compared to smaller regions, because of the neighbouring pixels greyscale similarity, which is very low [48]. The image processing can be accelerated by interfacing MATLAB with CUDA in parallelizing the larger portion of MATLAB white balance code in the image processing. The obtained results indicate that the acceleration is proportional to the size of image size until a maximum at 2056 x 3088 pixels and beyond these values the acceleration decreases. The performance with GPU enhances above a factor of 14~15 as compared with CPU. The demonstration of a mixed programming concept by the integration of MATLAB with CUDA is done by replacing the parts of the Algorithms running in MATLAB CPU which are time consuming and porting them to GPU. In this way, the programming features of MATLAB white balance implementation can be achieved by load balance between CPUs and GPUs. It is based on an accurate prediction of execution codes, profiling those codes in the CPU and GPU [49].

The programming of CUDA provides parallelism by writing simple code C that runs in thousands of threads of parallel, which are managed by demonstrating parallel works as kernels that is the sequence of tasks to be executed in every thread, mapped over the threads to be a target. The data to be processed by the GPU are transferred to the memory of the graphic board. Data transfer is persistently present until they are de-allocated, in this way it remains available for next kernels. The C-CUDA technologies have been made available for various applications of image and video processing for example image segmentation, edge detection for video segments and coding, that have been ported to CUDA. The computing in the GPU field is demonstrated in various applications in

different domains. The survey of CUDA based principles for image processing and video processing in multiple areas have been shown as to how many applications in these domains have been parallelized using CUDA, to achieve very high performance in terms of processing time meanwhile keeping the accuracy performance same [50]. GPU acceleration in operations of image processing, for example, the filtering, estimation of histogram estimation, distance and the interpolation transforms. These are the most used Algorithms in medical imaging field areas of image registration, denoising and segmentation. The Algorithms that are specific to single computing programs such as Ultrasound, Microscopy and Optical Imaging [51].

Various Algorithms of image processing have been coded CUDA for Pure Data such as RGB to grayscale transformation, thresholds, convolution, etc. It was of opinion that in order to get the full potential of the GPU, there are several procedures that are to be processed or the calculations are to be made complicated. Thus, when using the Algorithm on four or more function blocks the gain in computation time is real. For the first time program, efforts will be provided for developments of new CUDA blocks, including a “PIX_DRAW_CUDA” function. The purpose of it is to display processing results directly from the GPU, avoiding the transfer from GPU to CPU. This will improve performance in image processing [52]. Parallel processing of image techniques on GPU framework using the CUDA and the parallelism in medical image processing techniques have been well established. The main reason behind the image morphological applications and the importance of extracting image components that are useful in describing the region of image shape. Such experiments have been improvised on CUDA and its programming use in a highly parallel GPU architecture. The Algorithm for a morphological operation like the dilation and erosion got consequences with the effective use of the CUDA on the framework of GPU. The performance increase varies with the image’s dimensions and sizes, more performance gain is achieved with a bigger image size with larger cores in CUDA [53]. In investigating the merits and potential of the bottlenecks of using the best and perfect Algorithm, the most prominent distortion on GPU recommends that an understanding of the GPU and CPU embedded platforms, combined with detailed knowledge of the Algorithm. This can cause speed-ups without affecting the accuracy of prediction. Either single or a multi GPU implementation represents speedup, over the implementations of CPU. A bottleneck investigation illustrates the highest run time for

kernels and reasons for the high runtimes of these program optimizations like blocking that map to the memory of CPU may not be well to direct the memory of GPU's. However, computing CUDA is easy to handle and is powerful in serving the purpose in general for the programming of GPU for accelerating image processes [54].

Commonly used Image Processing boards and kits from Xilinx are as follows:

- Spartan-6 FPGA Embedded kit
- Xilinx Kintex UltraScale FPGA KCU1500 Acceleration Development Kit
- Xilinx Virtex UltraScale FPGA VCU110 Development Kit
- Virtex-6 FPGA Broadcast Connectivity Kit
- Xilinx Kintex UltraScale FPGA KCU105 Evaluation Kit
- Xilinx Kintex UltraScale FPGA KCU1250 Characterization Kit
- Xilinx Kintex UltraScale FPGA KCU1500 Acceleration Development Kit
- Xilinx Kintex UltraScale+ FPGA KCU116 Evaluation Kit
- Xilinx Virtex UltraScale FPGA VCU108 Evaluation Kit
- Xilinx Virtex UltraScale FPGA VCU110 Development Kit
- Xilinx Virtex UltraScale FPGA VCU1287 Characterization Kit
- Xilinx Virtex UltraScale+ FPGA VCU118 Evaluation Kit

2.9 Shortcomings in the Literature Survey and Contributions from this Research Work

Robots have been used in pick and place objects for many years. These Robots can deal with different types of shapes like (Novel objects, 3D objects and Irregular objects) in the industries using MV. The grasping of different objects required the different Robot end effectors and Algorithm to act on. Currently the Robots can catch the 3D object in the air, grasping the objects from clutter environment as well as working in the kitchens to palatize the plates and dishes. The Robots are also dealing with irregular objects by grasping them from the conveyor of different shapes and size. The different types of end effector are being developed to deal with such objects. However, these end effectors have a huge limitation with respect to the variations in the object. The research unlocks the freedom to absorb a high level of variations in the object dimensions. The main contribution is to palletise such objects, which have high variation in geometrical shape and size. These objects can be completely different from each other. The Algorithm is

developed to collect the raw data from the environment about the object location, size and shape. These objects may have sharp edges, perforation more than 50% and the centroid is not located on the object. The MV system develops a point-based trajectory to find the best available spots to grasp it. This can be further elaborated using the example of a geometrical shape star with a hole in the centre. Such scenarios where the centroid is not on the object due to perforation and it has sharp edges has not been researched yet. This Algorithm is capable to deliver the best possible locations in the form of point-based trajectory to grasp the objects by the Robot. The formulation will avoid the centre because there is no material and it will not be close to the sharp edge, so the end effector is unable to pick it. Further, contribution in the research is made during the research internship by the practical application of MV system for the generation of bonding points on the medical devices.

2.10 Summary

This chapter summarises the work which have been developed in academic research and industries showcasing the role and importance of MV applications in irregular polygons. The challenges involved in MV technology and contextual studies from the literature are studied. Understanding the industrial case studies of MV in the field of irregular shapes have been explored in detail. It describes the use of hardware for the testing of MV Algorithms in real time that includes CPU, GPU and FPGA along with the comparison between them in terms of data processing speed and applications. These boards are tailored for MV applications, even most are just plug and play. Once the image processing simulation is completed on the MATLAB software, this hardware can be deployed in seconds for the validation of the Algorithm in real environment. Some discussion about the CUDA programming for GPUs is also covered in detail. Few highlights on the camera structure, frame grabber and their application interface has been explored. This chapter also described global survey on the MV availability, growth and necessity to integrate with Robots. A summary of the different methodologies used in the literature survey and contribution from the research has also been showcased in this chapter. Furthermore, the insight to the modelling of point-based trajectory using the software packages like MATLAB are presented in detail in Chapter 4.

Chapter 3

Chapter # 3 Irregular Polygons Feature Extraction by Analytical and Numerical Method

- 3.1 Introduction
- 3.2 Shape Description and Feature
- 3.3 Analytical Method Formulation
- 3.4 Numerical Method Algorithm
- 3.5 Summary

3.1 Introduction

This chapter gives an insight into feature extraction by MV using MATLAB. It also illuminates how the analytical methods formulae and numerical methods Algorithm deals with different irregular polygons. A shape can be defined using different methods and it has more than 25 features to understand the geometrical characteristics of any shape. It is very important to know each feature of the shape before proceeding to the trajectory development. Furthermore, a shape is of infinite type because it is anything that can be drawn on a paper in a closed loop. Despite formulation of each shape is impossible, still there are many different analytical methods available to explain much details about the shape that can be used to prepare the object for further processing. Since, numerical methods work differently because almost any shape can be defined numerically, and it is independent of shape provided in a closed loop. Different MATLAB Algorithms are used and explained in detail to understand complex shape and their features even if they are not possible analytically. Thus, these methods would not only have a substantial impact on the industrial palatizing of irregular shapes however, it also provides detail information to Robot controller to enhance the dynamic stability for grasping the shapes.

3.2 Shape Descriptor and Feature

The understanding of items in multimedia content is a difficult task and requires a mixture of various fundamental visual and sound features by means of an information-based inferring process. Ordinarily, visual features which give reciprocal data, for example, shape, shading and surface are chosen. The shape is obviously a significant prompt for understanding, since people can normally perceive trademark queries exclusively based on their shapes. Normal criteria utilized for shape portrayal for dependable shape coordinating includes uniqueness, invariance to interpretation, scale, axis and symmetric changes, adaptability, minimization, extraction and coordinating effectiveness and strength to various types of expressions. Indeed, even because of 2-D outlines, there can be two ideas of similarity. Items having comparative 3-D, can have altogether different blueprint shapes and the other way around. A shape descriptor exemplifies the shape properties of the object's blueprint (outline). It ought to recognize shapes that have comparable shape properties. Such descriptors are exceptionally productive in applications where high intraclass fluctuation in the shape is normal, because of distortions in the item (inflexible or nonrigid) or axis disfigurements. The most

notable object measurements are based on depicting the shape. Shape measurements are known as physical dimensional measurement of a shape which shows the closeness of an object. The main purpose here is to use the least diffusely method to measures object. The nature of any shape measurements is based on the idea of the picture and how well objects are pre-processed. Those objects which are low in quality, for instance, little gaps, noise or commotion can bring poor measurement results which can cause misleading measurements. The term pose is basically known to describe the insinuate area, direction and size. Shape feature extraction is described as the deliberate investigation of geometric shapes, for example using a computer to examine the relatively shaped objects in a database or areas that fit together. In order to normally distinct a computer program need to process geometric shapes; the objects must be taken into consideration with a definite structure. Usually a point of internment picture is utilized to represent the object with its boundaries. Nevertheless, other volume-based depictions or point based representations are used to address the shape. At the point when the objects are already provided, either by illustration or by means of 3-D scanner they should be enhanced before a connection can be established. The unrevealed representation is known as the “shape descriptor”. These depictions are aimed to provide most of the huge information at the same time being easier to manage, to store for later use and to consider the shapes genuinely. The shape descriptor is a representation which can be used to systematically reproduce the main object.

Shape descriptors speak to unequivocal characteristics as for the geometry of a feature. All things considered, shape descriptors or shape features are a few courses of action of numbers that are conveyed to portray a given shape. The shape may not be totally reconstructed from the descriptors. Be that as it may, the descriptors for different shapes should be adequately various that the shapes can be isolated. Shape features can be portrayed into two kinds, area features and boundary features. Shape descriptors can be grouped by their invariance as for the changes permitted in the related shape definition. Numerous descriptors are invariant concerning congruency, implying that harmonious (shapes that could be deciphered, spun and reflected) will have a similar descriptor (for instance minute or round symphonies-based descriptors or Procrustes examination working on point mists). Another class of shape descriptor called “natural shape descriptors” is invariant as for isometry. These descriptors do not change with various

isometric embeddings of the shape. Their favourable position is that they can be connected pleasantly to deformable objects (for example an individual in various body stances) as this misshapeness do not include much extending yet are close isometric. Such descriptors are regularly founded on geodesic separations measures along with the outside of an object or on other isometry invariant attributes, for example, the Laplace-Beltrami range. There are other shape descriptors, for example, diagram-based descriptors like the average axis or the Reeb chart that catch geometric or potentially topological data and rearrange the shape portrayal. However, it cannot be as effectively analysed as descriptors that deal with shape as a vector of numbers. From this exchange, it turns out to be clear, that distinctive shape descriptors target of various parts of shape can be utilized for an application. In this way, contingent upon the application, it is important to dissect how well a descriptor catches the features of intrigue.

3.3 Analytical Method Formulation

Analytical methods are defined as the set of techniques that allow us to know quantitatively the composition of any shape. There are twenty-five features that are explained in detail to define irregular shapes. Following are the common measurements of a shape.

1. Area
2. Perimeter
3. Major and Minor Axis Length and Angle
4. Compactness
5. Elongation
6. Eccentricity
7. Circularity
8. Sphericity
9. Convexity
10. Convex Hull
11. Solidity
12. Rectangularity
13. Bounding Box
14. Shape Variance
15. Curvature

-
16. Bending Energy
 17. Total Absolute Curvature
 18. Spatial Moment
 19. Central Moment
 20. Normalized Central Moment
 21. Moment Invariant
 22. Radial Distance Measure
 23. Signature Analysis
 24. Fourier Descriptor
 25. Hough Transform

Area

The area can be characterized as the space occupied by an object or the outside surface of an item. The area of a figure is the number of unit squares that spread the outside of a figure. The area is projected in square units, for example, square centimetres, square feet, square inches and so on. The area is defined as the total space which comes in the boundary of a flat or 2-D object, for example, a triangle or circle, or the total covered area of a 3-D object. It can also be defined as the number of pixels in shape. The source of the word area is from 'area' in Latin, which means an empty level ground. The inception further prompted an irregular deduction of the area as a specific measure of room contained inside a set of a boundary. The floor area of a room is measured on daily basis to decide the size of the rug to be purchased, covering the floor with tiles, covering the wall with paint etc. All things considered, only one out of every simple plane figure can be distinguished as a square shape or a triangle. Surface Area is the area of the outside surface of a 3-D object. For example, a rectangular crystal has six rectangular bases. In this way, the entire surface area is known as the sum of the areas of all the 6 square shapes.

Perimeter

The perimeter is known as the boundary around a 2-D shape. Other definition of perimeter says that the span of the sum of pixels around the boundary of the object is called perimeter. The word perimeter implies a way that encompasses an area. It originates from the Greek word ‘peri’, which means around and ‘metron’, which means measure. In science, the perimeter alludes to the all-out length of the sides or edges of a polygon, a 2-D figure with edges. When portraying the estimation around a circle, it utilizes the word periphery, which is basically the perimeter of a circle. There are numerous reasonable applications for finding the perimeter of an item. Realizing how to discover the perimeter is helpful for finding the length of fence expected to encompass a yard or garden. Additionally, knowing the perimeter, or outline, of a wheel will explain that how far it will move through one revolution. The fundamental formula for finding the perimeter is simply to include the lengths of the considerable number of sides together. In any case, there are some specific equations that can make it simpler, contingent upon the shape of the figure. The perimeter of the convex hull that encloses the object is called the convex perimeter can be calculated using equation (3.1).

$$\text{perimeter} = \sum_{i=1}^{N-1} d_i = \sum_{i=1}^{N-1} |x_i - x_{i+1}| \quad (3.1)$$

Perimeter is significant term in mathematics. This applies to any shape of the field, irregular or normal. The perimeter is the boundary around the object. For instance, a home has a fenced yard. The perimeter is the length of the fence. On the off chance that the yard is 50 ft × 50 ft, so the fence is 200 ft in length.

Major and Minor Axis, Length and Angle

The major axis is known as the endpoints x and y of the lengthiest line which can be drawn over the object. The major axis endpoints x1, y1 and x2, y2 are created by gauging the pixel boundary between each of the boundary pixels in the measured object limit and then gauging the sum with the length. The major-axis length of an object is the pixel boundary between the major-axis endpoints is stated in equation (3.2).

$$\text{major - axis length} = \sqrt{(x_2 - x_1)^2 + (y_2 - y_1)^2} \quad (3.2)$$

The outcome is proportion to length. The major-axis point can be defined as the edge point between the major-axis and the x-axis of the measured object equation (3.3).

$$\text{major - axis angle} = \tan^{-1}\left(\frac{y_2 - y_1}{x_2 - x_1}\right) \quad (3.3)$$

The minor-axis length of an item is the pixel boundary among the minor-axis endpoints is stated in equation (3.4).

$$\text{minor - axis length} = \sqrt{(x_2 - x_1)^2 + (y_2 - y_1)^2} \quad (3.4)$$

The major and minor axes of a circle are distances across the round shape. The major axis is the longest width and the minor axis the briefest. If they are equivalent long, at that point the oval is a circle. Every axis is the opposite bisector of the other. That is, every axis cuts the other into halves and every axis crosses the other at right points.

Compactness

The compactness measure of a shape is a number that tells about how much shape is minimal. Compactness is described in equation (3.5) as the percentage of the object's area to its perimeter's area.

$$\text{Compactness} = \frac{4\pi \cdot \text{area}}{(\text{Perimeter})^2} \quad (3.5)$$

Objects with complex or irregular shapes have low compactness rather than smooth ones. For a circular shape, its maximum value is 1.

Alternate formula in equation (3.6) for the calculation of compactness is:

$$\text{Compactness} = \frac{(\text{Perimeter})^2}{4\pi \cdot \text{area}} \quad (3.6)$$

Objects with complex or irregular shapes have more compactness rather than smooth ones. For a circular shape, its minimum value is 1.

The importance of "compactness" here is not identified with the topological idea of minimized space. Different compactness measures are utilized. Notwithstanding, these measures share the accompanying for all intents and purpose, they are relevant to every geometric shape. They are autonomous of scale, direction and dimensionless numbers. Compactness is not excessively subject to a couple of outrageous focuses on the shape. It concurs with natural ideas of what makes a shape smaller. Typical utilization of

compactness measures is in redistricting. The objective is to amplify the compactness of appointive regions, subject to different requirements and accordingly to evade gerrymandering. Another utilization is in zoning, to manage the way wherein land can be subdivided into structure lots. Another utilization is in example characterization extends with the goal that it can group from different shapes.

Elongation

Shape elongation is one of the fundamental shape descriptors that has an exceptionally clear natural importance. That is the explanation behind its pertinence fit as a fiddle order undertaking. In its least complex structure elongation is the proportion among the object bounding box's width and length as shown in equation (3.7):

$$\text{Elongation} = \frac{\text{Width bounding-box}}{\text{Length bounding-box}} \quad (3.7)$$

The calculated value by this formula is some place in the scope of 0 and 1. If the proportion is equal to 1, the object is commonly square or circular shaped same as Figure 3.1. As the proportion value decreases from 1, the object ends up being increasingly stretched.

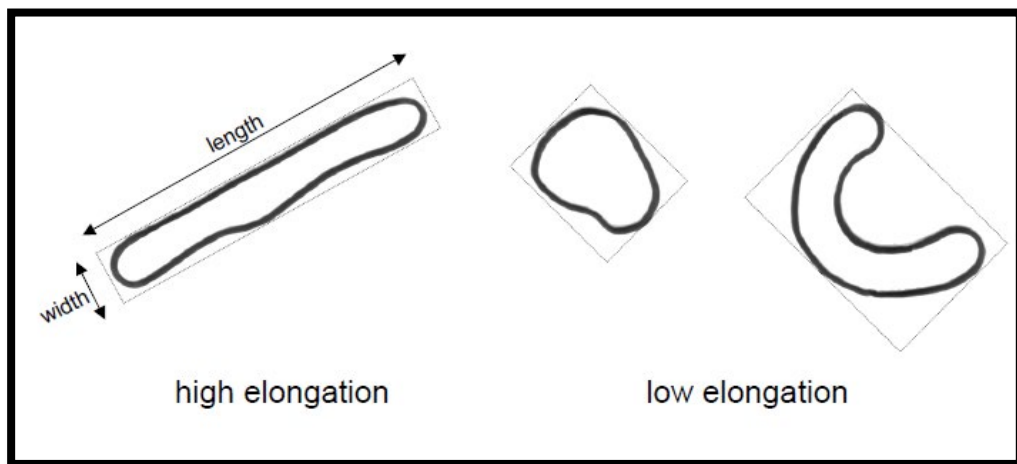


Figure 3.1 High and Low Elongation

Eccentricity

Eccentricity (also known as ellipticity) is the proportion of the length of the short axis length to the long axis length of an object formulated in equation (3.8).

$$\text{Eccentricity} = \frac{\text{axis length}_{short}}{\text{axis length}_{long}} \quad (3.8)$$

The outcome is a degree of object eccentricity which is provided as a value somewhere in the range between 0 and 1.

Alternative formula for eccentricity in equation (3.9) is as follows:

$$\text{Eccentricity} = \frac{(\mu_{02} - \mu_{20})^2 + 4\mu_{11}}{\text{area}} \quad (3.9)$$

A wide range of conic segments arranged with expanding eccentricity to note that ebb and flow diminish with eccentricity and none of these bends converge. In science, the eccentricity of a conic area is a non-negative genuine number that particularly portrays its shape. More formally two conic areas are comparative if and just on the off chance that they have a similar whimsy. One can think about the flightiness as a measure of how much a conic segment veers off from being roundabout. Specifically, the unpredictability of a circle is zero. The eccentricity of an oval as shown in Figure 3.2 which is not a circle is higher than zero, however under 1. The eccentricity of a parabola is 1 and of a hyperbola is much higher than 1.

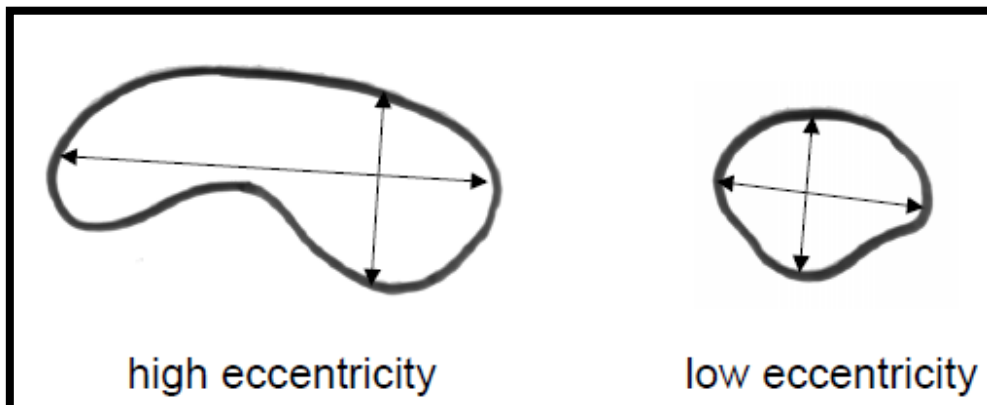


Figure 3. 2 High and Low Eccentricity

Circularity

Circularity is valuable to as it is used to measures the convexity or roundness of an object (3.10). Roundness or circularity which circumvents its nearby irregularities is the ratio of the area of an object to the area of a circle with the corresponding convex perimeter.

$$\text{Roundness} = \frac{4\pi \cdot \text{area}}{(\text{convex perimeter})^2} \quad (3.10)$$

This measurement rises from 1 for an indirect object and lower than 1 for an object that goes incorrect from circularity. The circularity picture is used to depict how close an object should be to an authentic circle. Now and again called roundness, circularity is a 2-D obstruction that controls the general kind of a circle promising it is not exorbitantly curved, square, or out of round. Roundness is self-governing of any datum feature and simply is for each situation not actually the expansiveness dimensional opposition of the part. Circularity fundamentally makes a cross section of a cylinder shaped or round feature and chooses whether the float confined in that cross portion is round.

Sphericity

Sphericity is the measure of how intently the shape of an object approaches the shape of a circle. For instance, the sphericity of the balls inside a metal roller decides the nature of the bearing, for example, the heap it can hold up under or the speed at which it can turn without falling flat. Sphericity is a case of a minimization measure of shape. Characterized the sphericity, of a molecule is the ratio of the surface area of a circle (with a similar volume as the offered molecule) to the surface area of the molecule. Up to what extent an object approaches the shape of a "circle" is sphericity. For a circle, the highest is the limit of 1.0. Sphericity can be calculated using equation (3.11).

$$\text{Sphericity} = \frac{R_{\text{inscribing}}}{R_{\text{circumscribing}}} \quad (3.11)$$

Convexity

Convexity is known to describe the extent an object which varies from a convex object (3.12). Usually the measure of convexity which can be gotten by enclosing the ratio of the border of an object's convex body to the border of the object itself. While this

will take the approximation of 1 for a convex object and on the other hand it will be under 1 if the object is not convex.

$$\text{Convexity} = \frac{\text{convex perimeter}}{\text{perimeter}} \quad (3.12)$$

To be convex is to be bent outwards, this definition makes it genuinely clear what it implies for a shape to be convex. Formally, all together for a shape to be convex, draw two points at any place inside the shape, and the line associating them cannot go outside of the shape. If it associates inside a shape where the line interfacing them goes outside the shape, at that point the shape is not convex. When a shape is a polygon, there is another standard for deciding whether it is convex. A polygon known to be a convex shape which most of its inner edges are not exactly or equivalent to 180° .

Convex Hull

The convex hull of an item is known as the least convex shape which covers the measured object. The convex hull is an omnipresent structure in computational geometry. Even though it is a valuable apparatus and is useful in developing different structures like Voronoi charts, and in applications like solo picture examination. It can be imagined that what the convex hull resembles by a psychological study. Envision that the focuses are nails standing out of the plane, take a versatile elastic band, stretch it around the nails and let it go. It will snap around the nails and expect a shape that limits its length. The area encased by the rubber band is known as the convex hull. This prompts an elective meaning of the convex hull of a limited set that focuses in the plane. This is the novel convex polygon whose vertices are focused and contains all purposes. Some of the uses of the convex hull are:

Crash evasion: If the convex hull of a vehicle keeps away from impact with snags at that point so does the vehicle. Since the calculation of ways that dodge crash is a lot simpler with a convex vehicle, at that point it is frequently used to design ways.

Smallest box: The smallest area square shape that encases a polygon has, at any rate, one side flush with the convex hull of the polygon, thus the hull is processed at the initial step of least square shape calculations. Correspondingly, finding the smallest 3-D box encompassing an article relies upon the 3D-convex hull.

Shape examination: Shapes might be grouped for coordinating their "convex lack trees", structures that depend for their calculation on convex hulls.

Recognizing edges of the convex hull is simple. An edge is extraordinary if each point is on or to the other side of the line controlled by the edge. It appears to be least demanding to recognize this by regarding the edge as coordinated and indicating one of the two potential headings as deciding the "side". Expressed adversely, a coordinated edge is not extraordinary if there is some point that is not left of it or on it.

Solidity

Solidity calculates the density of an object. A measure of solidity is the proportion of the object's area of an object to the area of a convex frame of the object, mathematical representation in equation (3.13) is given.

$$\text{Solidity} = \frac{\text{area}}{\text{convex area}} \quad (3.13)$$

A value of 1 implies a strong object, and value smaller than 1 tells an object having an unpredictable limit or containing openings. Solidity does not evaluate roundness apart from square shape, solidity is 1 (the greatest possible highest). Roundness (or similitude to a circle) can be advantageously processed by contrasting the area and the square of the edge, or the area of the result of the width and tallness (search for Feret breadths to register these). Another methodology is to decide the coefficient of variation of the separation of every limit pixel to the geometric focal point of the object. Solidity is valuable to measure the sum and size of concavities in an object limit. Gaps are likewise frequently included. For instance, it recognizes a star from a circle, yet does not recognize a triangle from a circle.

Rectangularity

Rectangularity can be defined as the amount of the area of measured item in the square shape mathematically equation (3.14) represents rectangularity. Suppose F_k is the proportion of the area of square shape, the square shape having the bearing k .

$$\text{Rectangularity} = \max (F_k) \quad (3.14)$$

Rectangularity has a value of 1 for a splendidly rectangular item. The measures rely upon two parameters which empower their adaptability, for example, the likelihood to

adjust regarding a solid application. A few rectangularity estimates exist in the writing, and they are intended to assess numerically how much the shape thought about varies from an ideal square shape. None of these measures recognizes square shapes whose edge proportions vary, for example, they expect that all square shapes (counting squares) have a similar shape. Such property can be a disservice in applications. The new rectangularity measures are invariant as for interpretation, revolution and scaling changes. They go over the interim $[0, 1]$ and accomplish the value 1 just for ideal square shapes with an ideal edge proportion. The standard technique for evaluating rectangularity is to utilize the proportion of the locale's area against the area of its base bounding square shape MBR (Minimum Boundary Rectangle). A shortcoming of utilizing the MBR is that it is delicate to bulges from the locale. Indeed, even a tight spike standing out of a locale can endlessly inflate the area of the MBR, and in this way produce very poor rectangularity gauges. Also, there is an asymmetry among bulges and spaces, since the last can have no impact on the MBR (even though obviously the rectangularity measure is influenced).

Bounding Box

The bounding box is defined as the item which have a square shape that surrounds the item. The parts of the bounding box are known as the major and minor axes. The area of the bounding box is calculated using equation (3.15).

$$area = (major\ axis\ length) \times (minor\ axis\ length) \quad (3.15)$$

The base bounding box is the base area that limits the shape. Encircled square shape or bounding box is the smallest square shape that contains the majority of the given focuses. Attempt this Drag any of the four underneath. The bounding box will alter as needs be. The encircled square shape, or bounding box, is the minor square shape that can be drawn around many focuses with the end goal that every one of the focuses is inside it, or precisely on one of its sides. The four sides of the square shape are in every case either vertical or even, parallel to the X-Axis or Y-Axis. In the Figure 3.3, the bounding box is demonstrated drawn around the vertices of a quadrilateral. It is known as the bounding box since it frames a limit, like a fence, around the shape or set of focuses. This is utilized broadly when discovering area of different shapes utilizing coordinate geometry. (For instance, observe Area of a triangle (box technique)). This strategy includes first drawing the bounding box and afterwards subtracting the areas of straightforward shapes made around its edge to discover the area.

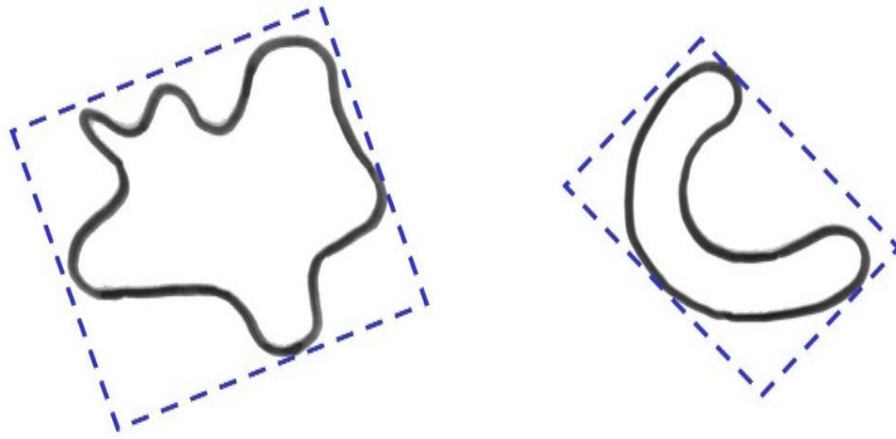


Figure 3.3 Bounding Box

Shape Variance

Most of the time a shape is compared with some other shape or a format. A circle is one of the most used shape which is compared with other shapes. The round variance is the corresponding mean-squared difference to the circle. If the value is zero it is an ideal circle and increments in the shape means the shape is multifaceted in nature and extension. Elliptic variance is another name for the round variance. In the Elliptic variance an oval is used in place of the circle and then the mean square difference is calculated. Primates have shoulders adjusted to a wide scope of locomotor capacities from earthly pronograde quadrupedal to exceptionally arboreal suspensory practices. The shape of the scapula firmly pursues these useful contrasts. Investigations of primate postcranial, including the scapula, show that quadrupedal monkeys are less factor than non-quadrupeds. The distinction is because of a connection between the quality of balancing out choice and the practical requests of the upper appendage. Here it is demonstrated that intraspecific scapular shape variance is exceptionally connected with the level of submitted quadrupedal. Primates that take part in incessant suspensory practices (for example gorillas and monkeys) normal double the amount of shape variance as quadrupeds (for example Old World monkeys and Saimiri). Since this distinction fit as a fiddle variance is evident in newborn children and does not increment or lessening considerably over ontogeny, it is not likely that distinctions in postnatal development, neuromuscular control or ecological factors, for example, environment structure/organization are the essential supporters of contrasts fit as a fiddle variance. Rather variance in embryonic elements that influence the shape/size of the scapula or epigenetic variables related to muscle connections are more probable applicants.

Specifically, the heterogeneous utilitarian requests of the non-quadrupedal shoulder presumably diminish the stringency of balancing out determination, bringing about the ingenuity into adulthood of expanded amounts of embryonically created scapular shape variance.

Curvature

The shape of a circle is conveyed equitably over its whole surface on a block, the arc is amassed in equivalent parts at every one of the eight equally dispersed vertices. Mathematicians have different approaches to characterize the arc for progressively complex shapes. To start with, envision a flat surface. Naturally, it has no bend (the surface is flat, all things considered). To see that numerically, draw a hover around a point on that surface with an edge of 360°. Presently envision a cone sticking out of the surface like a mountain. Take that cone out, make a straight slice from the peak to the base, and lay the cone flat. A part of a circle will be seen — that is, a hover with a missing piece, like Pac-Man with his mouth open. The edge of the missing piece of the circle is the curvature of the cone. It can likewise get a "negative" arc with shapes like a pony's seat. One way (in accordance with the head and tail) it bends up, while in the other bearing (opposite to the primary) it bends down. If it is somehow manage to slice it open and Endeavor to flatten it, as the cone, it would cover itself, since it has an excessive amount of edge. The surplus point is the negative curvature of the seat. Craftsmen exploit negative curvature in the peculiar quest for "hyperbolic knitting" — they include join into a flat yarn hover to make a negative shape and a twisted, space-time stylish.

Bending Energy

The absolute bending energy denominated as 'E_c' is a very famous shape descriptor. It is known as the limit of an energy which might be used to twist a pole to the ideal shape needed and can be determined of-squares of the limit bend κ(p) over the limit length L.

$$E_c = \frac{1}{L} \sum_{p=1}^L \kappa(p)^2 \quad \frac{2\pi}{R} \leq E_c \leq \infty \quad (3.16)$$

The base value 2π/R is concluded for a hover of sweep R in equation (3.16).

The bending energy of an object indicates the energy put away in its shape. Utilizing Elasticity hypothesis, one can demonstrate that the 2-D bending energy is

straightforwardly relative to the bending energy of a twisted around the pole. Also, it will demonstrate the connection between 3-D bending energy and the bending energy of an avoided flimsy plate. In 2-D just as 3-D, it has just thought to be isotropic bodies whose mis happenings keep Hook's law to a decent guess. That is, the twisting is corresponding to the applied power. Bending energy of a round bar is extended at certain focuses (convex side) and packed at others (sunken side). There exists, nonetheless, an impartial surface (or line) which experiences neither augmentation nor pressure. The length of the impartial line is unaffected by bending. Enormous bending redirections will cause a twisting that is a mix of bending and torsion. For little avoidances, it can expect that the bending happens in a solitary plane. The deviation of a marginally twisted bend from a plane (its torsion) is, in any event, one request of an extent littler than its curvature.

Total Absolute Curvature

The total absolute curvature is also known as the “third curvature”. This well-known shape descriptor is known as the measure of the total absolute curvature in the measured item and can be calculated using equation (3.17).

$$\kappa_{total} = \frac{1}{L} \sum_{\rho=1}^L |\kappa(\rho)| \quad 2\pi \leq \kappa_{total} \leq \infty \quad (3.17)$$

The total absolute curvature is the least value which can be found in the convex items. There are two basic kinds the curvature, extrinsic curvature and intrinsic curvature. The outward shape of bends in 2-D and 3-D is the main sort of curvature to be examined, which portray a space dimension completely as far as its “curvature” torsion, and the underlying beginning stage and behaviour. After the shape of 2-D and 3-D bends was considered, consideration went to the curvature of surfaces in three-space. The principle curvature that rose up out of this examination are the mean curvature, Gaussian curvature and the shape manager. Mean shape was the most significant for applications at the time and was the most considered, yet Gauss was the first to perceive the significance of the Gaussian curvature. Since Gaussian arc is “intrinsic”, it is perceivable to 2-D “occupants” of the surface, while mean curvature and the shape administrator are not perceptible to somebody who cannot ponder the 3-D space encompassing the surface on which it dwells. The significance of Gaussian curvature to an occupant is that it controls the surface region of circles around the occupant. Numerous summed up the idea of shape to sectional

curvature, scalar curvature, the Riemann tensor, Ricci bend tensor and a large group of other inherent and extrinsic ebbs and flows. General ebbs and flows never again should be numbers and can appear as a guide, gathering, groupoid, tensor field and so forth.

Spatial Moment

Spatial moment conditions additionally alluded to as pair approximations or related conditions that are generally new strategy in numerical science for understanding the conduct of gatherings of people developing and communicating in a spatial field. These models utilize an assortment of techniques to determine coupled conditions for both the mean densities and the spatial example of single or numerous connecting populaces; the spatial example is portrayed as far as the probabilities of two people occupying spatial areas. These probabilities can be communicated in various manners, as relationships or as contingent probabilities or as covariances. Moment conditions can be applied to populace dynamic models on discrete standard (generally square) cross-sections, in which case they are commonly called pair estimate conditions, on discrete normal or unpredictable systems, or to people situated at focuses in a consistent spatial field. Moment conditions have for some time been utilized in material science. However, they are presently utilized by an assortment of scientists in scientific nature, the study of disease transmission, and advancement as a method for approximating complex stochastic individual-based models in a manner that improves estimation and gives explanatory bits of knowledge. At an ongoing gathering of specialists met to talk about the eventual fate of these conditions. Spatial moment hypothesis, initially created in factual material science, can be utilized to examine the impact of spatial structure on populace level elements. The normal thickness of people managed in mean-field models is the primary spatial moment which holds no data on little scale spatial structure. One approach to access such data is to think about the second spatial moment, the normal thickness of sets of cells, communicated as a component of the separation r between them.

Equation (3.18) describe the (p,q) th-order moment.

$$m_{pq} = \sum_{x=0}^{M-1} \sum_{y=0}^{N-1} x^p y^q \quad \text{for } p, q = 0, 1, 2, \dots \quad (3.18)$$

Central Moment

In hypothesis and measurements, a central moment is a moment of a likelihood appropriation of an irregular variable about the arbitrary variable's mean that it is the normal value of a predetermined whole number intensity of the deviation of the irregular variable from the mean. The different moment's structure has one lot of values by which the properties of a likelihood appropriation can be helpfully described. Central moments are utilized in inclination to normal moments, processed as far as deviations from the mean rather than from zero, because the higher-request central moments relate just to the spread and shape of the appropriation. A central moment is one moment determined about some point. Central moments are translational invariant. This is significant in article recognition since it reveals to us that two generally indistinguishable masses (for example same size, shape, direction) that are in various pieces of our picture will have equivalent central moments. To ascertain the central moment of a mass about some point c , our standard condition turns into an addition to its area as formulated in equation (3.19).

$$\mu_{pq} = \sum_{x=0}^{M-1} \sum_{y=0}^{N-1} (x - \bar{x})^p (y - \bar{y})^q \quad \text{for } p + q > 1 \quad (3.19)$$

This is a substantially more computationally concentrated count than the crude moment. On the off chance to ascertain this for each pixel, it is going to haul down the exhibition of the framework. Central moments can be expressed as straight mixes of crude moments.

Normalized Central Moment

The central moments (3.20) can be normalized by utilizing the zeroth moment to produce the normalized central moment.

$$\eta_{pq} = \mu_{pq} / \mu_{00}^{\gamma} \quad (3.20)$$

$$\gamma = (p + q) / 2 + 1 \quad (3.21)$$

Central moment is known as the probability distribution for the variable which is random. Central moments or normalized central moments are used for the ordinary moments, which are computed in terms of difference in mean. As the higher order normalized central moments can be related to the shape distributor it can also be related to location. The primary central moment is a factual channel which estimates the fluctuation of degrees of a picture concerning the neighbourhood mean. The term moment

has been taken from material science. In material science, the moment of an arrangement of point masses is determined with a formula indistinguishable from equation (3.21), and this equation is utilized in finding the focal point of mass of the focuses. In insights, the qualities are never again masses. However, moments in insights still measure something comparative with the focal point of the values.

Moment Invariant

Moment invariants are properties of associated areas in twofold pictures that are invariant to interpretation, pivot and scale. They are helpful because they characterize an essentially determined arrangement of district properties that can be utilized for shape characterization and part acknowledgement. However, an autonomous premise set of invariants of a similar request containing just 6 invariants (and distinguishing the needy invariant in the set). Picture moments are a weighted normal of picture pixel forces. It is a straightforward guide to comprehend the past proclamation.

Radial Distance Measure

The state of a structure that is measured in equation (3.22) can also be dictated by investigating its limit, the varieties and shape of which establish the data to be evaluated.

$$d(n) = \sqrt{[x(n) - \bar{x}]^2 + [y(n) - \bar{y}]^2} \quad n = 0, 1, \dots, N - 1 \quad (3.22)$$

Transform the limit into a 1-D signal and investigating its structure. The outspread separation is estimated from the central point (centroid) to every pixel $x(n)$, $y(n)$ on the limit. To get the measurement of the normal radial distance it is acritude by normalizing $d(n)$ with the maximal distance. The quantity of the signal $r(n)$ crosses is known as the mean. There are other same kinds of metrics which are utilized to measure the boundary roughness. The sequence $r(n)$ is also observed with the shape metrics. Entropy is known as the proportion of a framework's energy for every unit temperature that is inaccessible for doing helpful work. Since work is gotten from requested atomic movement, the measure of entropy is additionally a proportion of the sub-atomic issue, or irregularity, of a framework. The idea of entropy gives profound understanding into the heading of unconstrained change for some regular wonders.

Signature Analysis

A signature is a 1-D representation of the boundary as shown in Figure 3.4.

- Computing the distance from the centroid of an object to the boundary as a function of angles, from 0° - 360° in any chosen increment.
- Harmonic analysis, or shape unrolling.
- The plot repeats at every 2π intervals.

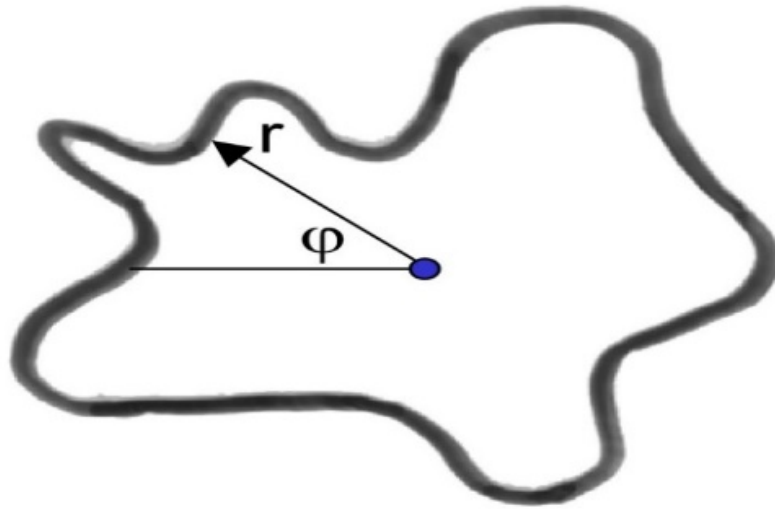


Figure 3. 4 Signature Analysis

Fourier Descriptor

Fourier descriptors and moment invariants are the most widely used shape representation schemes. The main idea of a Fourier descriptor is to use the Fourier transformed boundary as the shape feature. The information in the $r(n)$ signal can be further analysed in the spectral domain using the DFT (Discrete Fourier Transform) in the following equation (3.23):

$$a(u) = \frac{1}{N} \sum_{n=0}^{N-1} r(n) e^{-j2\pi nu/N} \quad u = 0, 1, \dots, N-1 \quad (3.23)$$

- The “low-frequency” terms, correspond to the smooth behaviour.
- The “high-frequency” terms correspond to the jagged and bumpy behaviour terms correspond to the roughness.

Hough Transform

The Hough transform is a global technique that finds the occurrence of objects of a predefined shape.

- Used to identify shapes within a binary image containing disconnected points.
- A cluster of such points may assume the shape of a line, a circle etc.
- The central idea of the Hough transform is to represent a line made up of many pixels by a single peak in parametric space to the accumulator array.
- This single peak has coordinated values in the accumulator array of two parameters necessary to describe the line, such as slope and intersect.
- Permits the detection of parametric curves example, circles, straight lines, ellipses, spheres, ellipsoids etc.

3.4 Numerical Method Algorithm

In numerical analysis, a numerical method is a mathematical tool designed to solve numerical problems and the implementation of a numerical method with an appropriate convergence check in a programming language is called a numerical Algorithm. This section describes the numerical tools used to describe the geometrical features of a shape and the development of numerical Algorithm, for each geometrical characteristic that are explored before. Furthermore, MATLAB toolboxes have also been used for image processing and image recognition to develop the numerical Algorithm. Following are the numerical methods used to describe the geometrical features of irregular shape.

Get the original image Figure 3.5 into the MATLAB enviroment

```
clc, clear all, close all, warning off
%Get image shapre from file

img = imread('28.jpg');

% Gray image
gray = rgb2gray(img);

% Binarise image using Sobel edge detector
BWs = edge(gray);
```

```
% Dilate the image
se90 = strel('line', 3, 90);
se0 = strel('line', 3, 0);
BWsdil = imdilate(BWs, [se90 se0]);

% Remove connected objects on border
BWnobord = imclearborder(BWsdil, 4);

% Keep only shape
BW = bwareafilt(BWnobord, 1);

%Show shape
figure, imshow(BW), title('Original Shape')
```

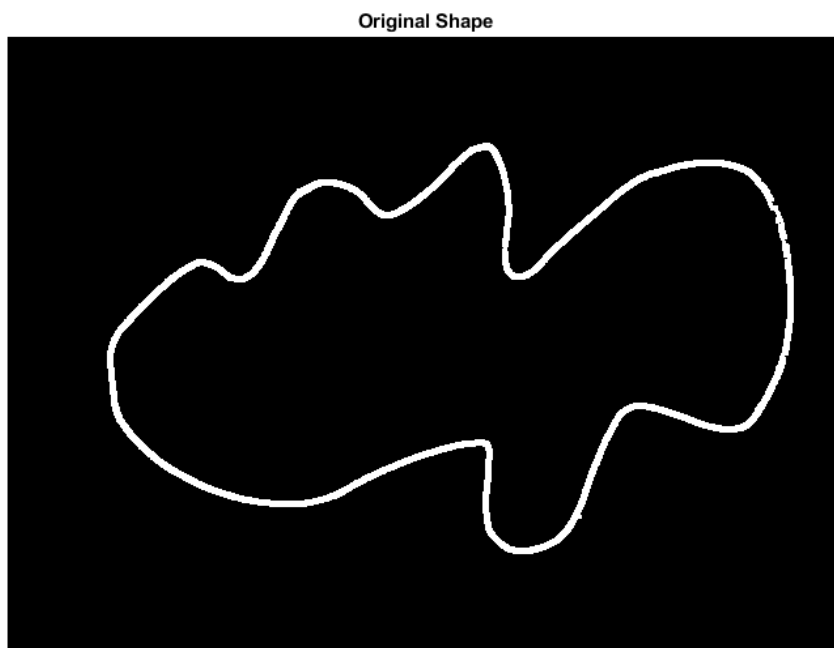


Figure 3.5 Original Image

Area

```
Area = regionprops(BW, 'area');  
Area = Area.Area;  
disp(['1. Area is ', num2str(Area)]);
```

1. Area is 8783

Perimeter

```
Perimeter = regionprops(BW, 'Perimeter');  
Perimeter = Perimeter.Perimeter;  
disp(['2. Perimeter is ', num2str(Perimeter)]);
```

2. Perimeter is 1643.358

Major and Minor Axis Length and Angle

```
MajorAxisLength = regionprops(BW, 'MajorAxisLength');  
MinorAxisLength = regionprops(BW, 'MinorAxisLength');  
Angle = regionprops(BW, 'Orientation');  
MajorAxisLength = MajorAxisLength.MajorAxisLength;  
MinorAxisLength = MinorAxisLength.MinorAxisLength;  
Angle = Angle.Orientation;  
disp(['3. Major Axis Length is ', num2str(MajorAxisLength) ', Minor Axis Length is ', ...  
      num2str(MinorAxisLength), ' and the Angle is ', num2str(Angle)]);
```

3. Major Axis Length is 639.47, Minor Axis Length is 380.07 and the Angle is 8.19.

Compactness

```
Compactness = Perimeter / Area;  
disp(['4. Compactness is ', num2str(Compactness)]);
```

4. Compactness is 0.18711

Elongation

```
BW2 = bwperim(BW);
```

```
Elongation = sum(sum(BW2)) / 2;  
disp(['5. Elongation is ', num2str(Elongation)]);
```

5. Elongation is 1466

Eccentricity

```
Eccentricity = regionprops(BW, 'Eccentricity');  
Eccentricity = Eccentricity.Eccentricity;  
disp(['6. Eccentricity is ', num2str(Eccentricity)]);
```

6. Eccentricity is 0.80421

Circularity

```
Circularity = 4 * pi * Area / Perimeter^2;  
disp(['7. Circularity is ', num2str(Circularity)]);
```

7. Circularity is 0.040868

Sphericity

```
EquivDiameter = regionprops(BW, 'EquivDiameter');  
Sphericity = EquivDiameter.EquivDiameter;  
disp(['8. Sphericity is ', num2str(Sphericity)]);
```

8. Sphericity is 105.7491

Convexity

```
ConvexArea = regionprops(BW, 'ConvexArea');  
Convexity = ConvexArea.ConvexArea;  
disp(['9. Convexity is ', num2str(Convexity)]);
```

9. Convexity is 124838

Convex Hull

```
disp(['10. Convex Hull is as in figure.']);
```

10. Convex Hull is as in Figure 3.6.

```
CH = bwconvhull(BW);  
figure;  
imshow(CH);  
title('10. Convex Hull');
```

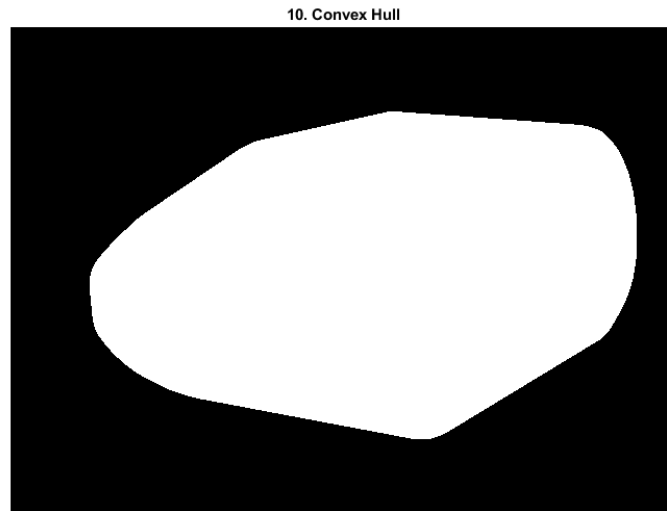


Figure 3.6 Convex Hull

Solidity

```
Solidity = regionprops(BW, 'Solidity');  
Solidity = Solidity.Solidity;  
disp(['11. Solidity is ', num2str(Solidity)]);
```

11. Solidity is 0.070355

Rectangularity

```
BoundingBox = regionprops(BW, 'BoundingBox');  
BB = BoundingBox.BoundingBox;  
RecArea = (BB(3) - BB(1)) * (BB(4) - BB(2));  
disp(['12. Rectangularity is ', num2str(Area / RecArea)]);
```

12. Rectangularity is 0.083867

Bounding Box

```
disp('13. Bounding Box is as in figure');
```

13. Bounding Box is as in Figure 3.7.

```
figure
imshow(BW);
rectangle('Position', BB, 'EdgeColor', 'red');
title('13. Bounding Box')
```

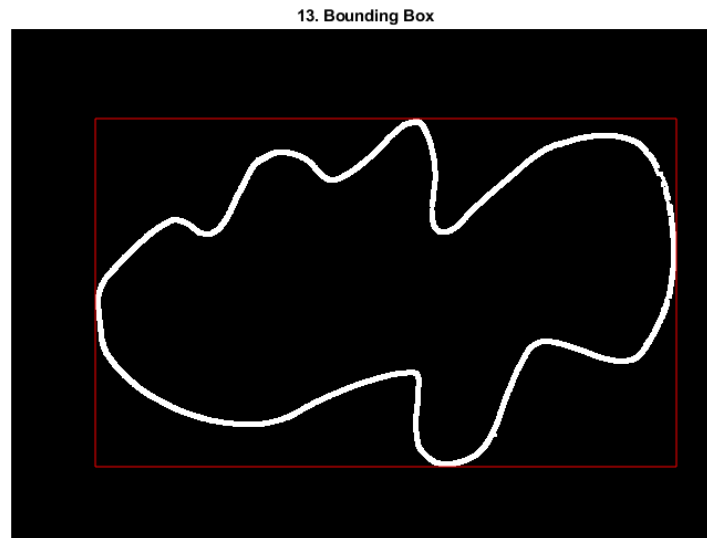


Figure 3.7 Bounding Box

Shape Variance

```
disp(['14. Shape Variance is ', num2str(Perimeter / 2 / (BB(3) - BB(1) + BB(4) - BB(2))));
```

14. Shape Variance is 1.2048

Curvature

```
boundaries = bwboundaries(BW);
x = boundaries{1}(:, 2);
y = boundaries{1}(:, 1);
windowSize = 10;
halfWidth = floor(windowSize / 2); % half window size
curvatures = zeros(size(x));
for k = halfWidth + 1 : length(x) - halfWidth
    theseX = x(k - halfWidth : k + halfWidth);
    theseY = y(k - halfWidth : k + halfWidth);
    % Get a fit.
    coefficients = polyfit(theseX, theseY, 2);
    % Get the curvature
```

```

curvatures(k) = coefficients(1);
end
disp(['15. Curvature is ', num2str(mean(curvatures(~isnan(curvatures))))]);

```

15. Curvature is 1.712470028766018e+25

Bending Energy

```

BE = 1 / 2 * abs(Elongation - Perimeter);
disp(['16. Bending Energy is ', num2str(BE)]);

```

16. Bending Energy is 88.679

Total Absolute Curvature

```

disp(['17. Total Absolute Curvature is ', num2str(sum(abs(curvatures(~isnan(curvatures)))))]);

```

17. Total Absolute Curvature is 8.852845808019289e+28

Spatial Moment

```

BW = im2double(BW);
[r c]=size(BW);
m = zeros(r, c);
for i = 0 : 1
    for j = 0 : 1
        for x = 1 : r
            for y = 1 : c
                m(i + 1, j + 1) = m(i + 1, j + 1) + (x ^ i * y ^ j * BW(x,y));
            end
        end
    end
end
disp(['18. Spatial Moment is ']);

```

18. Spatial Moment is

```

disp(m(1 : 2, 1 : 2))

```

8783 3080844

2024119 689520232

Central Moment

```
xb=m(2,1)/m(1,1);
yb=m(1,2)/m(1,1);
u = [ 0 0 0 0; 0 0 0 0; 0 0 0 0; 0 0 0 0];
for i = 0 : 3
    for j = 0 : 3
        for x = 1 : r
            for y = 1 : c
                u(i + 1, j + 1) = u(i + 1, j + 1) + (x - xb) ^ i * (y - yb) ^ j * BW(x, y);
            end
        end
    end
end
disp(['19. Central Moment is ']);
```

19. Central Moment is

```
disp(u)
```

```
1.0e+16 *
  0.0000  0.0000  0.0000 -0.0000
-0.0000 -0.0000 -0.0000 -0.0001
  0.0000  0.0000  0.0001  0.0012
  0.0000 -0.0000 -0.0008 -1.6838
```

Normalized Central Moment

```
disp(['20. Normalized Central Moment is ']);
```

20. Normalized Central Moment is

```
disp(u / Area)
```

```
1.0e+12 *
```

```

0.0000  0.0000  0.0000  -0.0000
-0.0000 -0.0000 -0.0000 -0.0001
0.0000  0.0000  0.0002  0.0013
0.0000 -0.0000 -0.0009 -1.9171

```

Moment Invariant

```

n = [ 0 0 0 0;0 0 0 0;0 0 0 0;0 0 0 0];
for i = 0 : 3
    for j = 0 : 3
        n(i + 1, j + 1) = u(i + 1, j + 1) / (u(1, 1) ^ (1 + (i + j) / 2));
    end
end
disp(['21. Moment Invariant is ']);

```

21. Moment Invariant is

```

disp(n)
1.0000  0.0000  2.8717  -0.4954
-0.0000 -0.2656 -0.0051 -1.8130
1.0662  0.0955  1.9678  0.1815
0.0828 -0.4920 -0.1292 -2.8296

```

Radial Distance Measure

```

C = regionprops(BW, 'Centroid');
Xs = boundaries{1}(:, 2);
Ys = boundaries{1}(:, 1);
C = C.Centroid;
RD = 0;
for i = 1 : length(Xs)
    x = Xs(i); y = Ys(i);
    RD = RD + sqrt((C(1) - x) ^ 2 + (C(2) - y) ^ 2);
end
disp(['22. Radial Distance Measure is ', num2str(RD)]);

```

22. Radial Distance Measure is 266859.0327

Signature Analysis

```
disp(['23. Signature Analysis is as in figure.']);
```

23. Signature Analysis is as in Figure 3.8.

```
distances = sqrt((Xs - C(1)) .^ 2 + (Ys - C(2)) .^ 2);  
t = 1 : length(distances);  
figure;  
plot(t, distances);  
title('Signature Analysis');
```

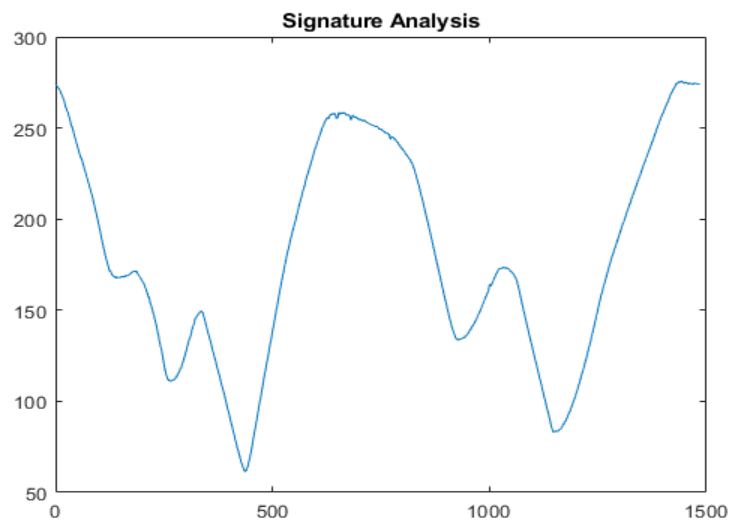


Figure 3. 8 Signature Analysis

Fourier Descriptor

```
boundary = boundaries{1};  
if mod(size(boundary, 1), 2) ~= 0  
    boundary = [boundary; boundary(end, :)];  
end  
np = size(boundary, 1);  
s = boundary(:, 1) + i * boundary(:, 2);  
descriptors = fft(s);  
descriptors = [descriptors((1 + (np / 2)) : end); descriptors(1 : np / 2)];  
disp(['24. Fourier Descriptor is ']);
```

24. Fourier Descriptor is

```
disp(descriptors(1 : 10))
```

```
1.0e+04 *  
(1.0401 + 0.0000i),  
(-0.6405 - 0.2835i),  
(-0.0716 - 1.2086i),  
(-0.8589 - 0.2010i),  
(-0.7884 - 0.3490i),  
(-0.0793 - 0.4891i),  
(-0.6154 + 0.3782i),  
(-0.4499 - 0.0372i),  
(0.9328 + 0.2875i),  
(0.9768 + 0.3307i).
```

Hough Transform

Calculate Hough transform

```
[H, T, R] = hough(BW, 'RhoResolution', 0.5, 'ThetaResolution', 0.5);  
disp(['25. Hough Transform is as in figure.']);
```

25. Hough Transform is as in Figure 3.9.

```
figure  
imshow(imadjust(mat2gray(H)), 'XData', T, 'YData', R, 'InitialMagnification', 'fit');  
title('Hough transform');  
xlabel('\theta'), ylabel('\rho');  
axis on, axis normal, hold on;  
colormap(gca, hot);
```

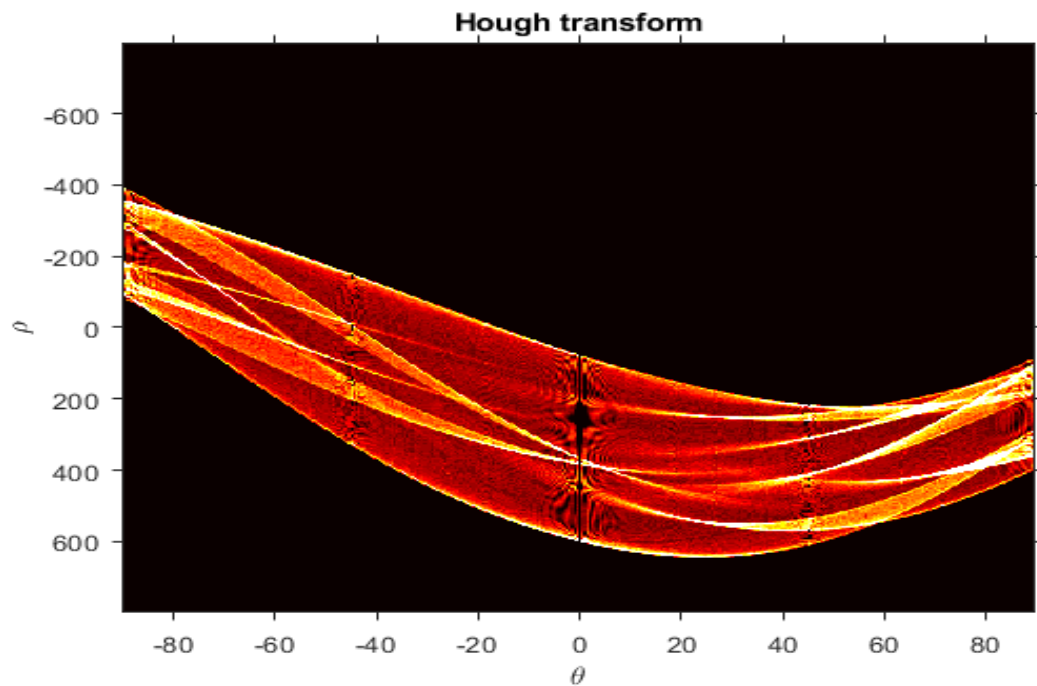


Figure 3.9 Hough Transform

3.5 Summary

This chapter covers both the methods to describe the feature of the shape. There are set of understandings about the numerical and analytical methods used to describe the geometrical features of irregular polygons and twenty-five geometrical characteristics of shapes are simulated using different Algorithms. The analytical methods formulae are described only, because these formulae are not capable to utilize on irregular shapes. The numerical Algorithms are calculated through MATLAB. These methods are further processed in the next chapter to develop the methodologies for finding the point-based trajectories of Robot end effector. This chapter further explores the different tools and techniques of image processing toolbox in MATLAB along with the Live editor, that is used to test the codes while creating them and the coding is exported directly to word file including graphs and images.

Chapter 4

Chapter # 4 Trajectory Development of Irregular Polygons in MATLAB

4.1 Introduction

4.2 Study of MATLAB Software and Image Processing

4.3 Shape Recognition of Polygon

4.4 Methodology to Develop Trajectory

4.5 Robot Coordinates and Communication

4.6 Summary

4.1 Introduction

There are different methodologies used to define the geometrical features of the shape. Considering the heuristic behaviours of MV System, designing them for diverse objectives. The analytical and numerical methods discussed earlier in sections 3.3 and 3.4 of Chapter 3 have been used. This chapter illustrates the most important aspects of Algorithm development in MATLAB software packages. These aspects are further incorporated in the analysis later in the thesis. While this study begins with the image recognition to find the shape basic features like information about type of polygon, number of polygons, centroid and length of it, to understand the initial aspects of the shape before trajectory formation. After that, the chapter illustrates step by step methodology to develop Robot end effector trajectory using MV. This chapter is the foundation for the next chapter because the positional information collected from image processing in section 4.5 will be communicated to the Robot using RCU through ‘G’ codes.

4.2 Study of MATLAB Software and Image Processing

Scientific computing is related to the execution of various machine Algorithms that are programmed in programming languages of different type. MV is employed to establish techniques and methods to automate actions such as processing, acquiring, understanding and analysing data coming from different sources [55]. The data is then mined from environment of the world and generate symbolic information from that to utilize MV. To put it in a nutshell, computers get the ability, from MV, to understand, analyse and process videos and images just like humans do [56]. There have been many advancements in machine learning tools, hardware and frameworks [57]. All these advancements have resulted in the MV’s implementation in many areas such as manufacturing, security and healthcare etc. High profile tech firms like Google, Facebook and Microsoft, shopping webs are investing a large amount in the development and research in this field. There are many libraries and tools that can be used for MV. Major tools of MV are MATLAB and OpenCV [58].

INTEL developed the software OpenCV which, is free for commercial use. OpenCV is one of the famous tools for MV that aim at giving a well-tested, well optimized and open source implementation for MV Algorithms. Some MV clients found OpenCV more complex. There are not many error handlings codes and documentation about this tool

[59]. MathWorks developed MATLAB. It has multi-paradigm numerical computing environment. It has more than three million users all over the world. It is considered as one of the most productive and easy to use language for scientists and engineers. It contains swift and powerful matrix library [60]. OpenCV and MATLAB are complementary software for the development of Algorithm, video and image analysis and vision system design [61]. The advantages of using these software packages is their ability to reduce system cost and the complexity of decision making thereby exposure to the new technologies. The description of MATLAB in which development environment, image processing techniques, different toolboxes, visualization of data, SIMULINK block diagram analysis of image processing etc. are involved as follows [62].

- Algorithm development;
- Math and computation;
- Data analysis, visualization and exploration;
- Simulation, modelling and prototyping;
- Engineering and scientific graphics; and
- Application development and to build GUI's for different purposes.

Whenever complex engineering problems solutions are needed, MATLAB is considered as a high-profile language. It assimilates visualization, computation and programming factors in an environment where solutions and problems are expressed using known mathematical symbols and formulae [63].

MATLAB's use arrays which has no requirement of dimensions. This lets the programmer solve various technical computing problems like solving matrix formulation problems and vector problems [64]. The whole complex processing is done in a fraction of time, which would have taken a good amount of time to be written in another scalar language such as Fortran and C [65]. The work environment of MATLAB is shown in Figure 4.1, which gives the description of software.

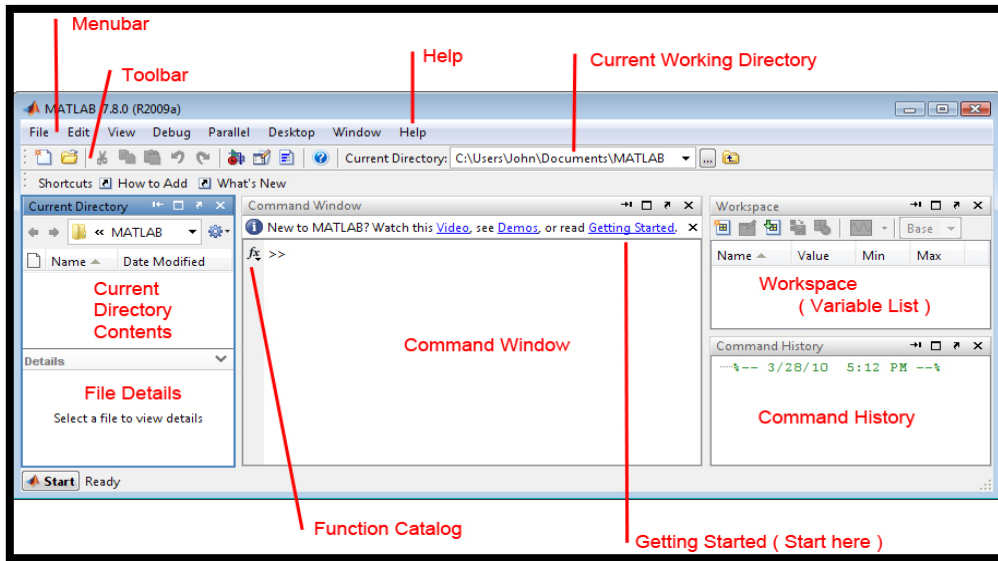


Figure 4.1 MATLAB Software Environment

4.2.1 MATLAB Toolboxes

MATLAB is designed to deliver convenient access to the EISPACK's and LINPACK's developed matrix software [66]. These two also are the state-of-the-art tools for the computation of matrix. The MATLAB also became famous because of its toolboxes. These toolboxes are image acquisition for image processing, database toolbox for exploration of data, statistics toolbox for stats [67]. Signal processing toolbox widely used in telecommunication industry, mapping toolbox for earth sciences, image processing toolbox discussed in Figure 4.2.

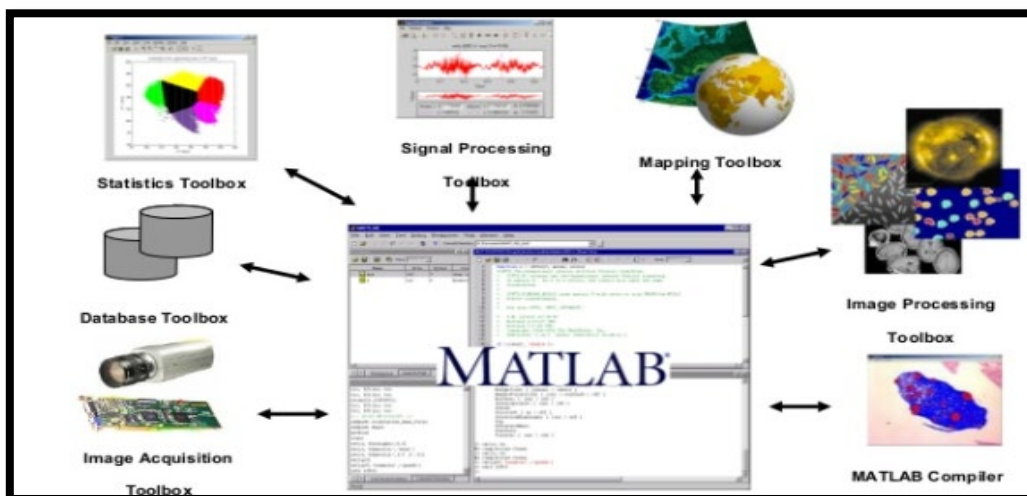


Figure 4.2 MATLAB Toolboxes

With input from many users over a period of years, there are many evolvments in MATLAB. For advanced courses of engineering, mathematics and science, which is the typical and compatible instructional tool for many universities' students [68]. In industry, for high level research, MATLAB is the tool of choice for development, research and analysis. This toolbox has a large importance for MATLAB's users. These lets the user to apply and learn specialized technology. These are many concise combinations of functions MATLAB adopt, which are used to solve categories of problems by extending the environment of MATLAB. In the fields of control system, there are many toolboxes used to solve control problems [69]. The image shown in Figure 4.3 is known as image processing toolbox, which is utilized, when there is functioning of image processing. It also includes aerospace and bioinformatics toolboxes for enhanced results.

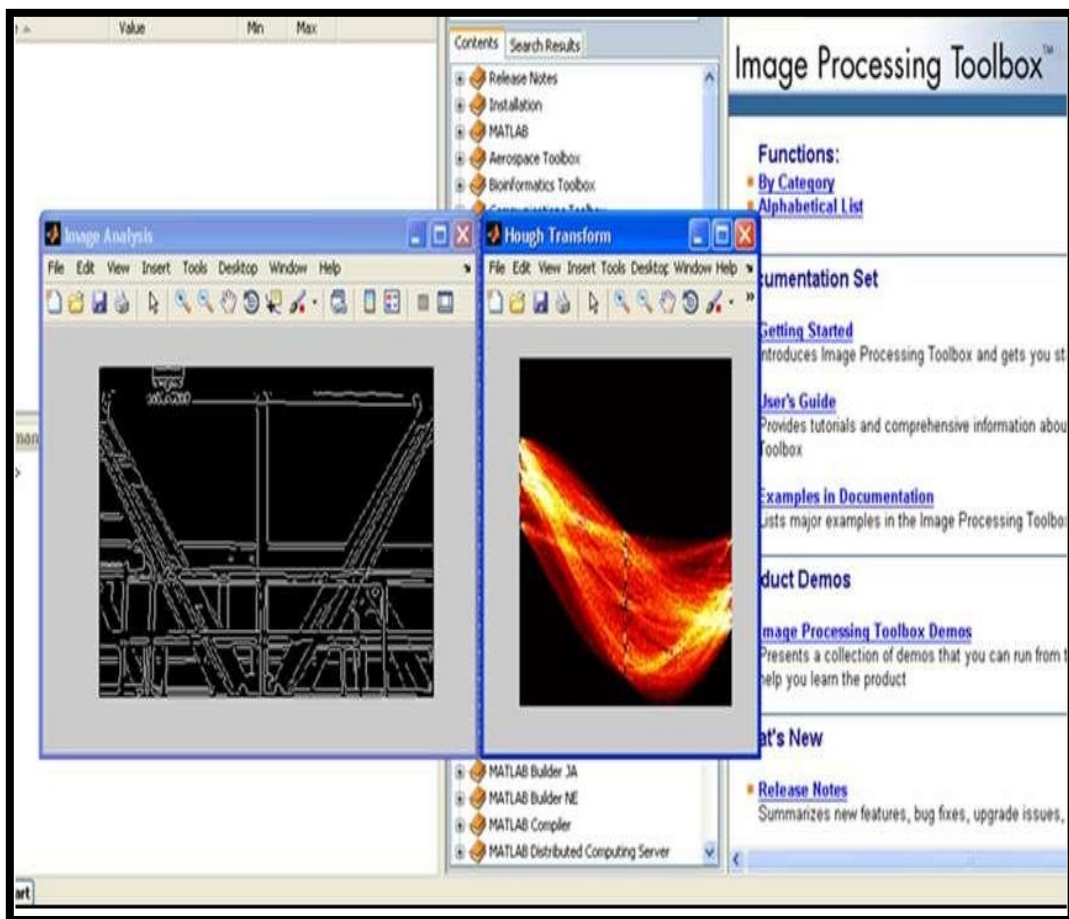


Figure 4.3 MATLAB Image Processing Toolbox

4.2.2 MATLAB Image Processing

The world is wondering about image processing techniques developed in few years because of video data analysis and extraction of valuable information. There are different types of text detection, image recognition and object detection are very common operations [70]. Image processing consists of three steps:

1. Initially the image is imported either by digital scanners, webcams or camera photography;
2. Analysing the data and to scrap the basics. MATLAB is sometimes used for enhancing the image pixels to process the data for compression and pattern spotting; and
3. Conclusion of the results are reported by software based on analysis and scrapping of data [71].

The steps of making analysis are given in a Figure 4.4 that shows analysis process for colour image processing wavelets, compression, segmentation, image acquisition, domain selection and object recognition [72]. Mining and exploration of data which includes the transformation of images, learning includes removal of image noise and creating images of high resolution from the low resolution with the aid of neural networks, segmentation which consists of region, texture, pixel analysis and filtering includes contrast adjustment, morphological filtering and the deblurring are involved, also processing of 3-D volumetric images in which all the above steps are performed for 3-D objects [73].

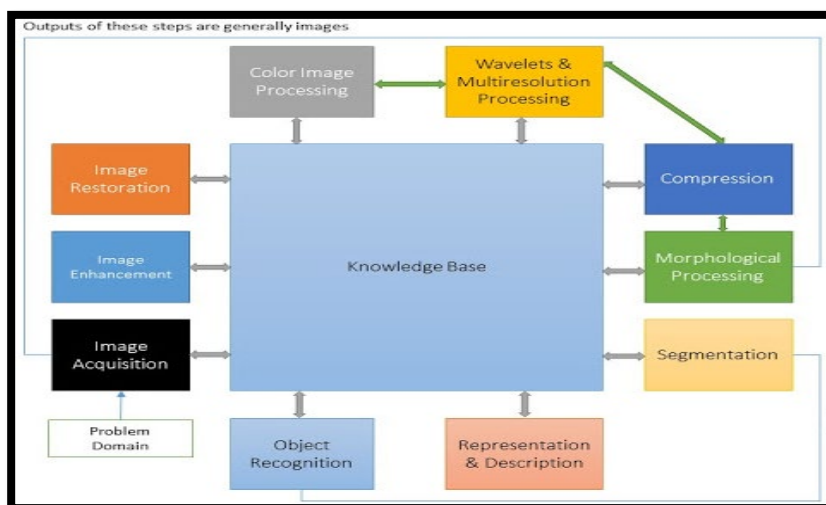


Figure 4. 4 Image Processing Techniques

Applications are involved in medical sciences, biometrics and satellite imaging technology. Moreover, it is utilized in many other fields of engineering. The blur images in medical imaging creates problem in investigation therefore the image pixel and clarity are improved. In the field of biometrics, it utilizes techniques to clear the result of fingerprints. In satellite technology, it is used to analyse large set of data and if the data contains raw data it also improves the dataset to analyse. Various types of mathematical Algorithm are used to develop new solutions to ensure the optimum result of the design process. Linear Algebra is used to predict whether the company will be in loss or profit after some years. MATLAB also utilizes to make various life and business decisions.

SIMULINK is a tool in MATLAB which provides the graphical programming environment. A model is created to simulate and analyse the results in multi domain dynamical systems. Block diagrams are drawn in SIMULINK and is customized according to the requirements. The step responses can be drawn in the field of control system to simulate the behaviour of circuits. MathWorks are the creator of SIMULINK module and its remarkable documentation that gives the complete knowledge of this tool [74]. A blank model of SIMULINK is shown in Figure 4.5, which is created by using command SIMULINK There are different blocks available according to the requirement in the SIMULINK library. Fuzzy logic toolbox, image acquisition toolbox, neural networks and many other types of blocks are available to make more prominent results accurately and comfortably.

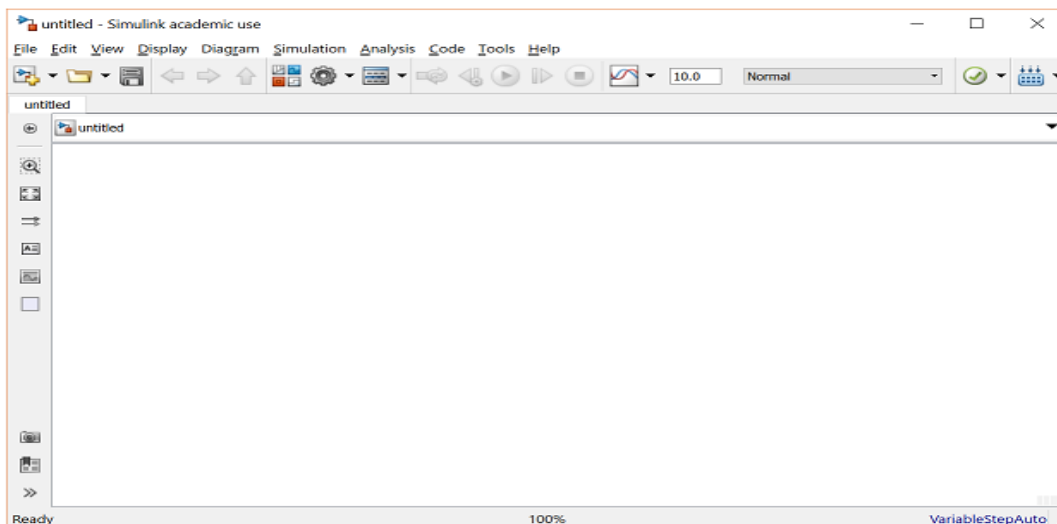


Figure 4.5 SIMULINK Software Environment

4.2.3 SIMULINK and Image Processing

SIMULINK model helps to generate the smallest elements from an image to convert it into segments to recognize. Previously there were many approaches used for video object segmentation Algorithm and morphological operation analysis. This technique is used in MRI to filter the image and focus on image pixels, which is used to localize other neighbouring elements. After that image is modified and transformed [75].

The basic model of SIMULINK is carried out using library that can select different blocks as shown in Figure 4.6. Once the block diagram is constructed the values can be modified. The configuration parameters like a solver pane stop time and solver type are selected in both 2-D or 3-D approach complete object region is given or provided as an input data. This technique provides an efficient result as 2-D recognizing problems. The feature-based model in which local features like eyes, ears, etc. are extracted and their location is saved as a matrix location, and this was given in the geometric appearance called the structural classifier. The experimental environment results are also extracted which gives the complete description of related work [76].

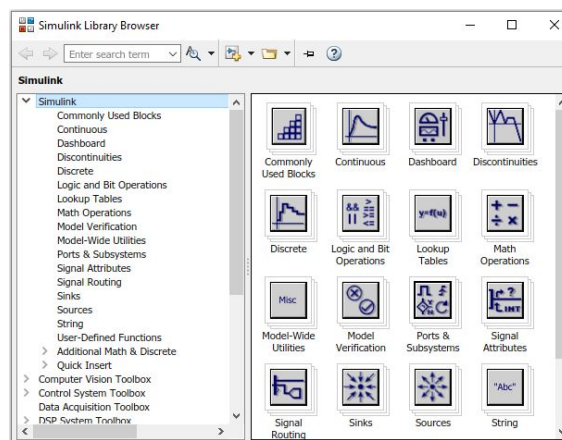


Figure 4.6 SIMULINK Library

4.3 Shape Recognition of Polygons

This section deals with Algorithm designing in the MATLAB to recognise different irregular polygon for extracting the features. There are five Polygons in the image named "Original Image" having regular and irregular.

The objective of this code is to recognise each object one after another, difference them between regular and irregular, name the type of polygon, calculate the number of sides, measure the area and centroid.

4.3.1 Codes to Call the Original Image into MATLAB

The original image is shown in Figure 4.7. This image is stored in a desired folder. Using command “imread”, the image will be imported into MATLAB environment for further processing.

```
cd 'D:\02 Education\01 PhD Administration\02D Towards Submission 03-10-2019\Tabish_Code_Towards-Submission'  
  
clear all;  
  
% Read image Read in  
a=imread('1.jpeg');  
  
RGB = a;  
figure;  
imshow(RGB);  
title('Original Image');
```

**Original Image
Regular and Irregular Polygons**

Name	Regular	Irregular
Triangle		
Quadrilateral		
Pentagon		
Hexagon		
Octagon		

Figure 4.7 Original Image

4.3.2 Codes to Convert Image from RGB to GRAY

```
% convert image from RGB to Gray, b is the later used
% rgb2gray(IMG);
b = rgb2gray(a);
GRAY = b;

% not required GRAY=histeq(GRAY);
% figure
% imshow(GRAY)
% title('Gray Image');

%*****
***

% Threshold the image Convert the image to black and white in order
% to prepare for further processing as shown in Figure 4.8.

threshold = graythresh(GRAY);
BW = im2bw(GRAY,threshold);

figure;
imshow(BW);
title('Binary Image');
```

Binary Image
Regular and Irregular Polygons

Name	Regular	Irregular
Triangle		
Quadrilateral		
Pentagon		
Hexagon		
Octagon		

Figure 4. 8 Binary Image

4.3.3 Invert the Binary Image and Morphological Operation

```
%*****  
**  
% Invert the Binary Image for faster processing  
%first remove clutter  
%  
se = strel('line',2,2);  
BWn = imdilate(BW,se);  
BWn=imfill(BWn,'holes');  
%BWn = ~ BWn;  
BW=~BW;  
BW=BW&BWn;  
%figure,  
%removed the unwanted shapes  
%*****  
***  
% Morphological operation  
se = strel('line',7,6);  
BWnn = imdilate(BW,se);  
BWnn=imfill(BW,'holes');  
BWnnn = bwareaopen(BWnn, 90);  
%BW=BW&BWnnn;  
% BW=~BW;not required  
BW=BWnnn;  
%I = im2uint8(BW);  
%  
figure,  
imshow(BW),  
title('Processed Image');
```

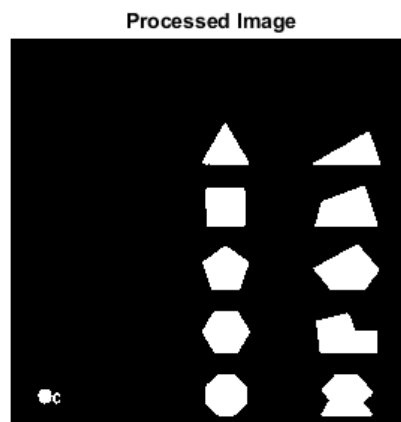


Figure 4.9 Processed Image

4.3.4 Coding for Polygons Recognition and Calculation

```
% Segmentation
%
CC = bwconncomp(BW);           % Finding connected components i.e shapes
%
% Next finding properties of region*****

centroids_ = regionprops(CC, 'Centroid');
blobs = regionprops(CC, 'Image');           % All different shapes
areas = regionprops(CC, 'Area');           % their Areas
locations = regionprops(CC, 'PixelList');   % Locations of each shape
number_objects = num2str(CC.NumObjects);   % number of Objects
%*****
***

% Shape Identification
%
for i=1:length(blobs) % iterate for all shapes found in image
shapz=blobs(i).Image ;

Xx = im2uint8(shapz);

%*****
***

% Compute distance of each shape from left bot corner of original image
%*****
***

[rox,cox]= size(BW);
cox=1; %always = 1
rx= centroids_(i).Centroid(1,2); %located from centroid not
locations(i).PixelList(1,1);
cx= centroids_(i).Centroid(1,1); %located from centroid not
locations(i).PixelList(1,2);
%distance from bottom left corner of i th object/ shape
d_stance(i)=sqrt(((cx-cox)^2)+((rx-rox)^2));
%*****
***
```

```

% Harris Corner detector detects corner in given shape
%*****
***
% Xx                                % Input image to corner detector
P_c= Xx; %rgb2gray(Xx);              % Input intensity image

%P_c=histeq(P_c);

st_dev=3;                            % Set standard deviation
Thr_shold=50000;                      % Threshold for Radi
Radi=3;                               % Window size in pixels (square)

%*****

% Derivatives of image
%
dx = [-1 0 1; -1 0 1; -1 0 1]; % Center divided diff derivative masks
dy = dx';                        % for Ix

Ix = conv2(P_c, dx, 'same');       % Image derivative in x direction
Iy = conv2(P_c, dy, 'same');       % Image derivative in y direction

Ix2=Ix.^2;                         % Square of image derivative
Iy2=Iy.^2;                         % Square of image derivative
Ixy=Ix.*Iy;                        % Product of derivatives in x and y

%*****

% Smoothing the derivatives using Gaussian Filtering
%
Gau=fspecial('gaussian',max(1,fix(6*st_dev)),st_dev); % Gaussian
Filter
Ix2=conv2(Ix2,Gau, 'same');        % Filter with Gaussian mask
Iy2=conv2(Iy2,Gau, 'same');        % and extract the central portion
Ixy=conv2(Ixy,Gau, 'same');        % corresponding to Ix2, Iy2, Ixy
%

%*****

% Corner response R using  $R = \det[M] - k (\text{Trace}[M])^2$ 

```

```

k=0.04          ;          % arbitrary
R = (Ix2.*Iy2 - Ixy.^2) - k*(Ix2 + Iy2).^2;
%
%Next displaying the corner response
%figure;
%imshow(R);title('Corner Response');

%*****

% R > Threshold
XR=R>Thr_shold;
%figure;

*****

% Local maxima detection and thresholding and displaying image
% Dilate intensity image
d_x=imdilate(R,strel('square',Radi));
R = (R>Thr_shold)&(R==d_x)      ;      % Find maxima and supressing
non

%[idx,co]=kmeans(R,2);          % maxima
%figure;
%imshow(R); title('Local Maxima');
[Radi,c] = find(R);            % find locations of
maxima
%
%*****

% Corners Detected in R

% next code calculates the distances between each corner point of
% sgmented shape

%*****

indx=1;

clear d;
d=0;

```

```

for z=1:length(c)

    Ro=Radi(z);
    Co=c(z);
    %
    %
    *****

        for y=1:length(c)
            if y ~= z
                d(indx)=[sqrt((Ro-Radi(y))^2+(Co-c(y))^2)];
                indx=indx+1;
            end
        end

    end

    %*****
    ***
    % Next part of the code identifies the shape
    %*****
    ***
    d=sort(d);
    str={};
    regular = abs(((d(1)-d(length(Radi)))/mean(d(1:length(Radi))))<0.1;

    % in sorted array of point-point distance first n distances are < 10% of
    mean
    % of smallest distances then this means a shape is regular.
    % because first n distances are supposed to be distances of polygon sides.
    % Regular = 1 if above condition is true.
    if regular==1
        switch(length(Radi))
            case 3
str={'Traingle', 'Regular', num2str(areas(i).Area), num2str(d_stance(i))};
            case 4

```

```

str={'Quadrilateral', 'Regular', num2str(areas(i).Area), num2str(d_stance(i)
)});
    case 5

str={'Pentagon', 'Regular', num2str(areas(i).Area), num2str(d_stance(i))};
    case 6

str={'Hexagon', 'Regular', num2str(areas(i).Area), num2str(d_stance(i))};
    case 7

str={'Heptagon', 'Regular', num2str(areas(i).Area), num2str(d_stance(i))};
    case 8

str={'Octagon', 'Regular', num2str(areas(i).Area), num2str(d_stance(i))};
    case 9

str={'Nonagon', 'Regular', num2str(areas(i).Area), num2str(d_stance(i))};
    case 10

str={'Decagon', 'Regular', num2str(areas(i).Area), num2str(d_stance(i))};
    case 11
        str={'11 Sided', 'Regular'};
    case 12
        str={'12
Sided', 'Regular', num2str(areas(i).Area), num2str(d_stance(i))};
    end
end

if regular==0
    switch(length(Radi))
        case 3

str={'Traingle', 'Irregular', num2str(areas(i).Area), num2str(d_stance(i))};
        case 4

```

```

str={'Quadrilateral', 'Irregular', num2str(areas(i).Area), num2str(d_stance(
i))});
    case 5

str={'Pentagon', 'Irregular', num2str(areas(i).Area), num2str(d_stance(i))};
    case 6

str={'Hexagon', 'Irregular', num2str(areas(i).Area), num2str(d_stance(i))};
    case 7

str={'Heptagon', 'Irregular', num2str(areas(i).Area), num2str(d_stance(i))};
    case 8

str={'Octagon', 'Irregular', num2str(areas(i).Area), num2str(d_stance(i))};
    case 9

str={'Nonagon', 'Irregular', num2str(areas(i).Area), num2str(d_stance(i))};
    case 10

str={'Decagon', 'Irregular', num2str(areas(i).Area), num2str(d_stance(i))};
    case 11
        str={'11
Sided', 'Irregular', num2str(areas(i).Area), num2str(d_stance(i))};
    case 12
        str={'12
Sided', 'Irregular', num2str(areas(i).Area), num2str(d_stance(i))};
    end
end

%*****
***

    % next showing shape with labels
%*****
***

    figure;
    imshow(b);           % Gray scale image.

```

```

text(locations(i).PixelList(1,1),locations(i).PixelList(1,2),str, 'Color',
'Color', 'red', 'FontSize',12);
    text(0,-15,'Total Number of Objects detected =',
'Color', 'blue', 'FontSize',12);
    text(265,-15,'10', 'Color', 'blue', 'FontSize',12);
    hold on;

plot(centroids_(i).Centroid(1,1),centroids_(i).Centroid(1,2), '*');

    %hold on;
    %
    % FORMAT OF DISPLAY
    % Name of shape
    % Regular / Irregular
    % Area
    % Distance from left bottom corner
    % Centroid is also shown

    %
    % displays length of sides in work space.
    %
    display('Types of Polygon, Length of Sides, Centroid etc')
    display(str);
    display(d(1:length(Radi)))

end
    % The End..

```

4.3.5 Results Generated from Algorithm

Following are the images that detects the information of regular and irregular polygons, types of polygons, length of sides and centroid. The coding is working properly, and the values are in pixels. There is an asterisk "*" mark in blue colour that illustrates the centroid and the red colour on the image describes some features. There are total of ten objects in the image.

Types of Polygon, Length of Sides, Centroid, Figure 4.10 etc

{'Traingle'} {'Regular'} {'480'} {'233.18'}
 25.5539 25.5539 26.9258

Total Number of Objects detected = 10
 Regular and Irregular Polygons

Name	Regular	Irregular
Triangle	 Traingle Regular 480	
Quadrilateral	 233.18	
Pentagon		
Hexagon		
Octagon		

Figure 4.10 Triangle

Types of Polygon, Length of Sides, Centroid, Figure 4.11 etc

{'Pentagon'} {'Regular'} {'643'} {'177.483'}
 15.8114 15.8114 16.6433 16.6433 16.7631

Total Number of Objects detected = 10
 Regular and Irregular Polygons

Name	Regular	Irregular
Triangle		
Quadrilateral	 Pentagon	
Pentagon	 Regular 643	
Hexagon	 177.483	
Octagon		

Figure 4.11 Pentagon

Types of Polygon, Length of Sides, Centroid, Figure 4.12 etc

```
{'Hexagon'} {'Regular'} {'677'} {'156.8286'}
13.8924 13.8924 13.8924 13.8924 13.8924 13.8924
```

Total Number of Objects detected = 10

Regular and Irregular Polygons

Name	Regular	Irregular
Triangle		
Quadrilateral		
Pentagon		
Hexagon		
Octagon		

Figure 4.12 Hexagon

Types of Polygon, Length of Sides, Centroid, Figure 4.13 etc

```
{'Quadrilateral'} {'Regular'} {'686'} {'204.9173'}
22 22 22 22
```

Total Number of Objects detected = 10

Regular and Irregular Polygons

Name	Regular	Irregular
Triangle		
Quadrilateral		
Pentagon		
Hexagon		
Octagon		

Figure 4.13 Quadrilateral

Types of Polygon, Length of Sides, Centroid, Figure 4.14 etc

```
{'Octagon'}    {'Regular'}    {'639'}    {'145.0904'}
9.8995    9.8995    10.0000    10.0000    10.0000    10.0000    10.0000    10.0000
```

Total Number of Objects detected = 10
Regular and Irregular Polygons

Name	Regular	Irregular
Triangle		
Quadrilateral		
Pentagon		
Hexagon		
Octagon	 639 145.0904	

Figure 4.14 Octagon

Types of Polygon, Length of Sides, Centroid, Figure 4.15 etc

```
{'Traingle'}    {'Irregular'}    {'545'}    {'292.2162'}
19.3132    19.3132    37.5899
```

Total Number of Objects detected = 10
Regular and Irregular Polygons

Name	Regular	Irregular
Triangle		 Traingle Irregular 545
Quadrilateral		 292.2162
Pentagon		
Hexagon		
Octagon		

Figure 4.15 Triangle

Types of Polygon, Length of Sides, Centroid, Figure 4.16 etc

```
{'Pentagon'} {'Irregular'} {'850'} {'248.0928'}
13.0384 13.0384 15.8114 15.8114 19.2094
```

Total Number of Objects detected = 10
Regular and Irregular Polygons

Name	Regular	Irregular
Triangle		
Quadrilateral		 Pentagon
Pentagon		 Irregular 850
Hexagon		 248.0928
Octagon		

Figure 4.16 Pentagon

Types of Polygon, Length of Sides, Centroid, Figure 4.17 etc

```
{'Octagon'} {'Irregular'} {'811'} {'266.864'}
1.0000 1.0000 2.2361 2.2361 9.0554 9.0554 11.1803 11.1803
```

Total Number of Objects detected = 10
Regular and Irregular Polygons

Name	Regular	Irregular
Triangle		 Octagon
Quadrilateral		 Irregular
Pentagon		 811 266.864
Hexagon		
Octagon		

Figure 4.17 Octagon

Types of Polygon, Length of Sides, Centroid, Figure 4.18 etc

```
{'Hexagon'} {'Irregular'} {'816'} {'230.6839'}
10.0000 10.0000 11.0000 11.0000 12.6491 12.6491
```

Total Number of Objects detected = 10
Regular and Irregular Polygons

Name	Regular	Irregular
Triangle		
Quadrilateral		
Pentagon		
Hexagon		
Octagon		

Figure 4.18 Hexagon

Types of Polygon, Length of Sides, Centroid, Figure 4.19 etc

```
{'Octagon'} {'Irregular'} {'772'} {'225.0063'}
6.0828 6.0828 7.0711 7.0711 7.2801 7.2801 9.0554 9.0554
```

Total Number of Objects detected = 10
Regular and Irregular Polygons

Name	Regular	Irregular
Triangle		
Quadrilateral		
Pentagon		
Hexagon		
Octagon		

Octagon
Irregular
772
225.0063

Figure 4.19 Octagon

4.4 Methodology to Develop Trajectory

There are different methods available and tested to define a trajectory. The method that shows the best results are based on the following steps.

1. Import the image into the MATLAB
2. Mesh the irregular shape into small regular square polygons of 25mm each
3. Define the asterisk into every 5 boxes horizontal and vertical that is about 125mm center to center distance in both direction
4. Remove all the meshing that is outside the shape
5. Remove the sharp edges from the boundry
6. Remove the asterisk that does not have a mesh
7. Remove the mesh as it does not required any more
8. Name the each asterisk starts from left top corner and advances horizontally
9. Describe the origin point of the shape
10. Calculate the cartesian coordinate values of each asterisk with respect to the common origin.

After that, this information will be processed to convert into 'G' codes and further communicate with RCU in real time. The image has a processing time of 15 seconds therefore every 15th seconds image can be changed. Following are the Algorithm used to perform the methodology.

4.4.1 Get the Original Image into MATLAB

clc, clear all, close all, warning off

```
img = imread('28.jpg');  
  
% Gray image  
gray = rgb2gray(img);  
  
% Binarise image using Sobel edge detector  
BWs = edge(gray);  
  
% Dilate the image  
se90 = strel('line', 3, 90);  
se0 = strel('line', 3, 0);
```

```

BWsdil = imdilate(BWs, [se90 se0]);

% Remove connected objects on border
BWnobord = imclearborder(BWsdil, 4);

% Keep only shape
BW = bwareafilt(BWnobord, 1);

boundaries = bwboundaries(BW);
x = boundaries{1}(:, 2);
y = boundaries{1}(:, 1);

BW = ones(size(BW, 1), size(BW, 2));
for i = 1 : length(x)
    BW(y(i), x(i)) = 0;
end
% Show shape
figure, imshow(BW), title('Original Shape') % Figure 4.20.

```

Original Shape

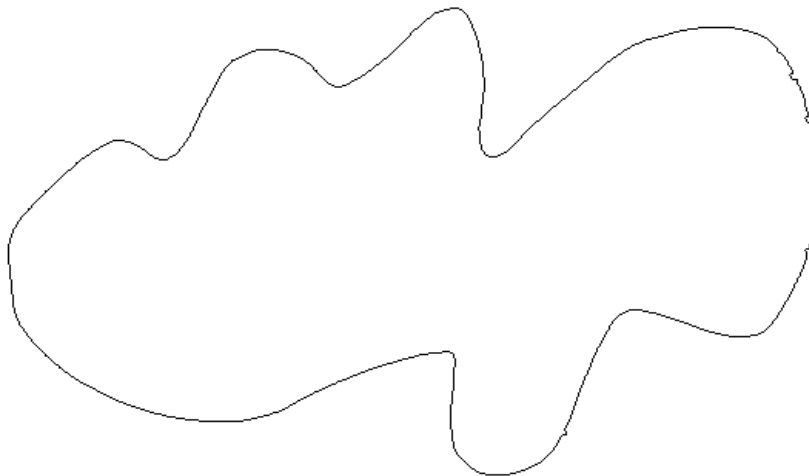


Figure 4. 20 Original Shape

4.4.2 Disintegrate the Irregular Polygons into Small Regular Polygons

```
% Get number of triangles
nc = round(297 / 2.5);
nr = round(210 / 2.5);

% Get rows and cols of image
[rows, cols] = size(BW);

% Get space
r_space = round(2.5 * 210 / nr);
c_space = round(2.5 * 297 / nc);

% Find rectangle positions
rect_pos = [];
x1 = round(cols / 2); % center x
y1 = round(rows / 2); % center y
xx = x1;

while xx > 0
    yy = y1;
    while yy > 0
        rect_pos = [rect_pos; [xx, yy, r_space, c_space]];
        yy = yy - r_space;
    end
    yy = y1 + r_space;
    while yy <= rows
        rect_pos = [rect_pos; [xx, yy, r_space, c_space]];
        yy = yy + r_space;
    end
    xx = xx - c_space;
end

while xx <= cols - c_space
    yy = y1;
    while yy > 0
```

```

rect_pos = [rect_pos; [xx, yy, r_space, c_space]];
yy = yy - r_space;
end
yy = yy + r_space;
while yy <= rows
    rect_pos = [rect_pos; [xx, yy, r_space, c_space]];
    yy = yy + r_space;
end
xx = xx + c_space;
end

rect_BW = insertShape(BW, 'rectangle', rect_pos, 'Color', [0, 0, 1]);
se = strel('disk', 4, 4);
BW2 = imdilate(1 - BW, se);
rect_BW2 = insertShape(1 - BW2, 'rectangle', rect_pos, 'Color', [0, 0, 1]);
figure, imshow(rect_BW2) % Figure 4.21 demonstrates the meshing.

title('2')

```

2

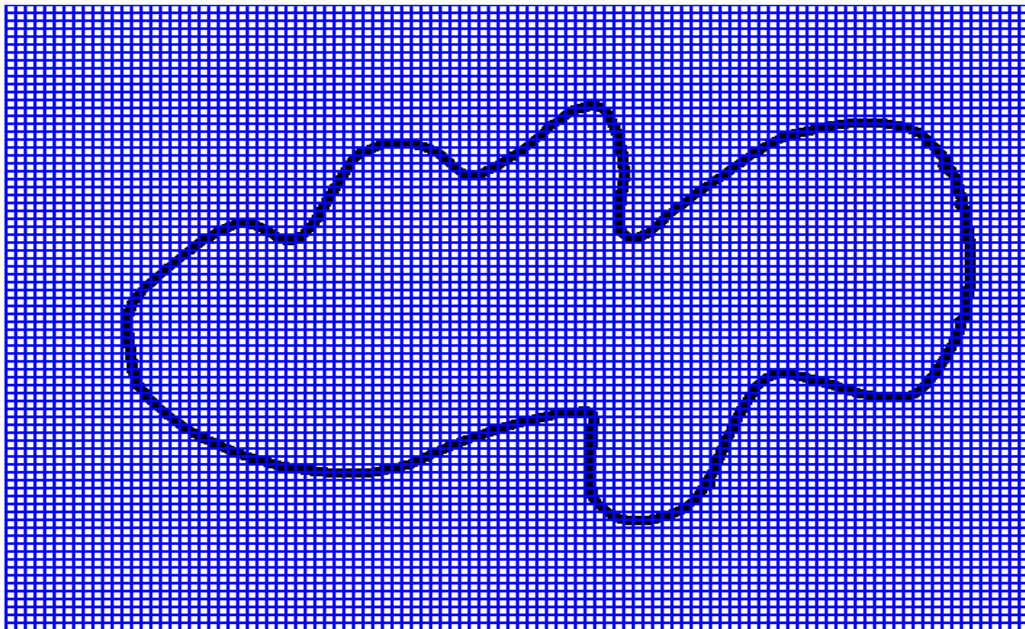


Figure 4. 21 Disintegrated Irregular Polygon

4.4.3 One Red Star Symbol '*' in the Centre of Every 5 Boxes

```
temp_pos = rect_pos(:, 1 : 2);
temp_pos(:, 1) = abs(temp_pos(:, 1) - cols / 2) / c_space;
temp_pos(:, 2) = abs(temp_pos(:, 2) - rows / 2) / r_space;
star_pos = [];
for i = 1 : size(temp_pos, 1)
    if rem(temp_pos(i, 1), 3) == 0 && rem(temp_pos(i, 2), 3) == 0 ...
        && rect_pos(i, 1) >= c_space * 2 && rect_pos(i, 1) <= cols - 3 * c_space ...
        && rect_pos(i, 2) >= r_space * 2 && rect_pos(i, 2) <= rows - 3 * r_space
        star_pos = [star_pos; rect_pos(i, 1 : 2)];
    end
end
star_pos(:, 1) = star_pos(:, 1) + c_space / 2;
star_pos(:, 2) = star_pos(:, 2) + r_space / 2;

star_BW = insertMarker(rect_BW, star_pos, 'star', 'color', 'red', 'size', 2);
star_BW2 = insertMarker(rect_BW2, star_pos, 'star', 'color', 'red', 'size', 2);
figure, imshow(star_BW2); % Figure 4.22 displays the asterisk at equal interval.
title('3')
```

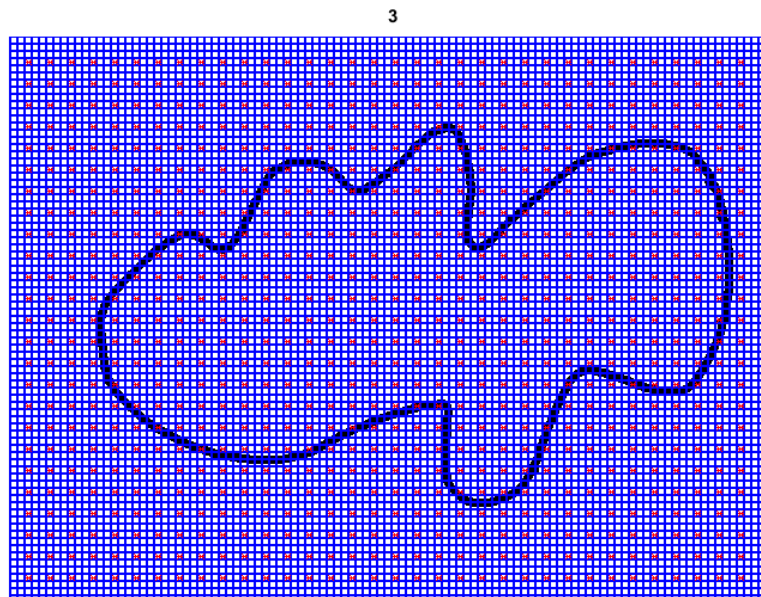


Figure 4.22 Mark the targets at specific sequence

4.4.4 Remove All the Boxes That Are Outside the Boundary

```
in_rect_pos = [];  
  
for i = 1 : size(rect_pos)  
    x1 = rect_pos(i, 1); y1 = rect_pos(i, 2);  
    x2 = x1 + rect_pos(i, 3); y2 = y1 + rect_pos(i, 4);  
    if inpolygon(x1, y1, x, y) && inpolygon(x1, y2, x, y) ...  
        && inpolygon(x2, y1, x, y) && inpolygon(x2, y2, x, y) ...  
        in_rect_pos = [in_rect_pos; rect_pos(i, :)];  
    end  
end  
  
% Draw Rectangle  
  
in_BW4 = insertShape(BW, 'rectangle', in_rect_pos, 'Color', [0, 0, 1]);  
figure, imshow(in_BW4) % Figure 4.23 Remove the mesh outside the boundary.  
title('4')
```

4

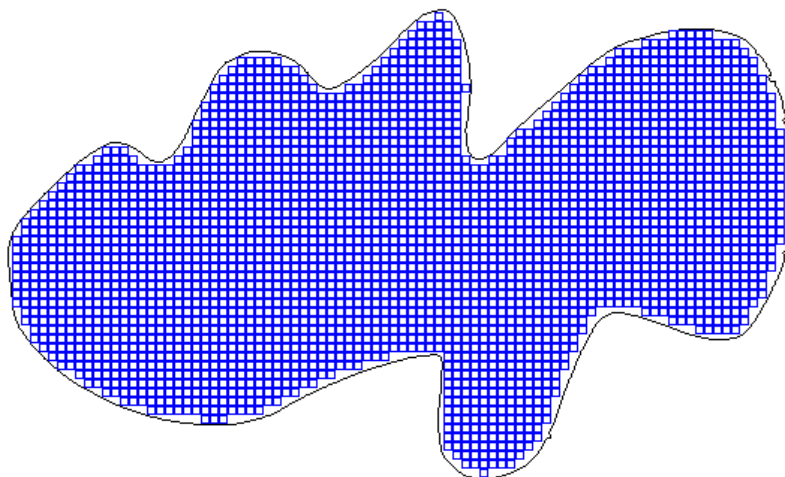


Figure 4. 23 Irregular Polygon with Clean Boundary

4.4.5 Remove the Sharp Edges from the Boundary

```
in_rect_pos = unique(in_rect_pos, 'rows');
i = 1;
while i < size(in_rect_pos, 1)
    pos = in_rect_pos(i, :);
    x_sub = in_rect_pos(in_rect_pos(:, 1) == pos(1), :);
    x_sub = x_sub((x_sub(:, 2) >= pos(2) - 4 * r_space) & (x_sub(:, 2) <= pos(2) + 4 * r_space), :);
    y_sub = in_rect_pos(in_rect_pos(:, 2) == pos(2), :);
    y_sub = y_sub((y_sub(:, 1) >= pos(1) - 4 * c_space) & (y_sub(:, 1) <= pos(1) + 4 * c_space), :);
    if size(x_sub, 1) < 5 || size(y_sub, 1) < 5
        in_rect_pos(i, :) = [];
    else
        i = i + 1;
    end
end
end
% Draw Rectangle
in_BW5 = insertShape(BW, 'rectangle', in_rect_pos, 'Color', [0, 0, 1]);
figure, imshow(in_BW5) % Figure 4.24 display the image without sharp edges.
title('5')
```

5

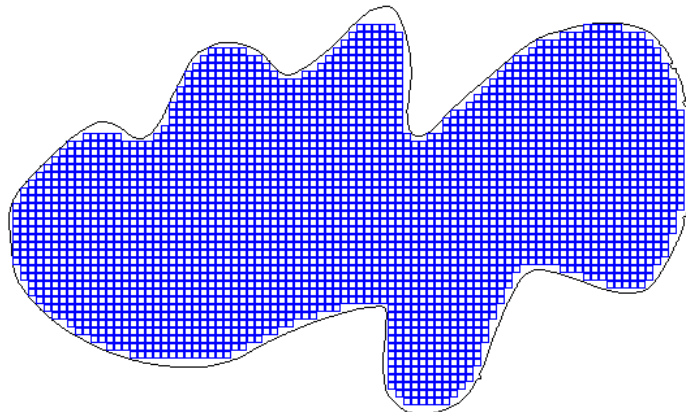


Figure 4. 24 Irregular Polygon without Sharp Edges

4.4.6 Remove All the ‘*’ that Are Touching or Outside the Boundary

```
in_star_pos = [];  
for i = 1 : size(star_pos)  
    x1 = star_pos(i, 1) - c_space / 2; y1 = star_pos(i, 2) - r_space / 2;  
    x2 = x1 + c_space; y2 = y1 + r_space;  
    if inpolygon(x1, y1, x, y) && inpolygon(x1, y2, x, y) ...  
        && inpolygon(x2, y1, x, y) && inpolygon(x2, y2, x, y) ...  
        in_star_pos = [in_star_pos; star_pos(i, :)];  
    end  
end  
in_star_pos = unique(in_star_pos, 'rows');  
  
% Draw Star  
in_BW6 = insertMarker(in_BW5, in_star_pos, 'star', 'color', 'red', 'size', 2);  
figure, imshow(in_BW6) % Figure 4.25 Reevaluate the asterisk.  
  
title('6')
```

6

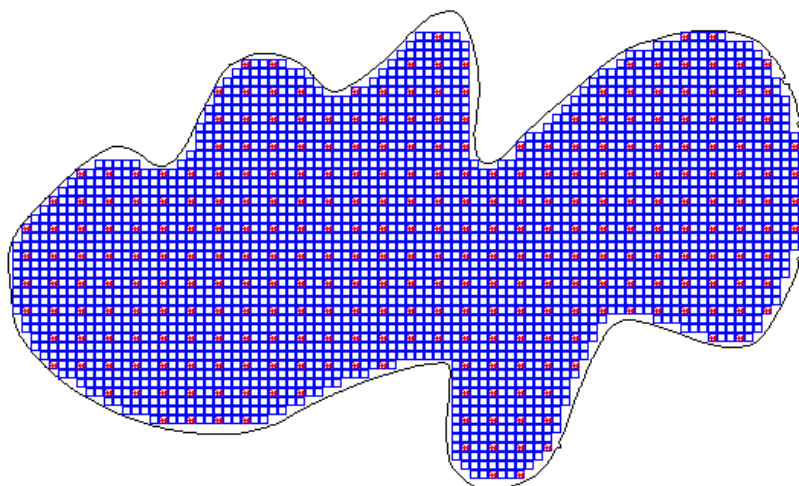


Figure 4.25 Final image including boxes

4.4.7 Remove All the Boxes Inside the Shape

```
in_BW7 = insertMarker(BW, in_star_pos, 'star', 'color', 'red', 'size', 2);  
in_BW7 = insertMarker(in_BW7, [0, rows], 'x-mark', 'color', 'red', 'size', 5);  
figure, imshow(in_BW7) % Figure 4.26 demonstrates the final trajectory to grasp.  
  
hold on  
title('7')
```

7

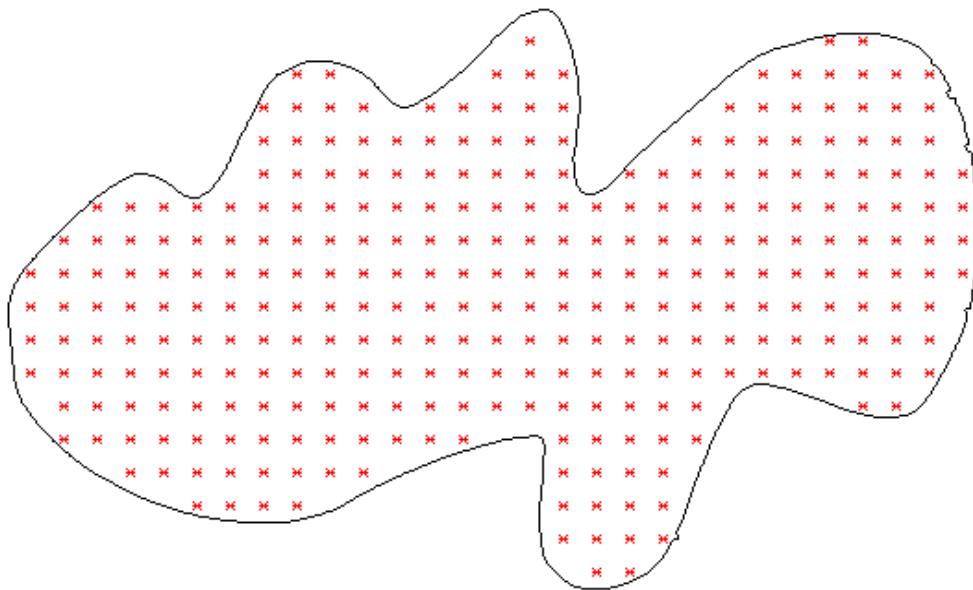


Figure 4. 26 The final trajectory of the polygon to grasp the object

4.5 Robot Coordinates and Communication

To define the position of every target in the trajectory domain it is necessary to name all those. The nomenclature begins with letter P and starts from top left corner as shown in Figure 4.27.

```
figure, imshow(in_BW7)
hold on
plot([1, cols], [rows, rows], 'red', [1, 1], [1, rows], 'red');
for i = 1 : size(in_star_pos)
    pt = in_star_pos(i, :);
    text(pt(1) - 7, pt(2) - 5, ['P', num2str(i)], 'FontSize', 5)
end
title('8') % Figure 4.27 displays the name each coordinate of the trajectory.
```

8

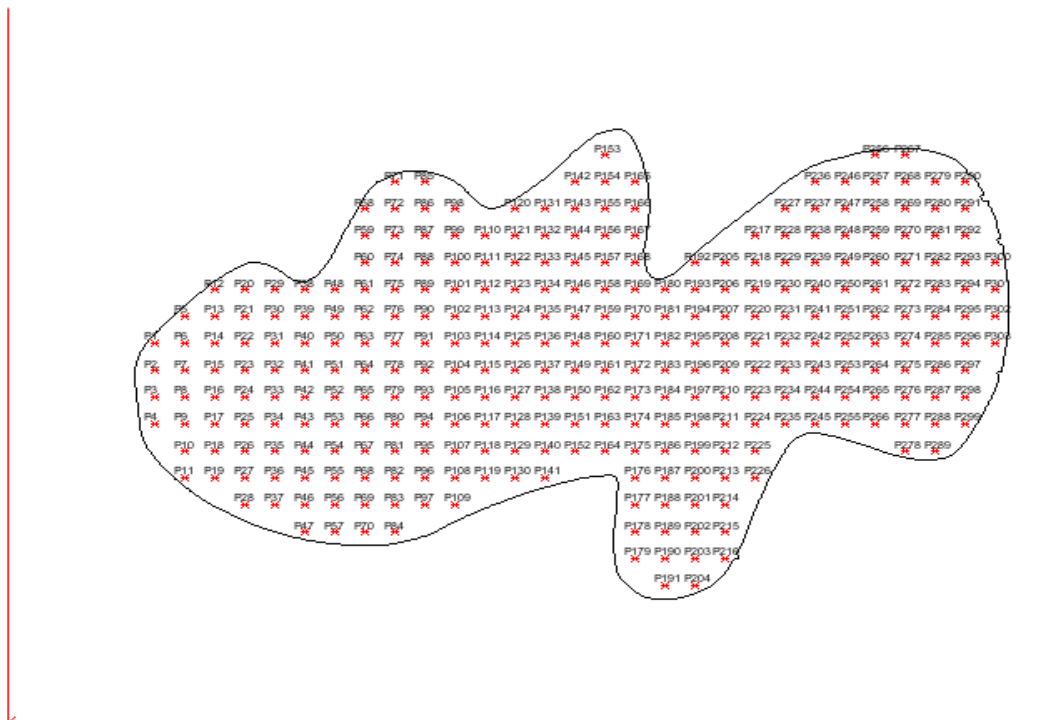


Figure 4.27 Robot Coordinates of trajectory

4.5.1 Distance in Cartesian Coordinates with Respect to Origin

The Cartesian coordinates are being calculated using following Algorithm.

```
[rows, cols] = size(gray);
rm = rows / 210;
cm = cols / 297;

% First Distance
fd = sqrt((in_star_pos(:, 1) / cm) .^ 2 + ((rows - in_star_pos(:, 2)) / rm) .^ 2);
fd_str = 'First distance is ';
for i = 1 : length(fd)
    fd_str = [fd_str, num2str(fd(i)), 'mm, '];
end
%disp(fd_str);

% Second Distance
sd = [];
for i = 1 : size(in_star_pos)
    pt = in_star_pos(i, :);
    dis = sqrt(((x - pt(1)) / cm) .^ 2 + ((y - pt(2)) / rm) .^ 2);
    sd = [sd, min(dis)];
end
sd_str = 'Second distance is ';
for i = 1 : length(sd)
    sd_str = [sd_str, num2str(sd(i)), 'mm, '];
end

out_str = "";
% for i = 1 : length(sd)
%     out_str = [out_str, 'P', num2str(i), ': (', num2str(fd(i)), 'mm, ', num2str(sd(i)), 'mm), '];
% end

for i = 1 : length(sd)
    out_str = [out_str, 'P', num2str(i), ': (', num2str(in_star_pos(i, 1) / cm), 'mm, ', num2str((rows -
in_star_pos(i, 2)) / rm), 'mm), '];
end

disp(out_str)
```

4.5.2 Cartesian Coordinates of Trajectory

P1: (41.3016mm, 111.5625mm), P2: (41.3016mm, 103.6875mm), P3: (41.3016mm, 95.8125mm), P4: (41.3016mm, 87.9375mm), P5: (49.6547mm, 119.4375mm), P6: (49.6547mm, 111.5625mm), P7: (49.6547mm, 103.6875mm), P8: (49.6547mm, 95.8125mm), P9: (49.6547mm, 87.9375mm), P10: (49.6547mm, 80.0625mm), P11: (49.6547mm, 72.1875mm), P12: (58.0078mm, 127.3125mm), P13: (58.0078mm, 119.4375mm), P14: (58.0078mm, 111.5625mm), P15: (58.0078mm, 103.6875mm), P16: (58.0078mm, 95.8125mm), P17: (58.0078mm, 87.9375mm), P18: (58.0078mm, 80.0625mm), P19: (58.0078mm, 72.1875mm), P20: (66.3609mm, 127.3125mm), P21: (66.3609mm, 119.4375mm), P22: (66.3609mm, 111.5625mm), P23: (66.3609mm, 103.6875mm), P24: (66.3609mm, 95.8125mm), P25: (66.3609mm, 87.9375mm), P26: (66.3609mm, 80.0625mm), P27: (66.3609mm, 72.1875mm), P28: (66.3609mm, 64.3125mm), P29: (74.7141mm, 127.3125mm), P30: (74.7141mm, 119.4375mm), P31: (74.7141mm, 111.5625mm), P32: (74.7141mm, 103.6875mm), P33: (74.7141mm, 95.8125mm), P34: (74.7141mm, 87.9375mm), P35: (74.7141mm, 80.0625mm), P36: (74.7141mm, 72.1875mm), P37: (74.7141mm, 64.3125mm), P38: (83.0672mm, 127.3125mm), P39: (83.0672mm, 119.4375mm), P40: (83.0672mm, 111.5625mm), P41: (83.0672mm, 103.6875mm), P42: (83.0672mm, 95.8125mm), P43: (83.0672mm, 87.9375mm), P44: (83.0672mm, 80.0625mm), P45: (83.0672mm, 72.1875mm), P46: (83.0672mm, 64.3125mm), P47: (83.0672mm, 56.4375mm), P48: (91.4203mm, 127.3125mm), P49: (91.4203mm, 119.4375mm), P50: (91.4203mm, 111.5625mm), P51: (91.4203mm, 103.6875mm), P52: (91.4203mm, 95.8125mm), P53: (91.4203mm, 87.9375mm), P54: (91.4203mm, 80.0625mm), P55: (91.4203mm, 72.1875mm), P56: (91.4203mm, 64.3125mm), P57: (91.4203mm, 56.4375mm), P58: (99.7734mm, 150.9375mm), P59: (99.7734mm, 143.0625mm), P60: (99.7734mm, 135.1875mm), P61: (99.7734mm, 127.3125mm), P62: (99.7734mm, 119.4375mm), P63: (99.7734mm, 111.5625mm), P64: (99.7734mm, 103.6875mm), P65: (99.7734mm, 95.8125mm), P66: (99.7734mm, 87.9375mm), P67: (99.7734mm, 80.0625mm), P68: (99.7734mm, 72.1875mm), P69: (99.7734mm, 64.3125mm), P70: (99.7734mm, 56.4375mm), P71: (108.1266mm, 158.8125mm), P72: (108.1266mm, 150.9375mm), P73: (108.1266mm, 143.0625mm), P74: (108.1266mm, 135.1875mm), P75: (108.1266mm, 127.3125mm), P76: (108.1266mm, 119.4375mm), P77: (108.1266mm, 111.5625mm), P78: (108.1266mm, 103.6875mm), P79: (108.1266mm, 95.8125mm), P80: (108.1266mm, 87.9375mm), P81: (108.1266mm, 80.0625mm), P82: (108.1266mm, 72.1875mm), P83: (108.1266mm, 64.3125mm), P84: (108.1266mm, 56.4375mm), P85: (116.4797mm, 158.8125mm), P86: (116.4797mm, 150.9375mm), P87: (116.4797mm, 143.0625mm), P88: (116.4797mm, 135.1875mm), P89: (116.4797mm, 127.3125mm), P90: (116.4797mm, 119.4375mm), P91: (116.4797mm, 111.5625mm), P92: (116.4797mm, 103.6875mm), P93: (116.4797mm, 95.8125mm), P94: (116.4797mm, 87.9375mm), P95: (116.4797mm, 80.0625mm), P96: (116.4797mm, 72.1875mm), P97: (116.4797mm, 64.3125mm), P98: (124.8328mm, 150.9375mm), P99: (124.8328mm, 143.0625mm), P100: (124.8328mm, 135.1875mm), P101: (124.8328mm, 127.3125mm), P102: (124.8328mm, 119.4375mm), P103: (124.8328mm, 111.5625mm), P104: (124.8328mm, 103.6875mm), P105: (124.8328mm, 95.8125mm), P106: (124.8328mm, 87.9375mm), P107: (124.8328mm, 80.0625mm), P108: (124.8328mm, 72.1875mm), P109: (124.8328mm, 64.3125mm), P110: (133.1859mm, 143.0625mm), P111: (133.1859mm, 135.1875mm), P112: (133.1859mm, 127.3125mm), P113: (133.1859mm, 119.4375mm), P114: (133.1859mm, 111.5625mm), P115: (133.1859mm, 103.6875mm), P116: (133.1859mm, 95.8125mm), P117: (133.1859mm, 87.9375mm), P118: (133.1859mm, 80.0625mm), P119: (133.1859mm, 72.1875mm), P120: (141.5391mm, 150.9375mm), P121: (141.5391mm, 143.0625mm), P122: (141.5391mm, 135.1875mm), P123: (141.5391mm, 127.3125mm), P124: (141.5391mm, 119.4375mm), P125: (141.5391mm, 111.5625mm), P126: (141.5391mm, 103.6875mm), P127: (141.5391mm, 95.8125mm), P128: (141.5391mm, 87.9375mm), P129: (141.5391mm, 80.0625mm), P130: (141.5391mm, 72.1875mm), P131: (149.8922mm, 150.9375mm), P132: (149.8922mm, 143.0625mm), P133: (149.8922mm,

135.1875mm), P134: (149.8922mm, 127.3125mm), P135: (149.8922mm, 119.4375mm), P136: (149.8922mm, 111.5625mm), P137: (149.8922mm, 103.6875mm), P138: (149.8922mm, 95.8125mm), P139: (149.8922mm, 87.9375mm), P140: (149.8922mm, 80.0625mm), P141: (149.8922mm, 72.1875mm), P142: (158.2453mm, 158.8125mm), P143: (158.2453mm, 150.9375mm), P144: (158.2453mm, 143.0625mm), P145: (158.2453mm, 135.1875mm), P146: (158.2453mm, 127.3125mm), P147: (158.2453mm, 119.4375mm), P148: (158.2453mm, 111.5625mm), P149: (158.2453mm, 103.6875mm), P150: (158.2453mm, 95.8125mm), P151: (158.2453mm, 87.9375mm), P152: (158.2453mm, 80.0625mm), P153: (166.5984mm, 166.6875mm), P154: (166.5984mm, 158.8125mm), P155: (166.5984mm, 150.9375mm), P156: (166.5984mm, 143.0625mm), P157: (166.5984mm, 135.1875mm), P158: (166.5984mm, 127.3125mm), P159: (166.5984mm, 119.4375mm), P160: (166.5984mm, 111.5625mm), P161: (166.5984mm, 103.6875mm), P162: (166.5984mm, 95.8125mm), P163: (166.5984mm, 87.9375mm), P164: (166.5984mm, 80.0625mm), P165: (174.9516mm, 158.8125mm), P166: (174.9516mm, 150.9375mm), P167: (174.9516mm, 143.0625mm), P168: (174.9516mm, 135.1875mm), P169: (174.9516mm, 127.3125mm), P170: (174.9516mm, 119.4375mm), P171: (174.9516mm, 111.5625mm), P172: (174.9516mm, 103.6875mm), P173: (174.9516mm, 95.8125mm), P174: (174.9516mm, 87.9375mm), P175: (174.9516mm, 80.0625mm), P176: (174.9516mm, 72.1875mm), P177: (174.9516mm, 64.3125mm), P178: (174.9516mm, 56.4375mm), P179: (174.9516mm, 48.5625mm), P180: (183.3047mm, 127.3125mm), P181: (183.3047mm, 119.4375mm), P182: (183.3047mm, 111.5625mm), P183: (183.3047mm, 103.6875mm), P184: (183.3047mm, 95.8125mm), P185: (183.3047mm, 87.9375mm), P186: (183.3047mm, 80.0625mm), P187: (183.3047mm, 72.1875mm), P188: (183.3047mm, 64.3125mm), P189: (183.3047mm, 56.4375mm), P190: (183.3047mm, 48.5625mm), P191: (183.3047mm, 40.6875mm), P192: (191.6578mm, 135.1875mm), P193: (191.6578mm, 127.3125mm), P194: (191.6578mm, 119.4375mm), P195: (191.6578mm, 111.5625mm), P196: (191.6578mm, 103.6875mm), P197: (191.6578mm, 95.8125mm), P198: (191.6578mm, 87.9375mm), P199: (191.6578mm, 80.0625mm), P200: (191.6578mm, 72.1875mm), P201: (191.6578mm, 64.3125mm), P202: (191.6578mm, 56.4375mm), P203: (191.6578mm, 48.5625mm), P204: (191.6578mm, 40.6875mm), P205: (200.0109mm, 135.1875mm), P206: (200.0109mm, 127.3125mm), P207: (200.0109mm, 119.4375mm), P208: (200.0109mm, 111.5625mm), P209: (200.0109mm, 103.6875mm), P210: (200.0109mm, 95.8125mm), P211: (200.0109mm, 87.9375mm), P212: (200.0109mm, 80.0625mm), P213: (200.0109mm, 72.1875mm), P214: (200.0109mm, 64.3125mm), P215: (200.0109mm, 56.4375mm), P216: (200.0109mm, 48.5625mm), P217: (208.3641mm, 143.0625mm), P218: (208.3641mm, 135.1875mm), P219: (208.3641mm, 127.3125mm), P220: (208.3641mm, 119.4375mm), P221: (208.3641mm, 111.5625mm), P222: (208.3641mm, 103.6875mm), P223: (208.3641mm, 95.8125mm), P224: (208.3641mm, 87.9375mm), P225: (208.3641mm, 80.0625mm), P226: (208.3641mm, 72.1875mm), P227: (216.7172mm, 150.9375mm), P228: (216.7172mm, 143.0625mm), P229: (216.7172mm, 135.1875mm), P230: (216.7172mm, 127.3125mm), P231: (216.7172mm, 119.4375mm), P232: (216.7172mm, 111.5625mm), P233: (216.7172mm, 103.6875mm), P234: (216.7172mm, 95.8125mm), P235: (216.7172mm, 87.9375mm), P236: (225.0703mm, 158.8125mm), P237: (225.0703mm, 150.9375mm), P238: (225.0703mm, 143.0625mm), P239: (225.0703mm, 135.1875mm), P240: (225.0703mm, 127.3125mm), P241: (225.0703mm, 119.4375mm), P242: (225.0703mm, 111.5625mm), P243: (225.0703mm, 103.6875mm), P244: (225.0703mm, 95.8125mm), P245: (225.0703mm, 87.9375mm), P246: (233.4234mm, 158.8125mm), P247: (233.4234mm, 150.9375mm), P248: (233.4234mm, 143.0625mm), P249: (233.4234mm, 135.1875mm), P250: (233.4234mm, 127.3125mm), P251: (233.4234mm, 119.4375mm), P252: (233.4234mm, 111.5625mm), P253: (233.4234mm, 103.6875mm), P254: (233.4234mm, 95.8125mm), P255: (233.4234mm, 87.9375mm), P256: (241.7766mm, 166.6875mm), P257: (241.7766mm, 158.8125mm), P258: (241.7766mm, 150.9375mm), P259: (241.7766mm, 143.0625mm), P260: (241.7766mm, 135.1875mm), P261: (241.7766mm, 127.3125mm), P262: (241.7766mm,

119.4375mm), P263: (241.7766mm, 111.5625mm), P264: (241.7766mm, 103.6875mm), P265: (241.7766mm, 95.8125mm), P266: (241.7766mm, 87.9375mm), P267: (250.1297mm, 166.6875mm), P268: (250.1297mm, 158.8125mm), P269: (250.1297mm, 150.9375mm), P270: (250.1297mm, 143.0625mm), P271: (250.1297mm, 135.1875mm), P272: (250.1297mm, 127.3125mm), P273: (250.1297mm, 119.4375mm), P274: (250.1297mm, 111.5625mm), P275: (250.1297mm, 103.6875mm), P276: (250.1297mm, 95.8125mm), P277: (250.1297mm, 87.9375mm), P278: (250.1297mm, 80.0625mm), P279: (258.4828mm, 158.8125mm), P280: (258.4828mm, 150.9375mm), P281: (258.4828mm, 143.0625mm), P282: (258.4828mm, 135.1875mm), P283: (258.4828mm, 127.3125mm), P284: (258.4828mm, 119.4375mm), P285: (258.4828mm, 111.5625mm), P286: (258.4828mm, 103.6875mm), P287: (258.4828mm, 95.8125mm), P288: (258.4828mm, 87.9375mm), P289: (258.4828mm, 80.0625mm), P290: (266.8359mm, 158.8125mm), P291: (266.8359mm, 150.9375mm), P292: (266.8359mm, 143.0625mm), P293: (266.8359mm, 135.1875mm), P294: (266.8359mm, 127.3125mm), P295: (266.8359mm, 119.4375mm), P296: (266.8359mm, 111.5625mm), P297: (266.8359mm, 103.6875mm), P298: (266.8359mm, 95.8125mm), P299: (266.8359mm, 87.9375mm), P300: (275.1891mm, 135.1875mm), P301: (275.1891mm, 127.3125mm), P302: (275.1891mm, 119.4375mm), P303: (275.1891mm, 111.5625mm).

4.6 Summary

This chapter explores different MATLAB tools that has been used to design the Algorithms. Nonetheless, there are many studies on MATLAB software which is considered more reliable by many MV technology providers in Australia. The current study aims at exploring further MATLAB image processing tools and techniques to understand the MV for irregular shapes. As discussed earlier, the objective of the software analysis is to reduce the processing time using numerical methods. However, the analysis made by MATLAB is the best method of evaluating all the possible combinations to test and deploy them on the hardware in real time. This chapter mainly covered the step by step development of Algorithms. Section 4.4.1 to 4.4.7 has covered the seven stages, begins with the image acquisition till formulating the point-based trajectory. The cartesian coordinates developed in section 4.5.2 is the information of each spot on the irregular shape to grasp. These points are developed by avoiding the sharp edges and perforation because if the solenoid turns the vacuum on the perforated area, the total pressure of the vacuum system can be reduced that leads the risk to drop the object during palletising. However, the Robot end effector uses the coordinate information precisely to control the solenoids that are on the object and keep others turned off. The next chapter is to validate the information of the coordinate points that is formulated in this chapter by the integration of MV system with the Robot controller to run the validation tests in real time.

Chapter 5

Chapter # 5 Developing a Prototype to Test the Algorithm Experimentally

- 5.1 Introduction
- 5.2 Development of Robot Control Unit
- 5.3 MACH3 Configuration and Robot Programming
- 5.4 Preliminary Study of Robot Motion
- 5.5 Experiments on Irregular Shapes
- 5.6 Overall Performance of MV System
- 5.7 Summary

5.1 Introduction

Chapter 5 discuss the development of prototype using the Robot Mitsubishi RM-501 (5-Axis Serial Robot) to test the behaviour of Algorithm in real time. The control unit of the Robot is replaced by the new state of the art DSP controller F280049C. This controller is configured in MATLAB software to be used as a DC servo driver and integrated with CYTRON MDD10A board to operate the DC servo motors with incremental encoders. After the development of the board the Robot kinematics is tested with MACH3 software. MACH3 can run up to 6 axes simultaneously therefore parameters of the Robots are set in the software to test the motion. The programming language for the MACH3 is ‘G’ codes hence all the positional information is sent in terms of ‘G’ codes from the MV system that is developed in the research. There are various experiments conducted to validate the Algorithm. First test was to check the Robot accuracies and kinematics to make sure that it is working in tolerances. Afterwards the different irregular polygonal shapes are placed under the camera and the Robot moves on the designated trajectory points to verify the Algorithm.

5.2 Development of Robot Control Unit

RCU is developed using TSM320F280049C DSP controller. The DSP is capable for fast mathematical calculations and the selection of TSM320F280049C is based on its capabilities like high resolution 24-bit position counters, two independent channels for interfacing the incremental encoders and ten PWM channels outputs for controlling the Robot. The board also connects with MATLAB using USB interface and its support library is available in the environment through its software add on. The software also allows to collect the real-time data values that is used to process the information directly, which saves much time. The programming of this board is very complex but due to MATLAB SIMULINK libraries it gets easy to program and test the Algorithm on the hardware. The RCU (TMS320F280049C) is further integrated to DCM50202 Lead shine Motor and MDD10A CYTRON Actuator to develop a fully closed loop servo system as shown in Figures 5.1 and 5.2.

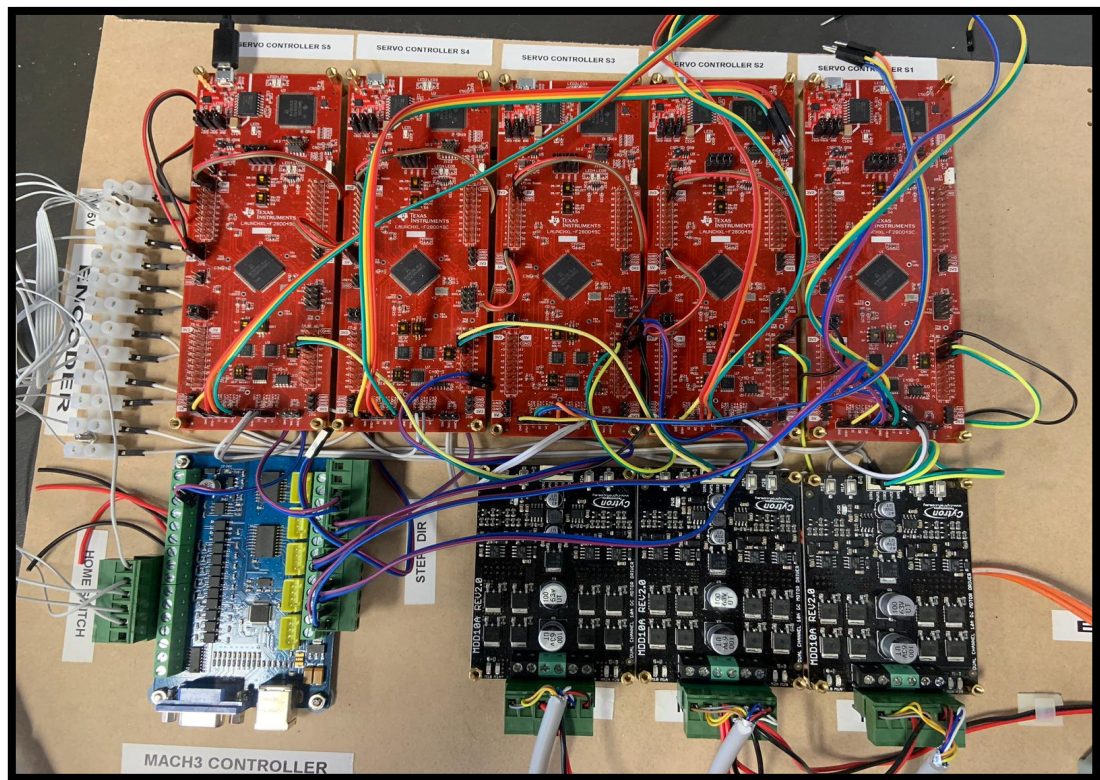


Figure 5.1 Robot Control Unit



Figure 5.2 Mitsubishi RM 501 5-Axis Serial Robot

5.2.1 RCU Part-1 F280049C DSP Micro-Controller

The C2000 LAUNCHXL-F280049C is minimal effort advancement board for the TI (Texas Instruments) Piccolo F28004x arrangement of MCUs. It is planned around the TMS320F280049C MCU and features the control, simple and correspondences peripherals, just as the incorporated non-volatile memory. The Launchpad additionally includes two autonomous Booster Pack XL extension connectors, on-board CAN (Controller Area Network) handset, 5V encoder connectors, FSI connector and a ready XDS110 troubleshoot test. The F280049CPZS is a 32-piece gliding point MCUs with 256KB Flash memory, 100KB RAM and works at 100 MHz (Megahertz). It incorporates propelled control peripherals, separated simple and different correspondences peripherals. The gadgets have been improved for elite applications and give an ease framework arrangement.

The greater part of the MCU's sign is directed to 0.1-inch (2.54 mm) pitch headers spread out to consent to the TI Booster Pack principles with a couple of special cases. An interior multiplexer permits distinctive fringe capacities to be doled out to every one of the GPIOs (General Purpose Input Output) cushions. The multiplexing alternatives can be found in the gadget explicit information sheet. When including outside hardware, consider the extra burden on the advancement board power rails. The F28004x Launchpad is a production line customized with a snappy beginning demo program. The speedy beginning program dwells in the on-chip Flash memory and executes each time power is applied, except if the application has been supplanted with a client program. The brisk beginning application uses the incorporated Simple ADC module to test the voltage on a stick, at that point yield the outcomes with the SCI (Sequential Communications Interface), UART (Universal Asynchronous Receiver-Transmitter) through the VCP (Virtual COM Port) of the XDS110 investigate test to a PC (Personal Computer) with a sequential screen running.

This controller has two incremental modules J12 and J13. J12 is used to collect the differential signals of the encoder that is 1000 line per revolution becomes 4000 step per revolution due to quadrature. These values are converted as a counter While J13 receives the commands signals from MACH3 that describes the target position of each actuator. These signals are processed to develop a servo system of the Robot. The values of J12 and J13 are compared to adjust the error through PID (Proportional Integral Differential).

Furthermore, header J6 pins 77 and 78 are used to transmit the PWM and DIR (Direction) signals to control the position and speed.

The prescribed strides for utilizing the F28004x Launchpad are:

Pursue the README First report incorporated into the unit. This helps to run the Launchpad for the first time. Inside only a couple of minutes, pre-modified brisk beginning application can control the Launchpad.

Trial with Booster Packs. This advancement unit conforms to the most recent amendment of the Booster Pack pinout standard. It has two autonomous Booster Pack associations with empowering an assortment of extension openings.

Venture out building up control applications. The F28004x Launchpad is supported by the C2000Ware advancement package. After C2000Ware is introduced, search for f28004x\examples\launchpad in the establishment index. Pre-designed model applications are available for this board just as for this board with chose Booster Packs. Any of the other models discovered withing the f28004x\examples index can be utilized with minor alterations to keep running on the Launchpad too.

Tweak and incorporate the hardware to suit end application. This advancement pack can be utilized as a kind of perspective for structure custom circuits dependent on C2000 Piccolo Series MCUs or as an establishment for development with custom Booster Pack or different circuits. This report can fill in as a beginning stage for this undertaking.

The LAUNCHXL-F280049C gives a simple approach to create applications with the F28004x Series MCU. Booster Packs are add-on sheets that adhere to a stick out standard. The TI and outsider environment of Booster Packs significantly grows the peripherals. Construct the customised Booster Pack by following the structure rules on website. TI even wants to elevate your Booster Pack to different individuals from the network. TI offers an assortment of roads to arrive at potential clients with all answers.

5.2.1.1 Insta-SPIN-FOC (Field Oriented Control)

The LAUNCHXL-F280049C incorporates the Piccolo TMS320F280049C that has the superset design of highlights empowered, including Insta-SPIN-FOC sensor less engine control innovation. A library is incorporated into on-chip ROM that can be retrieved by a lot of software APIs, as shown by ventures incorporated into C2000Ware Motor control Software Development Kit (accessible 2018Q4). Insta-SPIN-FOC innovation distinguishes engine parameters, self-tunes the sensor less FAST™ spectator, sets stable tuning for the present controllers, and enables to rapidly control three-stage engines under cutting edge, a superior field situated vector control without the requirement for mechanical rotor sensors.

LAUNCHXL-F280049C is an ease assessment and advancement apparatus for the Piccolo F28004x arrangement (counting Insta-SPIN-FOC capacity) in the TI MCU Launchpad biological system which is perfect with different fitting on Booster Packs. This all-encompassing adaptation of the Launchpad supports the association of two Booster Packs. The Launchpad gives an institutionalized and simple to utilize the platform to utilize while building up your next application.

The F28004x Launchpad incorporates two headers, J12 and J13, which are utilized for associating straight or revolving gradual encoders. These headers take 5 V flag that are down-changed over to 3.3 V and wired to the F280049C MCU. These signs are associated with the eQEP (Enhanced Quadrature Encoder Pulse) modules on the gadget. Every header has the EQEPA, EQEPB and EQEPI signals accessible for each eQEP module just as pins for GND (Ground) and 5 V.

5.2.1.2 Hardware Features

F280049C DSP hardware features are as follows:

- TMS320F280049C: 100 MHz C28x CPU with FPU and TMU, 256 KB Flash, Insta-SPIN-FOC empowered, 3x 12-piece ADC, CAN, encoder, FSI, UART and that is only the tip of the iceberg
- On-board XDS110 investigate test for ongoing troubleshoot and glimmer programming
- 80 stick Launchpad utilizing the Booster Pack environment
- Power space segregation for ongoing troubleshoot and blaze programming

-
- Separated CAN handset
 - Two encoder interface connectors
 - FSI interface connector
 - Hardware Files are in C2000Ware at
boards\Launchpads\LAUNCHXL_F280049C
 - C2000 Piccolo Series F280049CPZS MCU:
 - Enabled for Insta-SPIN-FOC™ engine control and CLB (Configurable Logic Block) capacity
 - Two free eQEP - based encoder connectors
 - Separate FSI connector
 - Two free Booster Pack XL standard connectors including stackable headers to amplify development through the Booster Pack biological system
 - Solid-Thinking Embed Support
 - Preparing Video: PMSM control arrangement, including Insta-SPIN-FOC
 - Power-sim PSIM Support
 - Insta-SPIN Processor-insider savvy and code age highlight

5.2.2 RCU Part-2 DCM50202 DC Servo Motor

Conventionally, DC motors are used for converting direct electric current into mechanical energy. A brushed DC motor consists of internal commutation, permanent magnets and moving electromagnets. DCM50202 is permanent magnet brushed servo motor. It is used in wide range of applications from industrial automation to CNC machines. The DCM50202 is mostly used in developing CNC machines, Robotics, cutting machines, engraving machines and medical appliances. The DCM50202 also contains an encoder which sends position feedback to the controllers. The primary benefits of preferring brushed DC motors over conventional motors include cost efficiency, high compatibility, low power consumption, low energy sink and relatively easy control.

In DC motors, a rotor consisting of coil is placed between two permanent magnets. The ending terminals of the rotor are always in contact with the carbon brushes through split ring. The permanent magnets create a magnetic field which is called stator field. The electric current is passed through the carbon brushes to the rotor. When the current passes through the rotor in the presence of stator magnetic field, a force acts on the rotor which is called Lorentz force. The direction of induced Lorentz force often points perpendicularly to the flux of stator magnet field. This generates torques are functions of rotor angle, and it results in torque ripple. This resultant torques start rotating the rotor.

An encoder is used for monitoring the rotations of motors. The encoder can be used for inspecting the rotations of motor for inferring its parameters like velocity and acceleration. The encoders can be ‘incremental’ and ‘absolute’; these are two basic types of encoders and Robot motor uses incremental encoder only. The incremental encoders can be further divided into two classes: quadrature encoders and non-quadrature encoders. A non-quadrature encoder provides a single pulse to the controller for every incremental motion, and the information obtained in this way is restricted to a constraint that it provides the information only when the position changes. For surmounting this constraint, the quadrature encoder can be used. A quadrature encoder provides two pulses on every incremental motion and these two pulses are out of phase. These two pulses can be used for detecting velocity and acceleration along with the direction also.

5.2.3 RCU Part-3 MDD10A CYTRON Actuator

The DC brushed motors are widely used for developing the systems and complex machineries. The relatively low power consumption of DC brushed motors makes them an appropriate choice for developing the systems. For controlling and regulating the various parameters, including speed, direction and position of DC brushed motors they require motor drivers. These motor drivers are used for regulating the parameters of the DC brushed motors without having any detrimental impact on the other circuitry of the system. MDD10A is also a motor driver which has the capability of driving two independent DC brushed motors. The MDD10A motor driver is one of the series launched by CYTRON.

MDD10A is an extended version of MD10C. MD10C can drive only single DC motor while MDD10A is a motor driver with the functionality of ‘dual channel’ that can

drive two DC brushed motors. MDD10A is also compatible with PWM signals having the characteristics of being ‘locked antiphase’ and ‘sign magnitude’. Most primary strength of MDD10A is solid state components. The solid-state components have no moving parts; the absence of moving parts extensively reduces the risk of wear and tear because moving parts like relay often suffer from the minor spark at the time of making contact and this spark results in degradation of the components.

5.2.3.1 MDD10A Features:

Following are the main features of MDD10A motor driver:

- It has bidirectional control for two DC brushed motors.
- It is packaged with two activating toggling buttons for manual activation of each of the two channels.
- It has functionality of regenerative braking which saves energy.
- It is compatible with PWM signals exhibiting the characteristics of ‘locked antiphase’ and ‘sign magnitude’ signals.
- It supports motor voltage ranging from 5V to 30V.
- It supports logic level 3.3V and 5V for DIR and PWM inputs.
- It exhibits fast response and behaviour due to solid state components.
- It consists of full NMOS H-Bridge which increases the efficiency and eliminates the need of heat sink.
- It supports the TTL PWM from MCUs.

The DC Servo Motor specification list is described in Figure 5.3.

Serial No.	Parameters	Min.	Typical	Max.	Unit
1	Power Input Voltage	5	-	30	Volt
2	I_{max} (Maximum Continuous Motor Current)	-	-	10	Ampere
3	I_{peak} – (Peak Motor Current)	-	-	30	Ampere
4	V_{in} (Logic Input – High Level)	3	-	5.5	Volt
5	V_{in} (Logic Input – Low Level)	0	0	0.5	Volt
6	Maximum PWM Frequency	-	-	20	KHz

Figure 5.3 DC Servo Motor Parameters List

The voltage input, DC battery having the DC voltage ranging from 5V to 30V, which is to be fed to the motors, is connected to the MDD10A driver. The manual activation buttons should be pressed for resetting or testing the MDD10A driver. MDD10A motor driver uses two input pins PWM and DIR for controlling the speed and direction of the

connected DC brushed motors respectively. These two input pins are fed with signals in following two operational ways:

➤ **Sign-Magnitude PWM Signal:**

In this approach, two different control signals are used for controlling the speed and direction of the connected motors. PWM input pin is fed with signals for controlling the speed of the connected motors while DIR input pin is fed with signals for controlling the direction of the connected motors.

➤ **Locked-Antiphase PWM Signal:**

In this approach, only one control signal is used for controlling the speed and direction of the motors. The PWM input pin is set to HIGH while the DIR input pin is fed with the PWM signal. The motor stops running on 50% duty cycle of the PWM and takes corresponding directions CW (Clockwise) or CCW (Counter-Clockwise) at duty cycle below or above the 50%. The decision whether the motor should follow CW direction or CCW direction below and above the 50% duty cycle completely depends upon the connections.

5.2.4 MATLAB Support Package for F280049C

Embedded Coder Support Package for TI C2000 Processors is known for creating an ongoing executable program that can be downloaded to TI board. Embedded Coder basically creates C code and embeds the I/O gadget drivers in your graph and these gadget drivers are embedded in the created C code. This support package is utilitarian for R2013b and previous versions.

The expanding need for the present-day industry for motion control makes the software increasingly intricate. The recreation platform and the hardware test platform in the conventional control arrangement of PMSM (Permanent Magnet Synchronous Machine) are regularly free of one another.

Software developers using this support package can make their calculations in MATLAB and SIMULINK, as well as can target, coordinate, troubleshoot, and test those models in PIL (Processor in the Loop) reproduction. The C code produced from Embedded Coder keeps running on the Robot MCU for the infinite time as the loop is set to run forever.

For the purpose of client interest in MATLAB and SIMULINK support, ST forcefully built up the abilities to go past complete Cortex-M processor support by making extra fringe squares. It further improves procedure. After that empowering DSP-standard devices to keep running on your Cortex-M processor-based items enables the clients to address a more extensive range of chances. This activity empowers designers and developers to effectively and proficiently create and investigate various models before producing advanced code for their processor-based ventures.

SIMULINK Coder, MATLAB Coder, and Embedded Coder yield the ANSI/ISO C/C++ code that can be aggregated and executed on TI C2000 MCUs by the means of Code Composer Studio IDE. Embedded Coder will enable effective design of the code created from MATLAB and the calculations to control software interfaces, advance execution performance, and limits memory utilization. Embedded Coder Support Package for TI C2000 Processors gives the accompanying highlights:

- Mechanized form and execution
- Square libraries for on-chip and on-board peripherals, for example, ADC, computerized I/O, ePWM, SPI, I2C
- Ongoing parameter tuning and logging utilizing an outer mode
- Processor improved code including DMC and IQMath libraries
- Capacity to perform processor-insider savvy (PIL) tests with execution profiling
- Models for PMSM FOC engine control and DC/DC buck converter

This software has a few unmistakable favourable circumstances. MATLAB enables one to utilize an advanced-level language, which is like C++, known as m-code. MATLAB has many worked in capacities which can be utilized to achieve practically any error possible. These fields incorporate math, insights, video, picture securing and handling, RF configuration, signal preparing, re-enactment and some more.

SIMULINK is a platform that has most of similar usefulness of MATLAB, yet permits specialists to structure frameworks graphically, with a square chart interface. SIMULINK has standard block sets that enable the client to execute basic errands, for example, I/O, summers, signal steering, scopes and so on. Extra block sets can be bought that add additional usefulness to SIMULINK.

State flow is a segment of SIMULINK, which is valuable for indicating the conduct of frameworks. Ordinarily before, architects would initially determine the general conduct of the framework on paper, in a square outline (or pseudocode). They would then interpret that graph into operational code. State flow makes those two strides and makes them one. It permits the designer to drag obstructs into the model that speaks to states, changes occasions and control rationale. All of which can execute on an embedded objective. Constant Workshop is a significant part of SIMULINK that enables clients to create SIMULINK models on their work PC and actualize them on different targets. These objectives can incorporate different PCs, embedded PCs, MCUs, DSPs and even FPGAs. Some of the supported embedded targets incorporate TI's C6000 and C2000 DSPs. It is a typical test for designers to create and test software to do different undertakings on embedded hardware. This can regularly be a dull procedure. Designers normally plan out the calculation graphically or with pseudocode. They make an interpretation of that into a significant level language, which includes composing numerous lines of code. This has been the regular technique for some years; there is a developing strategy that includes creating calculations with graphical instruments. This improves advancement time, diminishes programming multifaceted nature, and encourages sharing of the structure with collaborators. The main software package that fits this shape is MATLAB, from The Math Works. It has numerous amazing characteristics that make it reasonable for reproduction, information control, and end hardware focusing on.

MATLAB envelops various features of designing. These have applications in capacities managing video and picture preparing, channel structure, interchanges, control framework plan, just to give some examples. As opposed to be a specialist in each field, the designer can concentrate on taking care of the current issue. All that is required is a fundamental learning of the MATLAB improvement condition, the assistance framework, and MATLAB's modifying language. It is a basic matter to find and incorporate the suitable capacities to tackle the present issue. MATLAB has exceptionally great information show capacities. There are 2-D and 3-D plots for which the client can control numerous parameters. While on the other hand, SIMULINK is an expansion of MATLAB that empowers clients to structure and reproduce frameworks by making square charts. Frameworks can be displayed as nonstop or discrete, or even a half and

half of the two. Designers browse a huge rundown of squares and essentially drag them into a model. Squares can incorporate sign generators, scopes, work squares, and even client characterized squares. The mouse can be utilized to draw interfacing lines between squares to collect the framework.

This support package can collect the real time data when hardware in loop. Before downloading the c codes to hardware, the models can be simulated and optimized using software in loop. The main features for the development of Robot controller is Real Time PID auto tuning. This tool is very help because it can find the PID values in real time and reduces the time to find the unknown motors parameters. Once the controller is tune in real time the actual simulation model values can be updated to download the program in the Robot controller.

5.2.5 Parameter Estimation for DCM50202

Alberto et al. [77] have upgraded an industrial Robot in 2017 by changing the old motors and drives with new one and tested the controller kinematics for MACH3 and Linux CNC. Nowadays, the retrofitting has reached to second era where the motor and drive do not change simultaneously. There are many techniques available for identifying and optimising the parameters of DC motor. Lord et al. has found the parameters by step voltage as input and armature current as output. He develops a model to optimise the servo motor controller [78]. Schulz et al. used a frequency response method in 1983 [79]. Weerasooriya et al. used neural networks to find the parameters 1991 [80]. Researchers have developed different methods for achieving the best optimised values 1992 to 2010 [81-95]. They found that only seeking the parameters is good for some applications. When we discuss about retrofitting the parameters seeking is not enough. Hence, Galijasevic et al. identify the parameters and build a speed controller in 2011 [96]. Garrido et al. used a closed loop approach for servo mechanism in 2012 [97]. Obeidat et al. improved the DC motor parameters by real time technique using quantized sensor in 2013 [98]. The swarm optimisation technique is used to further optimise the DC motor parameters in 2013-2017 [99-104], Nayak et al. has recently used Whale Optimisation Algorithm for DC Motor Parameter in March-2019 [105].

Servomotor is a most widely used actuator in many control system or process. It becomes essential when motor behaves exactly as required. To achieve exact control of

the motor, the components that exist inside the motor and the relationship of these components must be well known. The input is given to the motor and the output is received from the motor in terms of mechanical work. This section deals with the modelling of a DC Motor and the parameter estimations in MATLAB. There are various parameters to consider while modelling a motor. They are:

J = Moment of inertia, B = Viscous friction, K=Torque constant, R=Resistance, L=Inductance.

Model the motor with voltage (V) as input (that is directly proportional to the duty cycle) and speed ($\dot{\theta}$) as output. The rotational position of the motor is given by θ and the time derivative of the rotational position gives the rotational velocity.

The equation (5.1) obtained by modelling the DC Motor is:

$$\dot{\theta} = \frac{d(\theta)}{dt} \quad (5.1)$$

The equation (5.2) shows us the relationship between the current that is drawn by the motor, the moment of inertia and damping in the motor.

$$J\ddot{\theta} + B\dot{\theta} = Ki \quad (5.2)$$

The equation (5.3) is obtained by simple applying Kirchhoff's Voltage Law to the internal closed loop of a DC Motor.

$$L \frac{di}{dt} + Ri = V - K\dot{\theta} \quad (5.3)$$

Takes the Laplace Transform of both the equations and solve simultaneously to obtain the transfer function of the model that was designed in equation 5.4. The transfer function is the Laplace Transform of output to the Laplace Transform of input and it is given by the transfer function H(s):

$$H(s) = \frac{\dot{\theta}(s)}{V(s)} = \frac{K}{(Js+B)(Ls+R)+K^2} \quad (5.4)$$

Parameter Estimation is a study which belongs to statistics. The coefficients of motor model are found that can be either a transfer function or difference equation, which consists of an error signal. The input to a method which estimates the parameters is the data that is measured by some means and the estimator gives the output, which are the parameters of the model. There are multiple techniques that are adopted to estimate the parameter of a model. The methods, which are learning based, are iterative in nature. While the classical methods use calculations to estimate the parameters. All the methods need an input and an output to find the parameters.

After, mathematical model of motor the Parameter Estimation toolbox is used for finding the parameters. The initial parameters were assumed as 0.1 except resistance that was 2.5Ω . The real time data collected in next section that is used here to get the results in almost 15 iteration as shown in Figure 5.4.

The values are found: $B = 6.4558e-5$, $L = 1.9819e-12$, $K=0.0032$, $J=9.8716e-7$, $R=.0071$.

The transfer function is found equation (5.5) by substituting the values in equation (5.4) is stated as:

$$H(s) = \frac{\dot{\theta}(s)}{V(s)} = \frac{0.0032}{1.956e-18 s^2 + 7.009e-09 + 1.07e-05} \quad (5.5)$$

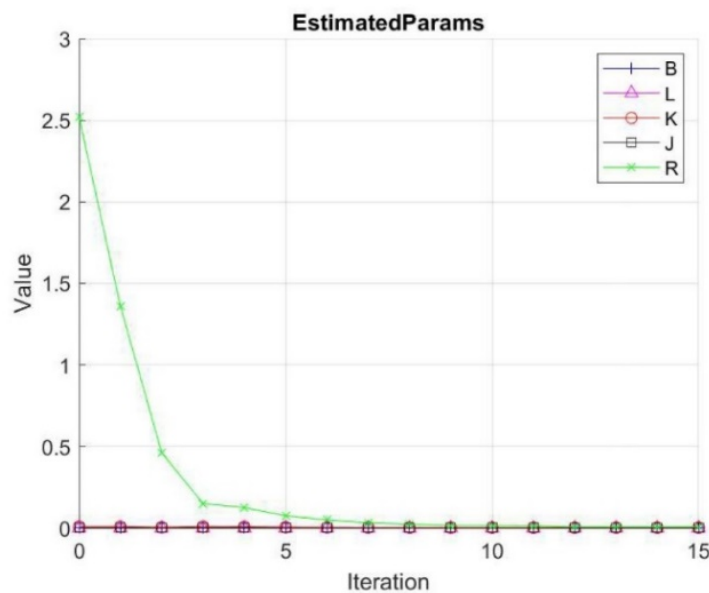


Figure 5.4 Parameter Estimation in MATLAB

5.2.6 Algorithm Development for RCU

This study is to design and develop an RCU to find DC Servo motor parameters by real time step testing method in a closed loop and deploy them to develop application specific controller that can be used with that Robot in real-time. This method is very useful for those Robots or machines whose all information has lost and they cannot work with the latest state of the art peripherals like MV system, torque sensors etc. This RCU Algorithm is designed on MATLAB SIMULINK and implemented on F280049C DSP controller. This application is tested on an old Robot RM-501 Move Master with MACH3 motion control.

5.2.6.1 Real Time Data Collection

LaunchXL-F280049C is 100 MHz DSP controller. All the data is collected using its quadrature encoder module. This controller is having two modules one for data collection by host MACH3 Controller and second is receiving the encoder signals. This module work in different modes. Counts direction mode for MACH3 data and CW and CCW mode for encoder is used. E-Capture module is used as APWM to generate PWM signals. Figure 5.5 displays the real time model in SIMULINK.

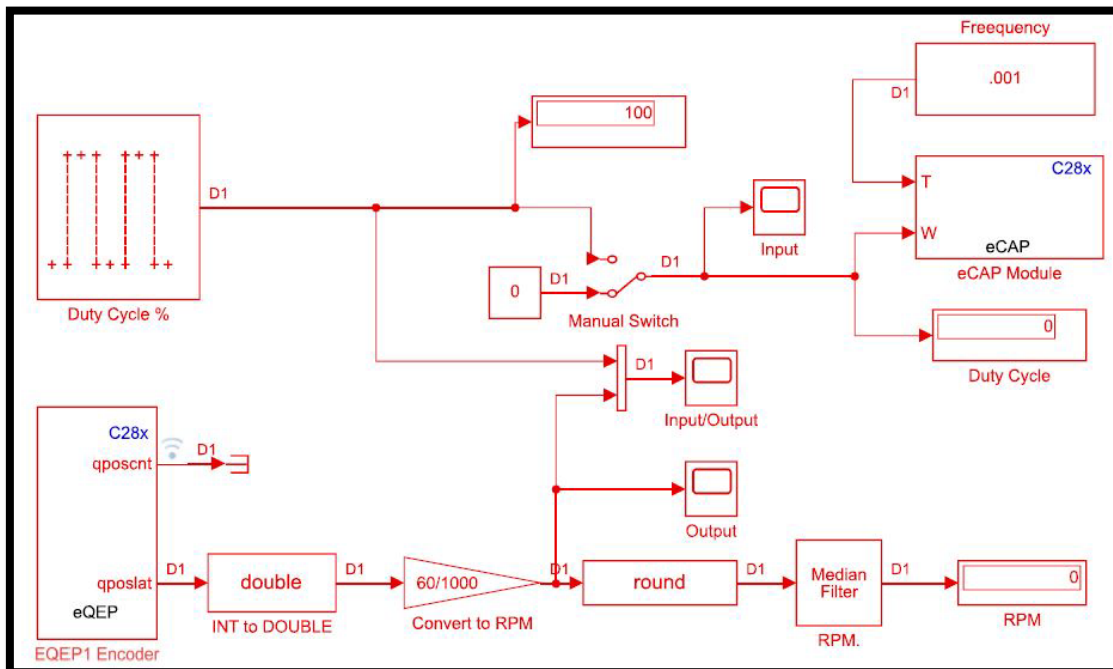


Figure 5.5 DC Servo Motor Real Time Data Collection DSP F280049C

The data is collected into two different way. The input pulses are duty cycle that is sent binary 0 and 1 (0% to 100%). The motor was running at maximum speed 3700RPM or at zero speed at fixed interval of five seconds. While in second test Step pulses are sent at different duty cycle (0, 25, 75, 100) at variable intervals. The measured speed is displayed in Figures 5.6 and 5.7.

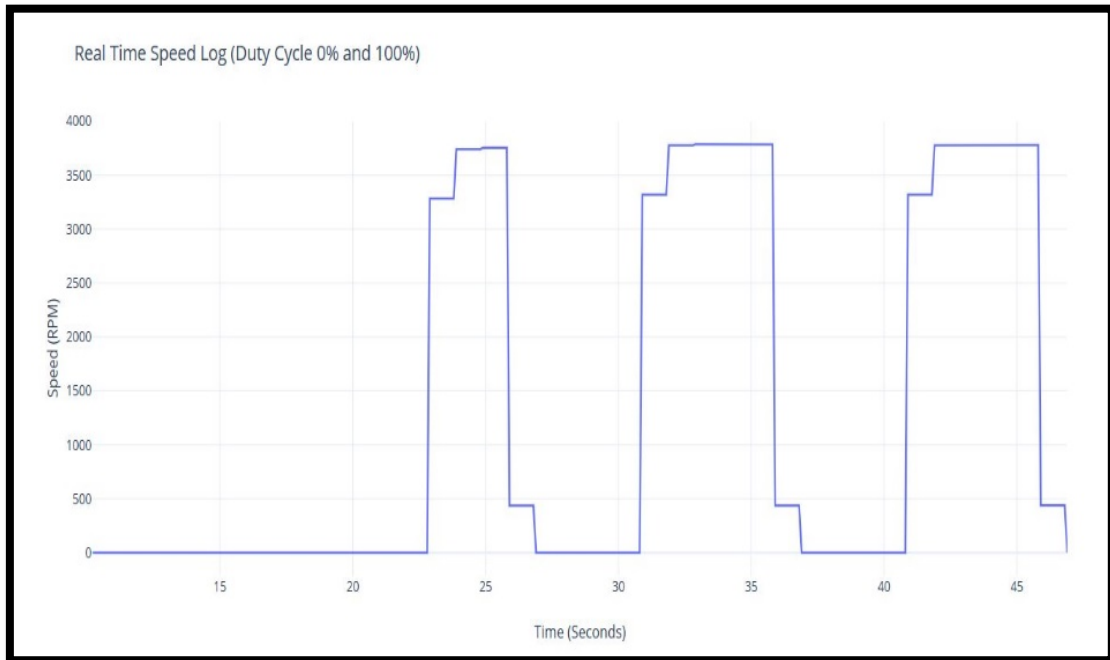


Figure 5. 6 Speed data in real time (Input is 0 and 1)

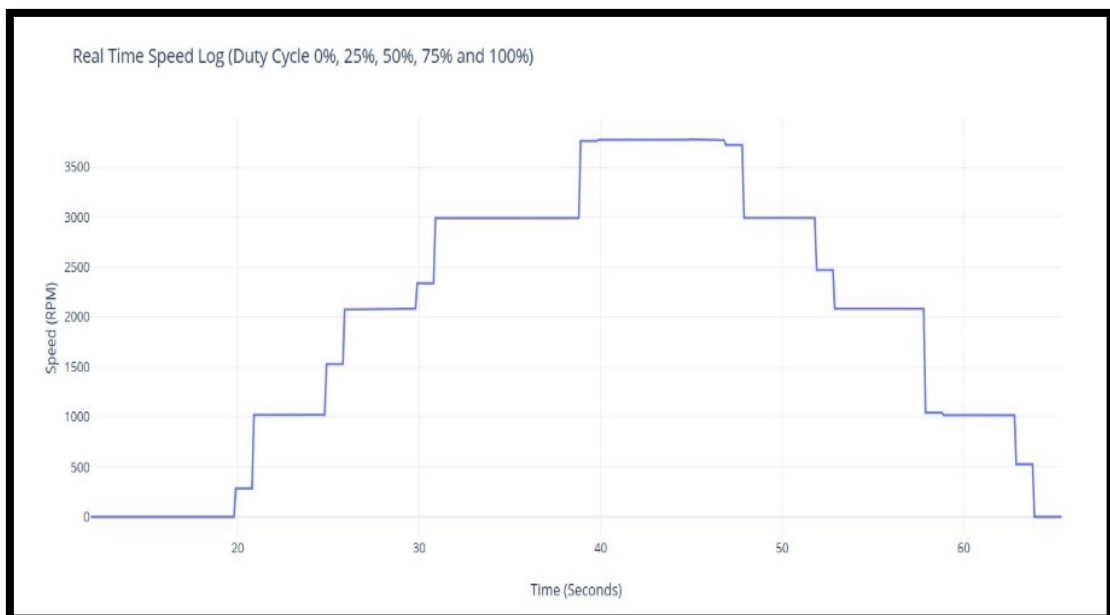


Figure 5. 7 Speed data in real time input is (0, 25, 75, 100)

5.2.6.2 Real Time PID Tuning

PID control can be described as the most used control system in the industry. It has been used in the mechanical control of different mechanical parts of many different kinds. Here the PID is used to control the position and speed of the DC servo motor that are connected into the Robot joints. The PID block in MATLAB has the capability to tune its value in real time that gives access to setup the parameters when software in loop. The block diagram in the Figure 5.8 is the RCU Control Algorithm modelled in SIMULINK.

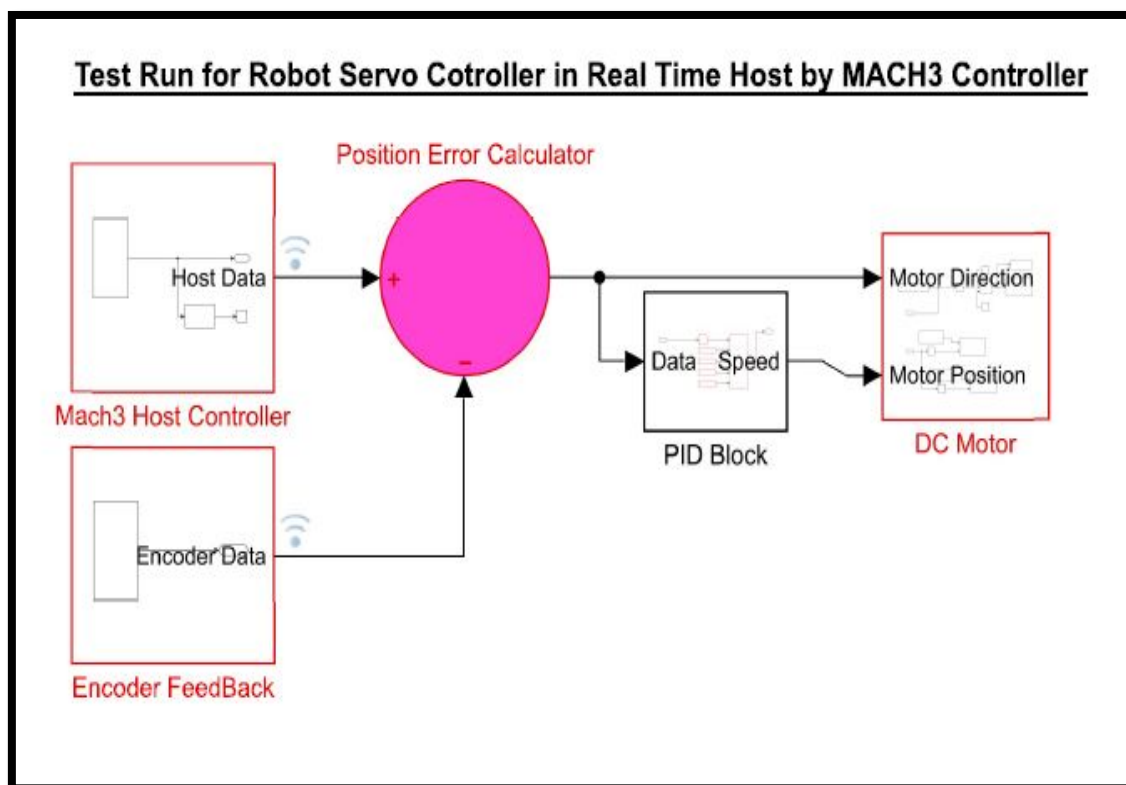


Figure 5.8 RCU Control Algorithm

5.2.6.3 Test the SIMULINK Model in Real Time

The Algorithm is tested by accelerating and deaccelerating the motor from zero speed to the maximum and vice versa as shown in Figure 5.9. The blue colour shows encoder feedback and yellow dots shows the MACH3 set point data. This is observed that the encoder is almost exactly following the set point that means the PID controller is tuned perfectly and the parameter estimation of the Robot motors was also the best optimised values.

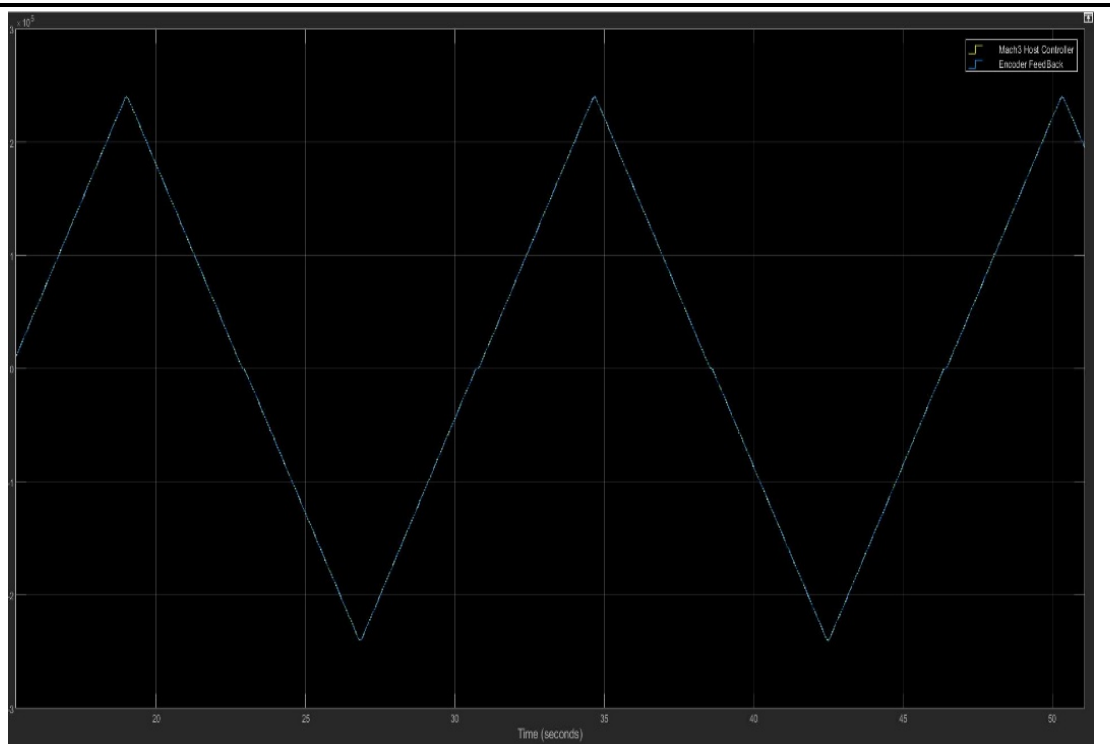


Figure 5.9 Test results of the designed controller

5.3 MACH3 Configuration and Robot Programming

MACH3 is a software package that is used for transforming a conventional computer into a CNC machine controller. MACH3 can be used for controlling different machines such as milling machines, text engravers, routers, plasma cutters, gear cutters, lathes, Serial Robot, Parallelogram even it can be used for controlling any machine comprising of motors up to 6-Axis as its screen does not support more than 6-Axis, provided a screen is developed for customized use. The MACH3 controller is hugely efficient and cost-effective alternative of conventional CNC and Robot controllers. MACH3 is equipped with extensive features that are like commercial controllers such as Fanuc, Yaskawa, Mitsubishi that further enhance the efficiency of CNC machines while optimizing the cost constraint for the system. MACH3 is being leveraged for developing systems at research and industrial level. The low cost makes MACH3 an appropriate choice for researchers and students for deploying their projects using typical computers. The system specifications requirement is very low even any desktop or laptop computer can run this software. The Figure 5.10 shows minimum requirement.

S. No.	Items	Range
1	System Configuration	Desktop PC or Laptop
2	Operating System	Windows 2000 to onwards all versions
3	Processor	> 1 GHz (Gigahertz)
4	RAM (Primary Memory)	> 512 MB
5	Graphic Card Memory	> 32 MB

Figure 5.10 System Specification for MACH3 Software

MACH3 takes ‘G’ codes as input for operating different components according to the instructions piled up in the ‘G’ codes. MACH3 communicated with the hardware through the Parallel ports which are conventionally used for printers. In case of unavailability of parallel ports, motion controller board can be used for creating the communication link between the hardware and MACH3 by leveraging Ethernet or USB port. MACH3 generate step pulses and direction signals according to the instructions of ‘G’ codes. These pulses and direction signals are used to drive stepper and servo motors in clockwise and anticlockwise direction as shown in Figure 5.11.

The configuration is setup in opposite direction as the MACH3 hardware will setup first and ‘G’ codes programming at last.

1. MACH3 Hardware Configuration
2. MACH3 Software Configuration
3. MACH3 Programming by ‘G’ codes

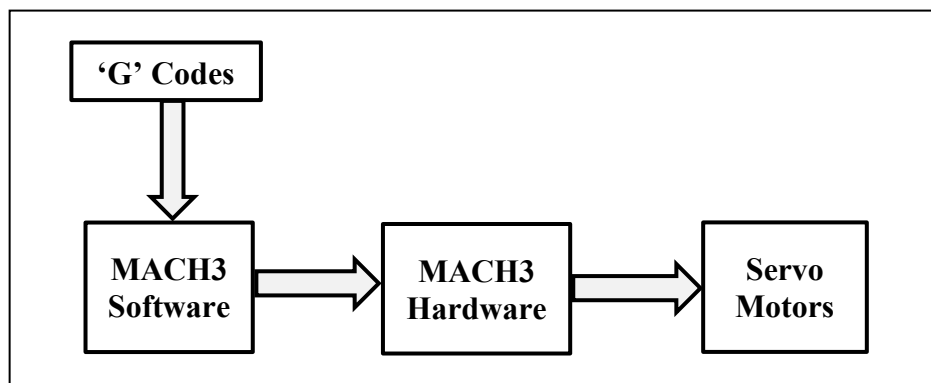


Figure 5.11 Flow of information from ‘G’ codes to the Actuators

5.3.1 MACH3 Hardware Configuration for Robot

MACH3 is widely used for transforming a conventional computer into a CNC controller. The computers cannot control and regulate the servo motors by itself. They require an intermediate hardware that can directly communicate with the servo motors while accepting commands from the computer. For establishing the communication link between computer and the servo system, a breakout board or hardware is used. The servo motors and other hardware components like limit switches are connected to this breakout board and then this board hardwired with the computer to communicate. MACH3 software is used for sending commands to the breakout board and the breakout board follows the instructions received from the computer for operating the servo motors. The intermediate breakout board helps in developing hardware in loop independently to reduce the processing of the computer processor to reduce jitter. Figure 5.12 shows the 5-Axis USB controlled BOB (Break Out Board) used in this project. Blue and purple wires demonstrate the pulses and direction while the grey colour are the limit and some sensors of the Robot.

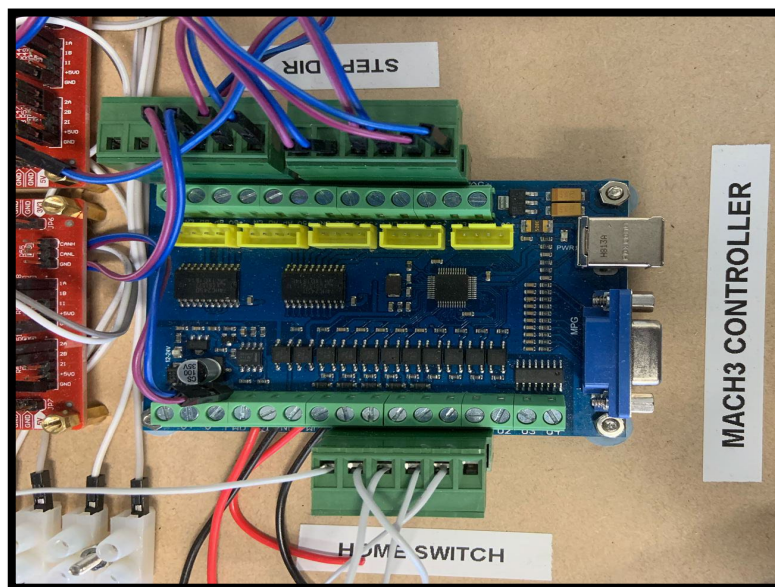


Figure 5. 12 MACH3 Hardware or Break Out Board

The first step of utilizing MACH3 for developing CNC controlling system is the development of programming file. The CNC programming is performed in the form of ‘G’ codes. These codes contain the necessary instructions which are required by the controller. The ‘G’ code files are fed into MACH3 software. The MACH3 software

interprets the files and sends the instructions to the hardware. Breakout board is supposed to be hardwired with the servo motors for performing motion control. This breakout board receives the instructions from the software and then it proceeds to taking the instructed steps of pulsing the motors step by step. This is a parallel computing therefore the one motor activates at a time. The kernel speed describes the smoothness of motion in curve. Higher the frequency promotes the smooth motion control according to the instructions.

The main features and functionalities that are provided by MACH3 breakout board is the capability of supporting 6-Axis stepper or servo motors and drivers. This hardware is also compatible with different CNC software packages the one of which is EMC2 (Enhanced Machine Controller). In order to maintain the electrical safety aspect of the board, a complete isolation is provided between USB power supply of the computer and peripherals powered phase. The safest form of isolation scheme is used in MACH3 breakout board that is Opto-isolation, it further enhances the protection of the hardware from unwanted signals. A 5-input interface has been provided for specifying the different CNC inputs like home sensors. It can tolerate the voltage ranging from 12 to 24 V DC. This feature protects it from variable voltage spikes which can arise due to malfunctioning of the hardware and disconnect the computer from the board when required. Furthermore, a relay output control interface is also provided for connecting the external components like Robot actuators. It provides the output Analog voltage ranging from 0 V to 10 V DC to control the Analog devices. MACH3 Hardware Specifications are in Figure 5.13.

S. No.	Items	Range
1	Input Power	USB port to directly get power from PC
2	Secondary Power	12-24VDC External power can be used
3	Compatible Motors	Stepper and Servo Motors
4	Pulse Type	Pulse and Direction Signals Control only
5	MPG Control	MPG (Manual Pulse Generator) works on 5V

Figure 5.13 MACH3 Board Electrical Properties

USB and Ethernet interface provide the facility of connecting the MACH3 enabled board with the computer without having any hurdle which arises due to parallel ports. Parallel port or Printer port is very old, and this hardware interface is not found in any new computer and laptops. Even the PCI (Peripheral Component Interconnect) boards are not being developed anymore for Parallel port interface because all the printers have been upgraded to USB, Ethernet and even wireless protocol through Wi-Fi. Therefore,

MACH3 hardware is compelled to upgrade the hardware interface to keep running their systems with new technology. Commonly all laptops and desktop have built-in USB, Ethernet and Wi-Fi ports. These hardware interfaces are very common and are currently used in millions of devices. Thus, the breakout boards are developed into two interface one is USB and second is Ethernet. There is some additional feature associated with the upgradation. Now, the boards do not require separate power supply to start their operations. These boards utilize the power from USB ports. The interface provides several important features and functionalities which can be used for enhancing the CNC systems as it advances the number of GPIOs to integrate with up to 132 different peripheral devices. GPIOs pins are attached with the motion interface cards which can be utilized for connecting several peripherals. In addition of providing the interface for the peripherals, the motion control interface cards also provide the protection by introducing the electrical isolation. This IO (Input Output) port isolation helps in protecting the attached circuitry from surges and spontaneous breakage. This board has completely supporting environment for all MACH3 versions. It supports the functionality of USB hot-swappable. The board has the capability of monitoring the status of USB connections at any time. It is equipped with an indicating LED that can show the USB connection and working status of the board by flashing.

MACH3 breakout board must be configured with MACH3 software. The configuration includes parameters and specifications of the breakout board. The basic configuration for connecting the MACH3 breakout board is performed at the time of setting up the MACH3 software. This fundamental configuration includes specifications of axis outputs, motor parameters, input signals, output signals and Robot actuator settings. For configuring the MACH3 software for USB or Ethernet motion interface card, following additional steps must be followed.

Click on Config on MACH3 software then Select Config Plugins. Plugin Control and Activation tab will be displayed. Click on CONFIG written against the plugin which is desired to be used for interface. A configuration interface will be displayed on the screen. This configuration interface consists of many important parameters which are used for specifying the USB motion card status. Following are the parameters which are required to be specified:

- Card Work Status

- IO Output Status
- Homing Status
- Homing Mode Selection
- Homing Offset Settings
- Robot Actuator Setting
- 'G' code Buffer Time Settings

5.3.2 MACH3 Software Configuration for Robot

Mostly, CNC devices are patched with built-in configuration of MACH3 due to increasing trend of MACH3. However, MACH3 can be configured for Mitsubishi Robot to jog it in cartesian coordinate system. There are following steps to configure the Robot. Open 'MACH3 CNC Controller' software interface as seen in Figure 5.14.

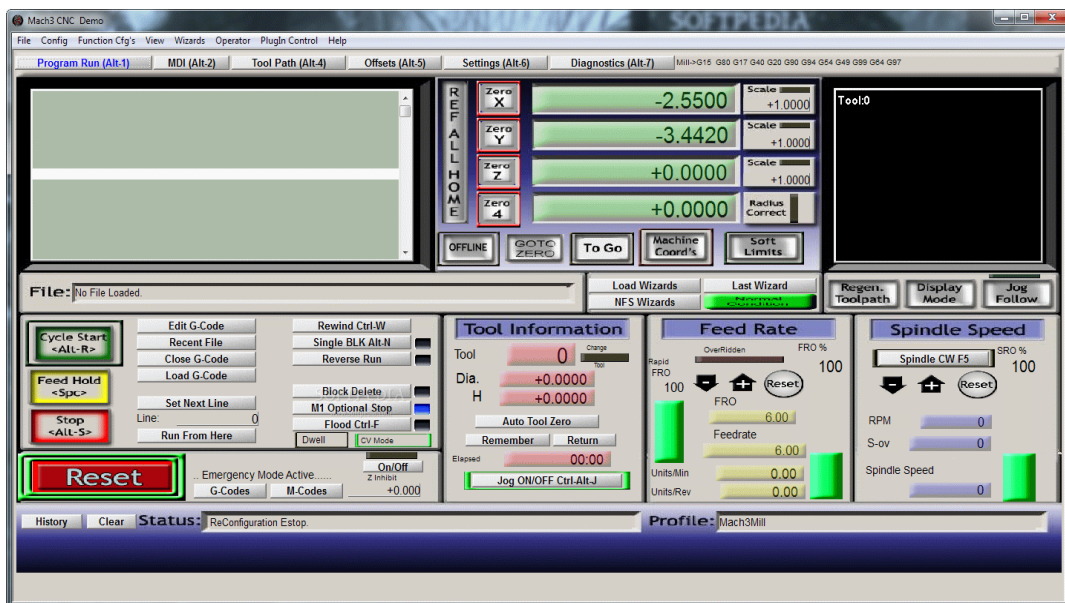


Figure 5.14 MACH3 Software Interface

Click on Config option in header tab and select Ports and Pins. Click on Port Setup and Axis Selection tab which is shown in the Ports and Pins dialog tab. If the MACH3 is aiming to use only one port located at motherboard, the address of 0x378 is automatically assigned to the Port 1 by default. If the user aims to use external PCI-extension port card, then the user is required to inspect out the port address by using the utility of control panel. The port address obtained from the control panel should be filled in the address field of the port. Similar approach can be used for filling out the address in the field of Port 2. Click on Apply button for saving the entered parameters.

There exists the option of selecting kernel speed on Port Setup and Axis Selection tab. The MACH3 driver can run from 25 kHz up to 100 kHz. The kernel speed is selected based upon the processor and the requirement of motors. The kernel speed determines maximum pulse rate for the motors. For example, 25 kHz pulse rate is suitable for driving stepper motor. 1 GHz processor can run at even 35 kHz, so high step rate can be used for driving fast motors like servo. The appropriate choice for Kernel Speed is 25 kHz that is set for the Robot.

Many other features are also available on Port Setup and Axis Selection tab. These features can be selected by ticking the check boxes. The Robot is 5 Axes serial. Therefore, J1 to J5 are selected as X, Y, Z, A and B.

The input and output signals can be defined on Port Setup and Axis Selection tab.

Output Signals: Select Output Signals Tab. Define the outputs by enabling them and assigning the suitable pin number. Click on Apply saving the parameters. The home sensors of the Robot are assigned from pin 11 to 15.

Select Encoder/MPG's tab for defining configuration parameters of the linear encoders or MPG. Enter suitable Counts/Unit value setting up the resolution of encoders and MPGs. For determining the scaling of the axis being controlled by MPGs, set up the corresponding velocity.

After passing through the basic configuration, the axis drives are to be configured. The axis drives can be configured by selecting Select Native Units by going into the Config tab. There are two units one is mm (millimetre) and other is inch. The Robot is configured in mm hence it is set.

After completing the steps described in subsection 5.3.2.1 to 5.3.2.6, it is required to set up the motors. For tuning up the motors, the first step is to determine the step pulses which should be sent to drive the motors according to the specified requirements. The motors used in the Robot is differential 1000-line encoder that becomes 4000 pulses per revolution. Since, the resolution of each axis is $360^\circ/4000\text{Pulses} = 0.09^\circ/\text{Pulse}$. After this step, the maximum speed, acceleration and deceleration of the motors are also set.

There are other additional configurations which can enhance the functionality. These additional configurations include system hotkeys, soft limits, position of home switches,

referencing speed and direction, slaving and general logic configuration. Do not setup these configuration as they are not required in the Robot RM-501.

5.3.3 Robot Programming by ‘G’ codes

The number of Robots is increasing rapidly. The majority of industrial sector relies upon Robots for manufacturing the products with greater granularity. The programming that is used for instructing Robots to perform the corresponding tasks is called Robot Programming. ‘G’ code is a programming language which instructs the machines tools to move accordingly. A ‘G’ code program is uploaded to the Robot controller and this Robot follows the instructions of ‘G’ code program line by line for setting up position, speed, direction and different parameters of servo system that are integrated with Robot controller.

Originally, ‘G’ code language was different from the conventional programming languages as it did not contain many programming features such as loops, programmer-defined variables and conditional statements. This earlier and original version of ‘G’ code lacked the capability of encoding the logic. The modern implementation of ‘G’ code is relatively different from the earlier implementation because the modern implementations include macro language capabilities which make it closer to conventional high-level programming language.

Manufacturers and researchers are using ‘G’ codes for controlling the different tools of the machine for manufacturing different parts. There are many applications of ‘G’ codes that are used in Robots, CNC Machines, Special Purpose Machines and 3-D Printing. Instead of following universal standard, some Robot vendors have developed their own ‘G’ codes for establishing their monopoly and security of their programs. The more notable actions which are instructed by the ‘G’ codes to the machines include Quick movements of the tools while performing any set of operations, switching between several coordinate systems, setting of important tool parameters for in-depth specifications of the operations being performed, precise and accurate control over the motor for moving in straight path, execution of synchronized series of multiple operations and monitoring of different parameters for inspecting the efficiency of the system. Figure 5.15 is the MACH3 software interface of teaching mode. Where the ‘G’ codes can be typed in the input column and press enter to execute the code.

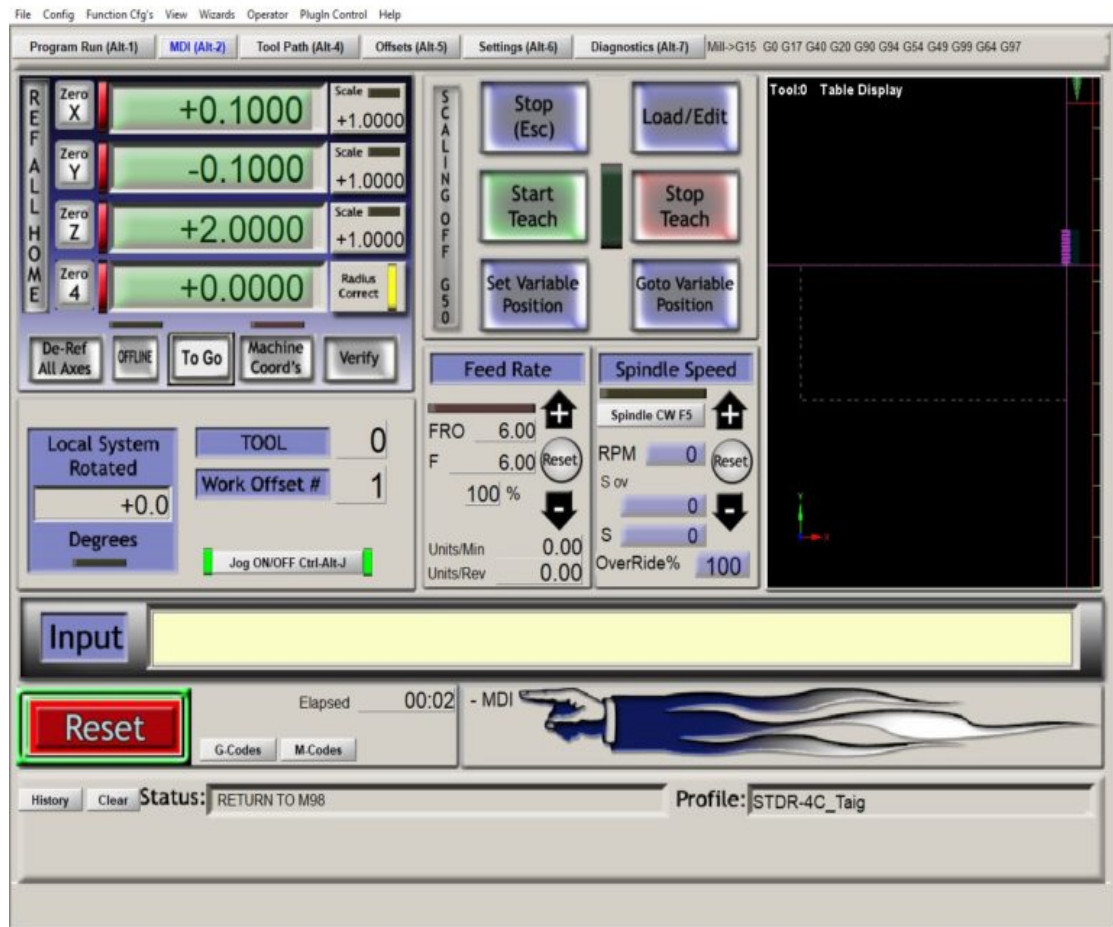


Figure 5. 15 MACH3 ‘G’ codes Programming in Teach Mode

A line of code in ‘G’ codes is referred as ‘block’. Each block consists of a new command. In order to send the instructions consisting of four commands, the user is required to write four lines or blocks of ‘G’ code. The commands consist of letters that are preceded by the number. The most prevalent letter used in CNC programming is G and the commands starting from the letter ‘G’ mostly refer to motion related commands. X, Y and Z are used for representing the axes.

Following steps should be followed for executing ‘G’ codes program in MACH3.

1. Generate ‘G’ code program file.
2. Open MACH3 software.
3. Click on **Load ‘G’ code** button.
4. Choose the ‘G’ code program file which is to be loaded on CNC machine.
5. Click on **Open** button.

These steps load the ‘G’ code file in MACH3. After loading and analysing the ‘G’ code program, MACH3 generates a tool path for it. This tool path is displayed on the screen and it establishes the program extrema for elucidating the information in visual representation. At this stage, the program can be run on MACH3 enabled machine.

Standard ‘G’ codes are used for moving the Robot in coordinate system. These ‘G’ codes are used for writing the blocks to build a program. When MATLAB Algorithm finally evaluate the trajectory and concludes the positional information the ‘G’ codes language is used to convert the information into Robot understandable language and send to the Robot Controller. A reference table can be observed in Figures 5.16 to 5.18. These are standards that are almost used in all general-purpose machines.

Code	Description
<u>G0</u>	Coordinated Motion at Rapid Rate
<u>G1</u>	Coordinated Motion at Feed Rate
<u>G2 G3</u>	Coordinated Helical Motion at Feed Rate
<u>G4</u>	Dwell
<u>G5</u>	Cubic Spline
<u>G5.1</u>	Quadratic B-Spline
<u>G5.2</u>	NURBS, add control point
<u>G7</u>	Diameter Mode (lathe)
<u>G8</u>	Radius Mode (lathe)
<u>G10 L1</u>	Set Tool Table Entry
<u>G10 L10</u>	Set Tool Table, Calculated, Workpiece
<u>G10 L11</u>	Set Tool Table, Calculated, Fixture
<u>G10 L2</u>	Coordinate System Origin Setting
<u>G10 L20</u>	Coordinate System Origin Setting Calculated
<u>G17 - G19.1</u>	Plane Select
<u>G20 G21</u>	Set Units of Measure
<u>G28 - G28.1</u>	Go to Predefined Position

Figure 5. 16 Reference Table A

G30 - G30.1	Go to Predefined Position
G33	Spindle Synchronized Motion
G33.1	Rigid Tapping
G38.2 - G38.5	Probing
G40	Cancel Cutter Compensation
G41 G42	Cutter Compensation
G41.1 G42.1	Dynamic Cutter Compensation
G43	Use Tool Length Offset from Tool Table
G43.1	Dynamic Tool Length Offset
G43.2	Apply additional Tool Length Offset
G49	Cancel Tool Length Offset
G53	Move in Machine Coordinates
G54-G59.3	Select Coordinate System (1 - 9)
G61 G61.1	Path Control Mode
G64	Path Control Mode with Optional Tolerance
G73	Drilling Cycle with Chip Breaking
G76	Multi-pass Threading Cycle (Lathe)
G80	Cancel Motion Modes

Figure 5. 17 Reference Table B

G81	Drilling Cycle
G82	Drilling Cycle with Dwell
G83	Drilling Cycle with Peck
G85	Boring Cycle, No Dwell, Feed Out
G86	Boring Cycle, Stop, Rapid Out
G89	Boring Cycle, Dwell, Feed Out
G90 G91	Distance Mode
G90.1 G91.1	Arc Distance Mode
G92	Coordinate System Offset
G92.1 G92.2	Cancel G92 Offsets
G92.3	Restore G92 Offsets
G93 G94 G95	Feed Modes
G96	Spindle Control Mode
G98 G99	Canned Cycle Z Retract Mode

Figure 5. 18 Reference Table C

5.4 Preliminary Study of Robot Motion

The Robot is calibrated after the integration of RCU to the manipulator. The calibration procedure is completed using two methods 3-Points and 5-Points as shown in Figure 5.19.

1. 3-Points P1P2P3 are three positions having the same tool control point. The motion of the tool coordinates will remain same as the motion of electrical coordinate system.
2. 5-Points P1P2P3 will remain same as the three points and the motion of tool coordinate will be set up by P3P4P5 where P3 means the original position P4 is the positive X-Axis and P5 is the positive Z-Axis.
3. Once the tool coordinate are set the Robot kinematics can be verified by jogging the Robot in X, Y and Z Axes. This test can be completed with the help of a cube. The Robot TCP (Tool Control Point) will move in cartesian coordinate system by following the edges of the cube. After that the repeatability test will be conducted same as described in section 6.6.

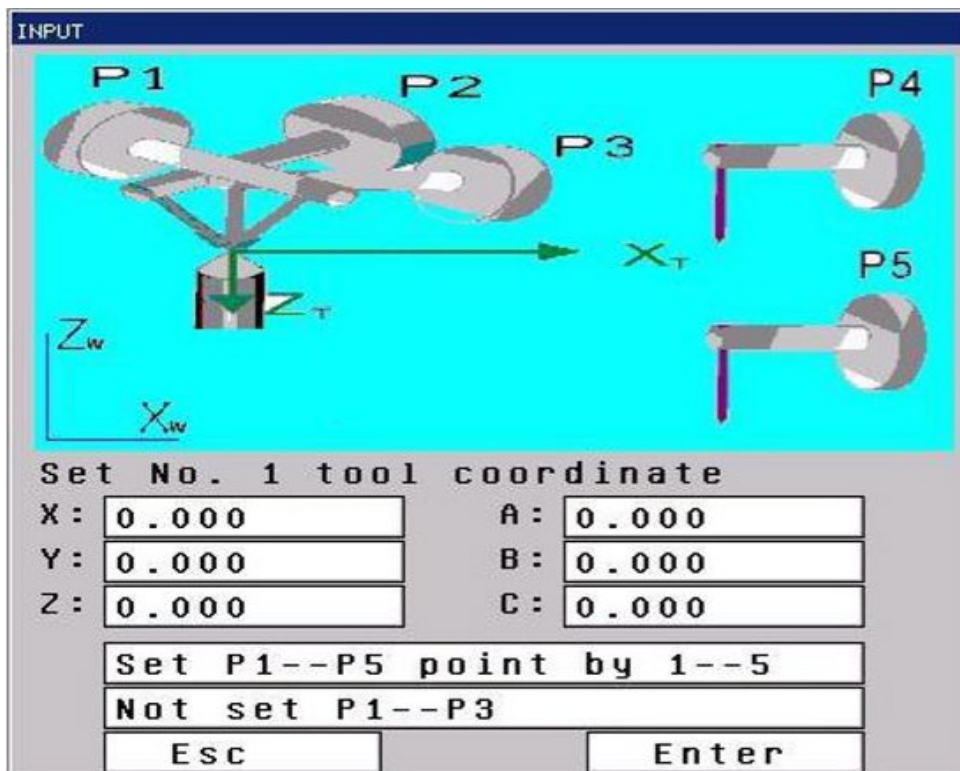


Figure 5. 19 3-Point and 5 Point tool coordinate system

5.5 Experiments on Irregular Shapes

The different shapes are drawn on A4 white paper as shown in Figure 5.20. The Algorithm developed in chapter 4 are tested in real time. The camera is mounted directly above the A4 board and connected to the MATLAB through USB. The images are taken by Algorithm after equal interval of time and once the processing is completed the 'G' codes are stored into the Robot memory automatically. Once RCU receives the information, the Robot moves directly above the shape and reduce the height until it reaches a millimetre above the boards. The pneumatic actuators turn on from specific locations to grasp the object. Different shapes are tested to verify the Algorithm. However, this code works for one shape at a time if there are more than one shape that becomes totally different scenario and it is discussed in section future scope.

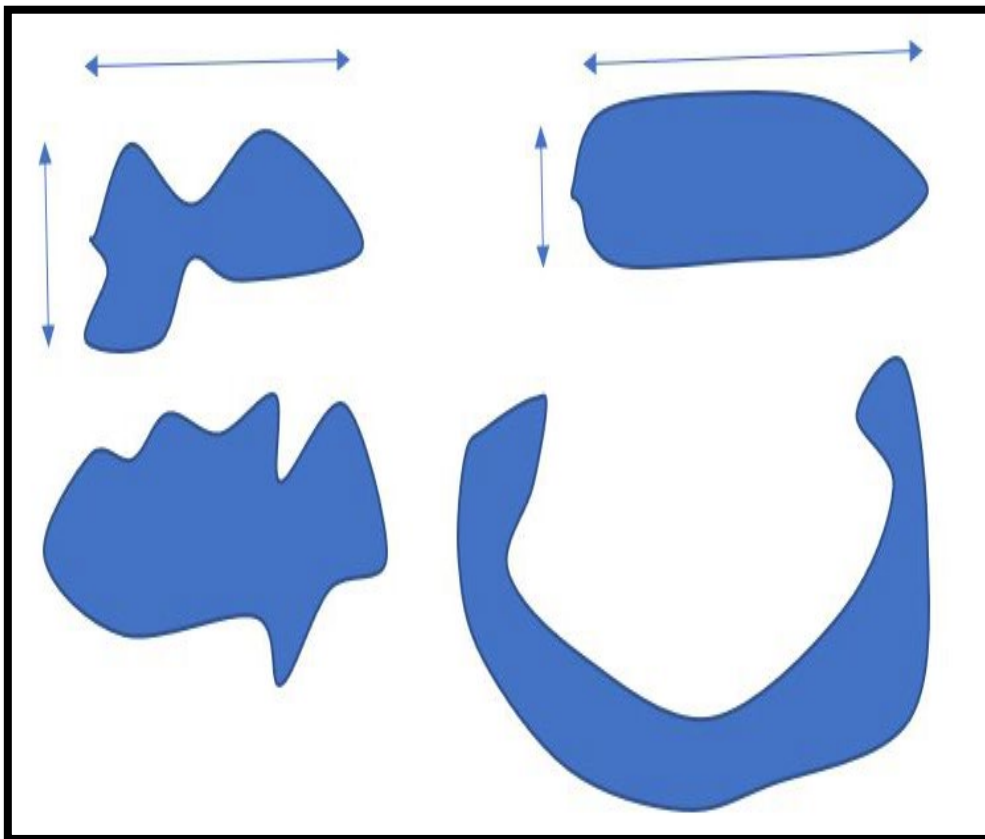


Figure 5. 20 Irregular shapes

5.6 Overall Performance of MV System

MV system is the integration of several units and each of the unit should work in a loop and communicate each other in milliseconds time. The MV system is used in the prototype is a low-cost camera with appropriate pixels because our system does not grasp very tiny objects hence high megapixel camera is not necessary for this type of operation. MATLAB software is installed on a core i7 laptop and used it as a main control unit for the development of coding. The software asks the camera to take image after specific interval of time. The image taken by camera is stored in a designated folder and read by our Algorithm. After that all the processing takes place in few minutes that includes the information about type and size of image, develop the end effector trajectory, and finally converts the positional information into 'G' codes. These 'G' codes are then further communicated to Robot RCU that turn the Robot movement on the designated position and activate the solenoids to grasp the object. This all system us fully automated and in a closed loop. The overall performance is analysed by changing the different shapes and the behaviour of the Robot against it. There are still many types of scenarios available where the Algorithm gets stuck and waits for human intervention that is discussed in detail in the section of future scope.

5.7 Summary

The prototype objective is to test the Algorithm in the real world and that is achieved in this section. The RCU of the Robot that is developed in SIMULINK and deployed in TI F280049c DSP controller communicated with the MATLAB and received the information without any difficulties. The MACH3 software is used as a Robot Controller interface, the calibration and kinematics configuration are tested and checked for accuracy and repeatability. Chapter 4 is the main input of the prototype because the Robot depends on the positional information supplied by the MATLAB and if this information is slightly wrong the Robot can go totally out of the way and that is why the external limit switches are installed as a secondary safety option. Two emergency switches are installed to disconnect the Robot power in case of accidents. Different types of shapes are tested to make sure the overall performance of the MV system. This work also supported to find the research internship to implement it in the industry environment. Further work on MV in PolyNovo R&D Lab is conducted in the next chapter.

Chapter 6

Chapter # 6 Industrial Application of Research

- 6.1 Introduction
- 6.2 PolyNovo Requirements for AUWS
- 6.3 Construction of 3-Axis Cartesian Robot
- 6.4 Parameterization of Panasonic AC Servo System
- 6.5 Programming of Daincube Robot Controller
- 6.6 Repeatability Test of Robot
- 6.7 Welding Test on Soft Material based Medical Devices
- 6.8 Welding Test on Irregular Shapes by MV Algorithm
- 6.9 Algorithm to Generate Different Bonding Pattern
- 6.10 Summary

6.1 Introduction

This chapter describes the significance of the research and one of its application domains in medical device industry. PolyNovo Biomaterials offered the research internship to Research and Development of an AUWS.

PolyNovo is a manufacturer of novel medical devices based on proprietary biodegradable polymers. The company has one product in commercial distribution (NovoSorb® BTM) and is developing several other products that require new manufacturing processes. One of these processes involves bonding of sheets of material together via a series of point bonds across the sheets. This process is currently conducted manually leading to slow production of devices and of variable quality at the bond-points. As the project ramps up, PolyNovo needs a larger amount of material for testing purposes and therefore requires a simple automated machine or Robotic arm to work with this existing bonding process to move the tool across the surface and activate the bonding tool in different pattern. This machine is needed to both improve the quality and reproducibility of the bonds and increase the throughput of material in this process.

The project requires the intern to develop an automated machine or mechanical arm as shown in Figures 6.1 and 6.2 that will move the existing bonding tool across the surface of the sheets to be bonded; the tool needs to be moved in both the X-Axis and Y-Axis directions to create a matrix of bond points. The machine needs to hold the bonding tool (which weighs less than 1 kg), lower it to the surface of the sheets, activate the control unit for a few seconds, raise the tool, then move it in the XY-Axes plane and repeat. The machine must have good reproducibility in the z-direction (vertical) so that the tool is always in the same vertical position relative to the surface of the sheets (to 0.1 mm if possible) to generate consistent bond points. The tolerance requirements in the X-Axis and Y-Axis directions are less stringent. The machine should allow the user to easily define both the pattern for the bond-points in the X-Axis, Y-Axis directions, and the position of the tool relative to the surface of the sheets in the z-direction. The sheets to be bonded are smooth, flat and 75 x 40 cm in size.

The contribution in the research is the welding of different shapes of medical devices and development of Algorithm to achieve 100% strong weld between the plastic materials.



Figure 6. 1 Automated Ultrasonic Welding System



Figure 6. 2 3-Axis Robot Control Unit

6.2 PolyNovo Requirements for AUWS

PolyNovo provided a set of requirements for the AUWS. The key requirements are as follows.

Power

The system must use single-phase mains power: 230 V AC, 50 Hz.

Spare Parts

Any specialized spare parts for the system shall be readily available.

Consumables

Any specialized consumables required to operate the system shall be readily available.

Operating Environment

The system shall be suitable for use in an ISO Class 7/8 clean room.

System Materials

- a. The product contact parts of the system shall be constructed from materials that do not rust or shed particulate material (e.g. 316 stainless steel).
- b. Product contact parts are defined as those parts that come into direct contact with the materials being processed.
- c. Material certification and surface treatment reports shall be provided for all product contact parts.

Contamination of Material

The system shall not transfer any contaminants (including residue, oil, grease, particulates, rust or dust) to the material being processed.

Processing Tools

The system shall be capable of accepting different welding tools to produce different welding styles and patterns for point to point programming mode.

Welding Large Material

The system shall be able to conduct multiple consecutive welds without operator intervention in order to weld the construct.

Weld Precision

- a. The system shall weld features in the input material to within a tolerance of ± 0.5 mm relative to each other the x and y directions
- b. The system shall weld features in the input material to within a tolerance of ± 3 mm relative to the edge of the processed material.

Input Material Thickness

The system shall be capable of processing material with thicknesses between 0.1 mm and 20 mm.

Input Material Size

The system shall be capable of welding material of at least 300 x 300 mm.

Operating Conditions

The system shall operate at temperatures between 15 and 25 °C and at humidity < 90% RH.

System Control

- a. The critical operating parameters of the system shall be set by the operator(s).
- b. The following parameters of the ultrasonic welder system shall be able to be set by the operator through an input interface of the Welder System
 - Weld Energy, Weld Amplitude and Maximum Weld Time

Display of Operating Parameters

The following operating parameters shall be displayed in digital readout to the operator(s):

- Weld Energy, Weld Amplitude and Weld Time

Welding Pattern

The system shall allow the operator to generate varying weld patterns.

Guarding

The system shall only be able to operate when there is no possibility of injury or harm to the operator.

Emergency Stop

- a. The system shall provide at least one Emergency Stop button in a location that can be reached by the operator(s).
- b. When the emergency stop button is activated:
 - All motion on the system shall stop immediately
 - Power to the system controller shall be disconnected (as a result operator cannot move Robot Axis by controller).
 - The system can only be re-started by an operator(s) in a safe mode procedure defined in manual.
 - No damage shall occur to the system

Power Failure

In the event of a power failure:

- All motion on the system shall stop as soon as practicable
- The system can only be re-started by an operator(s) in a safe mode
- No damage shall occur to the system

Recovery from Power Outage

1. After a power outage, the system shall be able to re-start with minimal set-up time and minimal loss of material.
2. After a power outage, the control software and recipe files back up procedure shall be available in the operating manual.

Documentation Required

The following documents shall be provided by the intern in pdf format:

1. Operating Manual, at a level understandable by a high school graduate.

6.3 Construction of 3-Axis Cartesian Robot

The Robot is the integration of several units. Begins with the mechanical design and fabrication of linear actuators, installation of electrical components to build a panel box and Robot controller configuration and calibration with the servo systems. Each of the sub section is defined in detail in the following sub-sections.

6.3.1 CAD Model of 3-Axis Cartesian Robot

The CAD Model is developed on CREO 5.0. The Robot has a total dimension of 1675X1375X775 mm and can develop the medical devices of no more than 750X750 mm as shown in Figure 6.3, with the maximum height clearance of 40 mm as shown in Figure 6.4. The CAD drawings for the Robot is developed on A3 pages and bill of material attached to the assembly drawings. There were many revisions required as the fabrication unit was installed in China. It is very important that the drawings deliver the accurate and clear information to the engineers. So that they can understand the requirements and act accordingly.

Architects, engineers and designers utilize computers to contribute in their design projects. The preferred designing method is to develop CAD (Computer Aided Design) model to design elaborate computerized models and materials before they are physically manufactured. CAD permit them to envisage their designs and oppose difficulties before they have consumed any of the resources essential to put them into physical form. Practically anyone with access to a personal computer can attain the software and abilities essential to produce simple CAD design. CREO software is a 3-D CAD modelling software tool for product engineers to yield a direct modelling method. It offers three CREO tools options: CAD, CAM and CAE. Its chief features are that it Curtails time-to-market, it fulfils customers' needs, it also please progressively more complex customer requirements and make variations to geometry briskly and smoothly. There are many forms of CAD modelling which is envisaged by the type of project being designed. Certain models are simple 2-D illustrations of numerous views of a material and the rest are elaborate 3-D cross-sections that express every aspect in great depth. Some CAD models are even animated, presenting how all the components of the model work together to accomplish its mechanisms in CREO mechanica module.

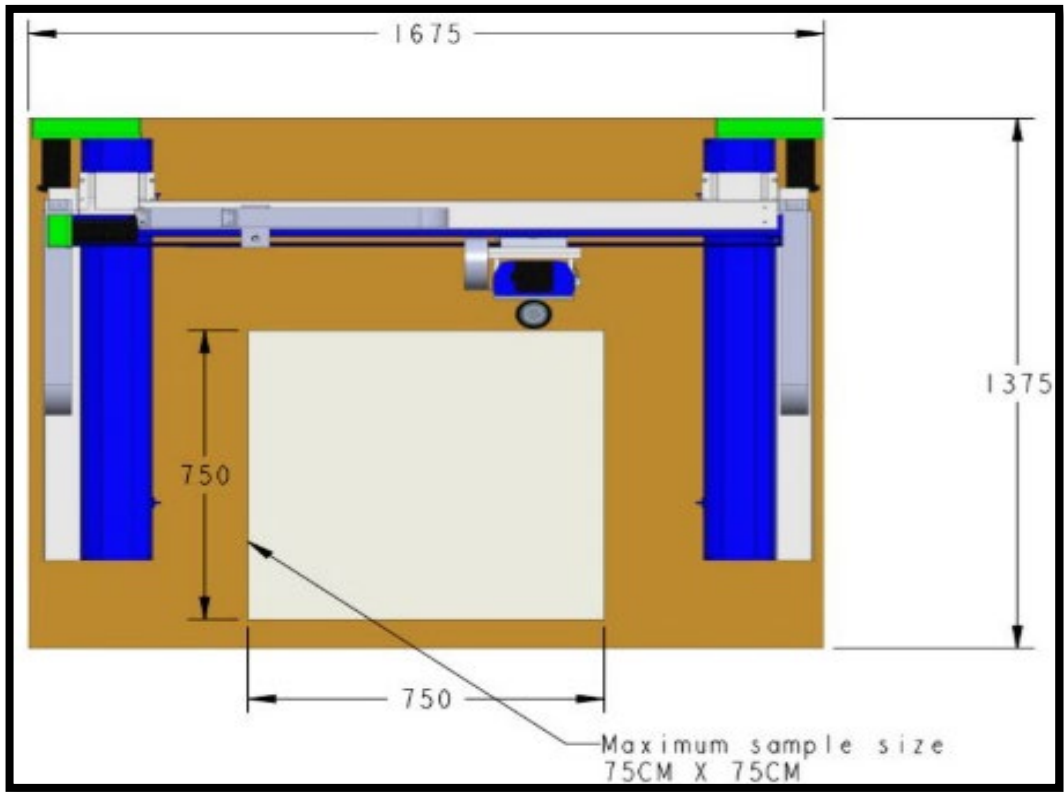


Figure 6.3 Top view of the 3d CAD Model

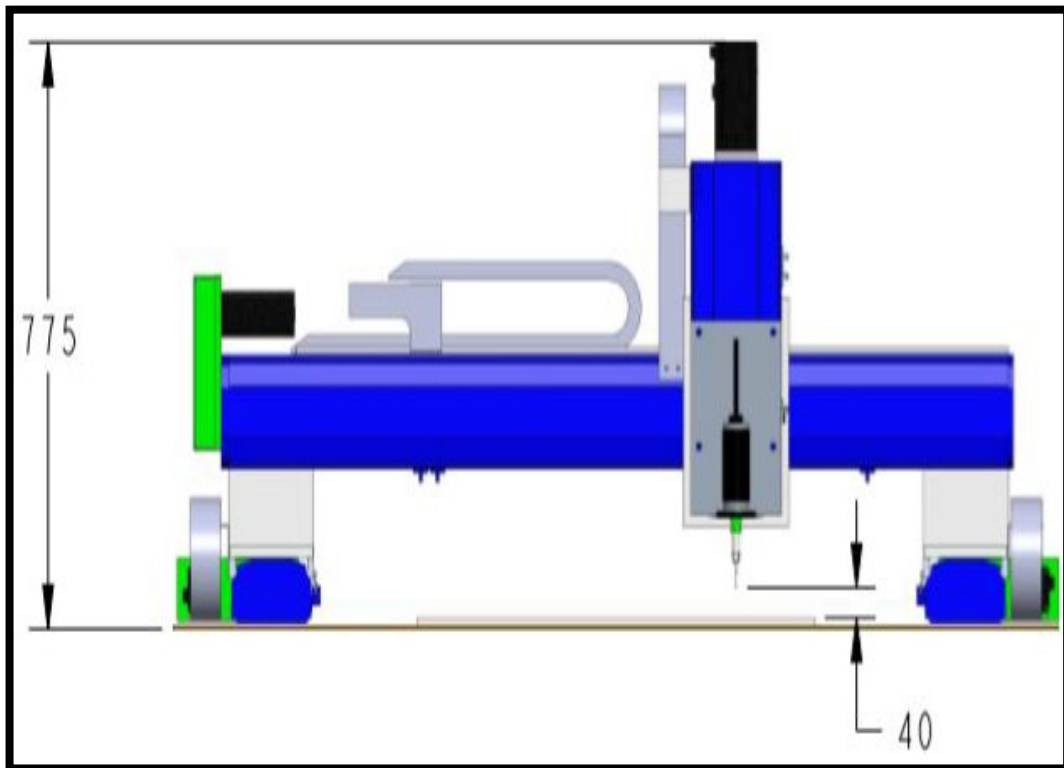


Figure 6.4 Front view of the 3d CAD Model

6.3.2 Linear Actuator Installation

There are several applications of Linear actuators across various industries such as medical equipment, farming machinery, high voltage switch gears, metro buses, trains, factory processes and assembly machines. Every linear actuator application has exceptional necessities. Across the world there are many manufacturers who offer countless models of linear actuators in an extensive variety of stroke, speed and sizes etc. They are also available in variety of models. Selection of choosing the right linear actuator for a particular application is a difficult task. Once the structure is personalized for an application, the precise necessities will affect both the manufacturing and design procedures. Irrespective of end use, an actuation system is planned by first recognizing basic requirements, then assessing certain key considerations that finally affect the complete system operation. Electro-mechanical linear actuators are planned to provide efficiency, precision, repeatability and accuracy in implementation and monitoring linear movement. Aluminium, polymer and zinc are the chief materials of Actuators and can be self-contained and prepared to mount for easy plug-in operation by stepper or servo motors. Actuators that are presenting both open architecture and modular design allow exchangeable external and internal components, as per the prescribed specification. The Robot is made up of four linear actuators as follows.

NSS-150-L10_S800_BR-P40B-C3, (X-Axis 800mm Stroke, Qty 1)

NSS-150-L10_S400_BR-P40B-C3, (400 Stroke) consists of ± 0.02 Repeatability as shown in Figure 6.5. It has a ball screw lead of three types 5, 10 and 20 mm and it has a maximum speed of 250, 500 and 1000 mm/s. It can carry both horizontal and vertical pay load per kg, it has a rate thrust of up to 1564 N, It has a stroke pitch between 100-1200 mm, It has a AC motor output of 400 W and a ball screw of C7 mm, it consists of 10x14 mm of motor coupling and a home sensors. Based on the available options the X-Axis guide is selected of 10mm pitch, 30,000mm/min speed and 800 mm of stroke to suit the application.

NSS-150-L10_S800_BL-P40B-C3, (Y-Axis 800mm Stroke, Qty 2)

The only difference in these two models (X-Axis and Y-Axis) is the side of motor installations as shown in Figure 6.5. There are four options available like left, right, top and front. The Y-Axis motor side is selected left.



Figure 6.5 Linear Guide for X and Y Axes

PSS-170-L10_S200_BC-T75B-C3, (Z-Axis 200mm Stroke, Qty 1)

PSS-170-L10_S200_BC-T75B-C3, (200 Stroke) consists of ± 0.01 Repeatability as shown in Figure 6.6, that is higher than X-Axis and Y-Axis because the repeatability requirement of vertical axis is more than horizontal axes. Based on the available options the Z-Axis guide is selected of 10mm pitch, 30,000mm/min speed and 200 mm of stroke and 750-Watt servo motor to suit the application.



Figure 6.6 Linear Guide for Z-Axis

6.3.3 Electrical Panel Box Design and Installation

The Electrical Enclosure consists of Panasonic absolute AC Servo System, Beckhoff I/O and Safety Devices

6.3.4 Panasonic Servo System

This Panel Box consists of MHMF042L1V2M and MBDLN25BE 400-watt Panasonic servo system for X-Axis and Y-Axis while MHMF082L1V2M and MCDLN35BE 750-watt servo system for Z-Axis Control as shown in Figure 6.7. This system includes breaks and absolute encoder to maintain the position stability in case of power outage.



Figure 6. 7 Panasonic Servo System

6.3.5 Beckhoff I/O

Ultrasonic Welder is controlled by digital I/O. Therefore, the Beckhoff EK1100 Ether Cat Coupler along with 24VDC EL1008 8-channel digital input terminal and EL2088 8-channel digital output terminal are used to connect the Welder. These I/O are controlled by EtherCAT and can be integrated with any controller as described in Figure 6.8. Further details of each unit are described below.

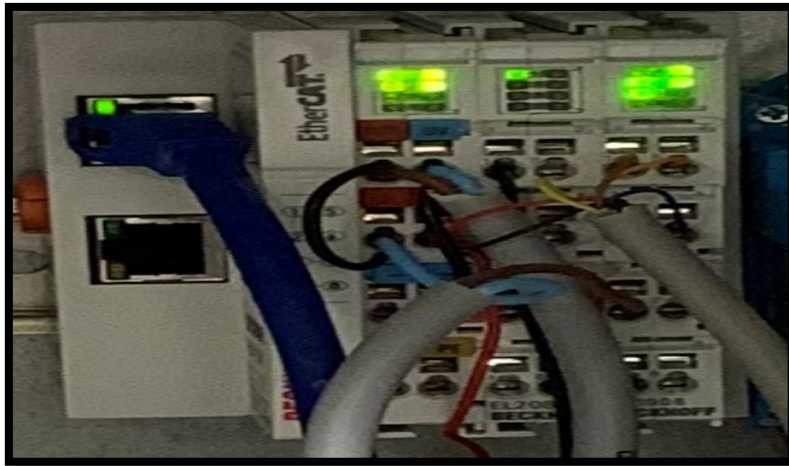


Figure 6. 8 Beckhoff Digital I/O

The EK1100 coupler is defined as a piece of equipment which provides connection between EtherCAT and the EtherCAT Terminals. It consists of one station, EtherCAT Terminals several in numbers, an EK1100 coupler and a bus node terminal station. Thus, the major purpose of the coupler will be the change of transient telegrams to the Electronic-bus signal representation from Ethernet 100BASE-TX. The coupler is then linked to network environment through higher Ethernet framework. The lower connector RJ45 socket is then used to link rest of the EtherCAT hardware in the same manner. In the said EtherCAT network, wherever under Ethernet signal transformation section excluded it, the EK1100 coupler may be installed directly to the switch.

The 24VDC EL1008 digital input terminal manages the Boolean control signals at the place from where the process level is present and then it transmits such type of signals to higher-level automation unit from an electrically isolated unit point. Thus, the Digital input points in the EL100x series have exactly 3ms number of input filter. Therefore, the EtherCAT points uses light emitting diodes to point their state. However, they can vary in the quantity of channels and the pin assignment.

The digital format output terminal EL2088 couples the Boolean control signal from the workflow unit to the drive at the phase level through electrical isolated environment. The EtherCAT terminal consists of 8 (0 V) switching outputs and generates load currents that withstand short circuits and overloads. It consists of 8 channels that show the status of the signal using LEDs. Connection technology includes a 1-wire system and 8 outputs. It requires 24V rated load voltage. It also has Reverse voltage protection which is an added advantage for its functioning.

6.3.6 Safety Devices

The general safety devices are used like RCD (Residual Current Device), MCB (Mini Circuit Breaker) and MC (Magnetic Contactor) as shown in Figure 6.9 to ensure the safety of the Servo system and Robot Controller. Each unit is discussed in detail below.

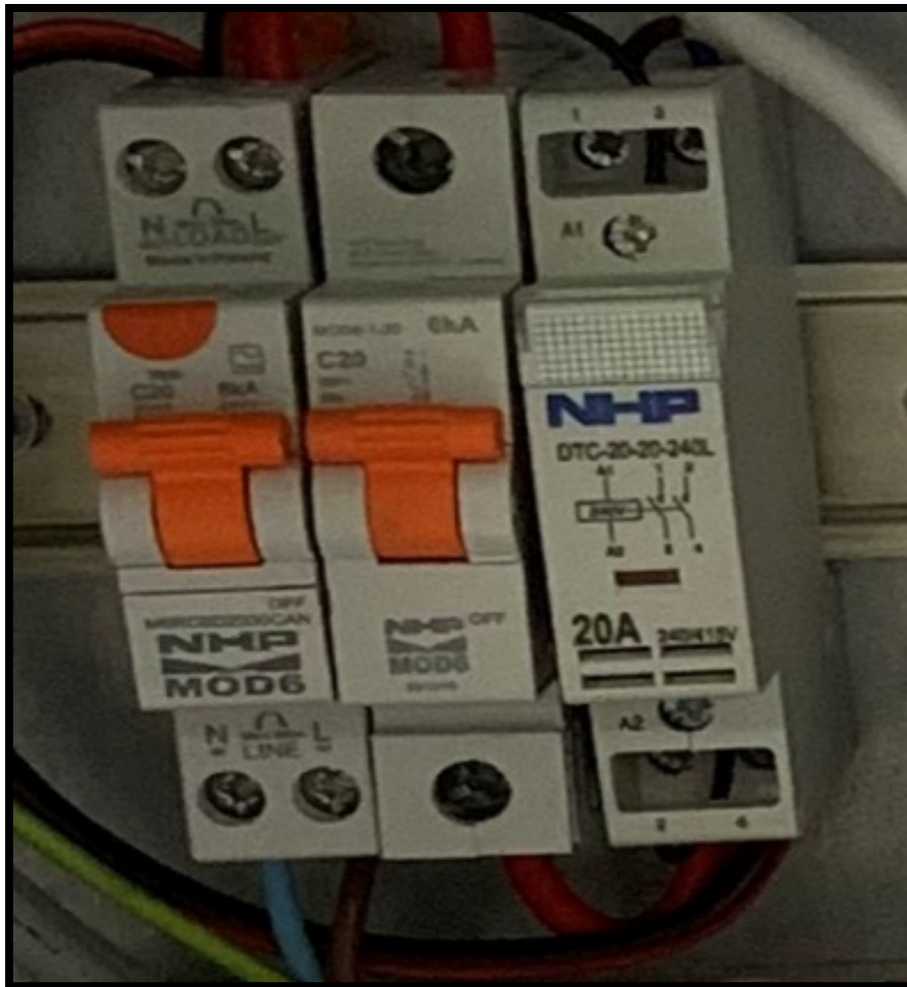


Figure 6.9 Safety Devices

It is an electromechanical device that is an absolute sheath that is prepared in insulation material. An important function of the MCB is circuit conversion. In other words, the development of a trip circuit when current exceeds from some specific point via MCB. It can be manually turn ON and OFF as needed to fit a regular switch. The mini “circuit breaker” is an electromagnetic device that signifies absolute enclosed unit in a prepared insulating system. The important characteristics such device is the transformation of the circuit, i.e., to release the circuit by design when the steady current

fleeting through it MCB surpasses the importance for which it can be fixed. It can be manually changed ON and then OFF as comparable to usual switch if needed. In order to choose the model selects a certain MCB for a precise application is a cautious task to guarantee reliable protection alongside overloads and short circuits. If it is not nominated rendering to the circuit requirements, there will be probabilities to lead to frequent undesirable tripping. If the rated load current is not evaluated, the MCB will cause a normal trip and the rated current of the MCB will not be greater than the rated load current, so the current will cross the line load. Similarly, if it is too large, it will not properly bind to the load. In this case, the MCB unit will not work even if the load is still consuming current. NHP 6KA C20 MCB is used to protect the panel box.

A magnetic contactor is a type of relay that comes from the largest electric motor. They act as a safety measure, acting as an intermediary between direct method power motors and high load on motors in order to standardize or balance the frequency deviations that may occur from the power source. Note that the shape is similar however, the magnetic contactor is not a circuit breaker. They do not individualize the connected unit amongst appliance, and other power source through a short circuit which can happen. They are removable in order to make it work with motor unit by the operator; strip or preserve it, and without which the likelihood of still live current transient via the device. NHP DTC-20-20-240V MC is used to protect the motors.

It is assumed that the RCD shuts off the power in the event of an accident. It is higher than a standard circuit breaker and works by observing the current movement between the current and neutral lines. Faults such as cable damage or short circuit can affect the flow of energy and immediately activate the circuit breaker. It is an added protection device vital by law in various workplaces and does not change supplementary safety features like fuses. These devices are also denoted to as ground fault circuit interrupters.

6.3.7 Integration of Ultrasonic Welder

The ultrasonic welder integration is the biggest task because the manufacturer of the welder does not supply any electrical diagrams to control the welder tool. After few experiments the welder was able to at least turn ON and OFF using a separate switch and later this switch is controlled by the Beckhoff relays that is integrated to Robot controller through EtherCAT.

The machine mounting plate has multiple threaded holes suitable for M8 bolts. For the ultrasonic welder, use Allen bolts to mount the tool holder onto the lowest two threaded holes; the bolts will align the tool holder parallel to the table (refer to Figure 6.10).

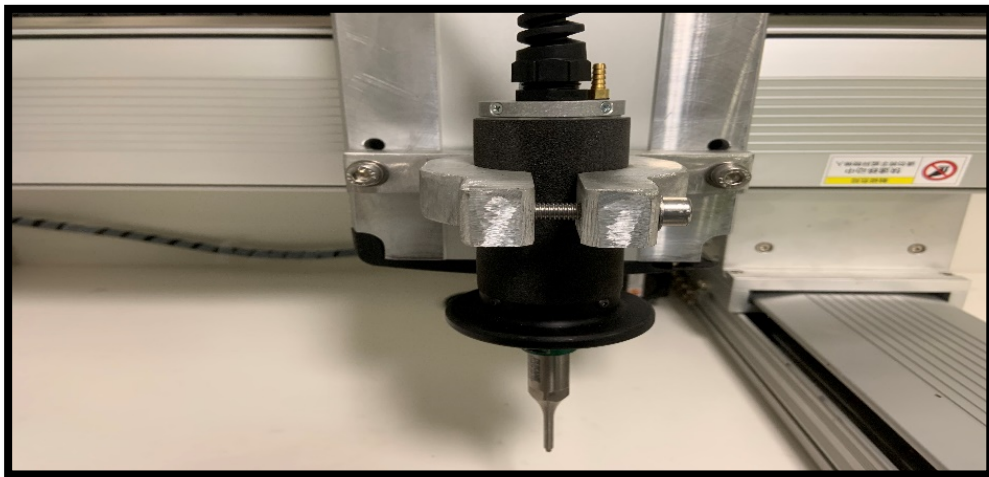


Figure 6. 10 Tool Installation

The following is the procedure to insert the welding head.

1. Remove the long 50 mm Allen bolt at the front of the tool holder.
2. Pass the welder wire through the tool holder.
3. Insert the welder into the tool holder.
4. Fix the bolt back again.
5. There are two extra screws on the side. These can be tightened if required to hold the welder securely.

In order to remove the welder from the ultrasonic welding head, use a spanner on the flat faces of the tool, screw another tool to the head and tighten using another spanner.

6.4 Parameterization of Panasonic AC Servo System

EtherCAT Servo drives and pulse I/O servo drives both are the hardware connections interface system. EtherCAT servo drives offer the functionality of a base Analog Drive, Indexing Drive, Can Open Drive and EtherCAT Drive, all in one product. Hence, this drive reduces the need of other drive and can perform multiple tasks. It is flexible and can transfer one bus type to another easily within a single drive. Thus, they are fast, feature-rich and easy to integrate into any application. Their performance, communication and power levels can vary depending on manufacturer body. Pulse I/O servo drive being the part of pulse module, it comprises of several component which can work on different task. The main function is to input the code directly from the LAN and send the output. There are the encoders that translates the codes to send the required pulse. The servo drives, over a period have proved more fast, compact and user friendly and it also fulfills the present-day need. They are made up of high inertia and lead wire. Both types of drives can function in the same way, the difference is only the interface.

The current rating and the power output of servo motors are different, for MHMF042L1V2M that is 2.1A, 400Watt and MHMF082L1V2M is 3.8A and 800 W. Considering other factors their dimensionalities of body, length of the wires and shaft diameters affects the mass due to which MHMF082L1V2M is heavier than the other. The torque of these motors is different due to the rating of current. Though both the motors rotate at a same frequency of 3000 RPM, still their recommended moment of inertia ratio of load and the rotor is different for both that is 30 and 20, apart from all their safety precautions are kept same.

A device that is used to gauge absolute or true angular position is termed as Absolute encoder. The difference with incremental encoders is to compute the modification in angular position. The examination as to whether an encoder is absolute or incremental can be found at power outage. The position value will remain same even after the motor shaft is rotated in the absence of power. If it outputs its true position, then it is absolute. Usually, the value of an absolute encoder is more precise than an incremental encoder.

6.4.1 EtherCAT Process Data Communication - PDO and SDO

The EtherCAT master functions uses telegram that pass through each node. Each device states the statistics addressed to it “on the fly” and supplements its facts in the frame as the frame is moving downstream. The hardware propagation delay time delays the frame. The opening port is detected by the parts/segment (or drop line) of a closing node and it also leads the communication back to the original one using Ethernet technology’s complete duplex characteristics. Over 90% rate of telegram’s maximum effective data is increased and as such the usage of the complete duplex feature, the theoretical aspect of effective data rate is much more than 100 Mbit/s (> 90 % of two spells 100 Mbit/s). There is only node within a parts/segment that permit to actively direct EtherCAT frame which is EtherCAT master; rest of the other nodes/edges in the segment are simply forward frames downstream data. This idea avoids irregular interruptions and assures real-time capabilities. Even beyond the additional computation and communication resources/processor, the master can use a standard Ethernet MAC (Media Access Controller). This also permits a master/main that can be applied on each hardware environment with an existing port of Ethernet, irrespective of which real-world and real-time system software. For example, Operating System or an application software is being utilized. It also utilizes an ESC (EtherCAT Slave Controller) to develop segments on the virtual environment, which makes the performance of network expectable that is free of the separately connected child device mechanism implementation.

The master device does not only prepare logical generation of addresses, it also direct a connected slave node through its location in the framework. This technique is implemented for the duration of network start up to regulate the entire network paradigm and associate it to the prearranged environment. It requires negligible effort to adjust conceivable respect of implementing the EtherCAT in hardware that remained formerly equipped with CAN open® and huge percentages of the CAN open® Firmware are even recyclable. It has the option to keep the legacy and 8-byte PDO, the limitation of which may be waived of, and then it is probable to implement the boost bandwidth of EtherCAT to provide support to the upload of the complete Object Dictionary. Therefore, to implement such types of mechanism, the device profiles, like the drive profile “CIA 402” is also reutilized for the purpose of implementing the EtherCAT.

6.4.2 Position Control

There are two types of position control method.

The Profile Position Method is defined as one of CAN open/EtherCAT Modes of Operation. It is configured with Object 0x6060. In this mode, the master will send data to Motion Task 0 in the AKD and the drive will execute the motion task.

Cyclic synchronous position method is comparable to adjust interpolation mechanism. In such type of method of control, the major/master can provide additional torque and speed to attain torque and speed feed forward flow control. The interpolation time of cycle describes the time for position to be targeted bring up to date. In this circumstance, interpolation cycle time is the like synchronized timings.

6.4.3 Velocity Control

There are two types of velocity control method.

In profile velocity method the drive flows till the desired speed/flow value has been touched and retains this velocity.

The cyclic synchronous velocity control modes allow the EtherCAT master to send desired velocities to the SOMANET drive. It is to make sure that the values of velocity are being reached by the connected motor.

6.4.4 Torque Control

There are two types of torque control methods.

Torque profile method functions the target value outputs controller. The output signals are being control by Servo drive in order to control the motor and to allow the target acceleration and torque.

Cyclic Synchronous Torque Method is implemented for the purpose of receiving controller gave the servo drive a target torque value sporadically and then motor is controlled by the servo drive as per the target values of torque.

6.5 Programming of Daincube Robot Controller

DTP7 DainCube Robot Controller is a 6-Axis simultaneous EtherCAT based Robot Controller. This controller is integrated with the Panasonic Servo Drives and Beckhoff I/O. The controller is opensource and can be configure to several compatible manufacturers of servosystem and digital I/O. CORECON is the operating software of this controller. The controller is configured as 3-Axis gantry Robot. The 32-bit absolute encoder for precise position control is setup. The main feature of the controller is the accessibility to external system I/O control. This gives number of privileges to control numerous things according to requirements as well as it can develop individual boards to integrate in with the projects.

DainCube Robot Controller DTP7 Series as shown in Figure 6.11. It has passed IP54 waterproof, dustproof and 1.5-meter drop test. This controller has many external switches on the body such as Emergency Rotary Switch, Double Enable Switch that meets the industrial safety regulations. In addition, Windows, Windows CE, or Linux can be installed so the user can develop various application of 6-Axis motion control. DTP7H-CORECON have an integrated Robot motion controller with teach pendant that contains high performance ARM Cortex-A9 processor to run real-time operating system and integrate motion control software CORECON.

The DTP7-CORECON is built-in the teach pendant that is a Robotic UI program. DTP7 and Servosystem uses the EtherCAT communication to send and receive commands in real time. This controller can work with different types of Robot configuration for example Orthogonal, SCARA, Delta, 6-Axis Vertical Articulated Robots, Serial Robot.

The controller is absolute and updates the positional values of each axis simultaneously. The controller configuration is very easy and begins with the selection of Robot Type, manufacturer of servosystem, encoder values and the speed. There are many features like operator and administrator control, dry run mode, integration of external peripherals like welding system, Spray painting makes it more versatile. This has all the features that are found in ABB, FANUC and YASKAWA Controllers.



Figure 6. 11 DainCube Robot Controller

Key Features of Daincube Robot Motion Controller

Features of the Robot Controller that make it stand out among different controllers are as follows:

- High reliability: waterproof, anti-corrosion, shock resistant
- Great cost performance
- Integrated Motion Controller and S/W with Teach Pendant
- Several Robot function (motion operation, setting, I/O, function, structure, operation, variable, constant)
- Quick response rate based on Real-Time Linux (Xenomai 2.6.5)
- Real-Time EtherCAT Master stack with 2ms cycle time
- Simply build GUI applications with the advanced version of QT 4.8.7
- Support for multiple devices via EtherCAT Master, Ethernet, RS-485
- High-speed non-volatile memory device (M-RAM)
- High performance, small size, lightweight, low power
- High-reliability, high-speed, self-made urethane shielded cable
- Certifications: KC, CE, ISO 9001, ISO 1400

CORECON Technical information

Robot Controller CORECON technical information is stated:

- ARM Cortex-A9 – 1GHz
- DDR3 1GB
- USB, SD Card
- Communicates with controller: RS-232, RS-485, Ethernet, EtherCAT
- EtherCAT Master interface
- Robot methodology (Cartesian, SCARA, Delta, Vertical multi-axis, Take-out, Gantry and WTR etc.)
- Operating mode (Teach / Repeat / Manual)
- Function of system logging and EtherCAT monitoring

A teach pendant clarifies Robot programming, but the internal electronics must be high-performance, low power and ready to withstand the harsh conditions of a factory floor. When producing their DTP7-P teach pendant for industrial Robots, Daincube took the DFI BT700 QSeven System-On-Module based upon the Intel Atom® processor.

Daincube is a most leading manufacturer company of industrial Robot controllers, including teach pendants, Robot motion controllers and safety controllers. The Daincube teach pendant is differentiated by its ergonomic design and adaptability to a wide range of automation applications.

Programming a Robot with manual instructions is time consuming and requires significant debug. Further, it is difficult to achieve 100% accuracy of movement in 3-D space. The most widely used method is to utilize a handheld device called a teach pendant. Like a touchscreen tablet, the teach pendant enables the operator to move the Robot through a desired range of motion. When a sequence has been fully specified, the Robot can play back the programming at full speed.

The operation mode of the Robot is classified into Manual or Repeat mode as shown in Figure 6.12. The operation mode can be switched using the Select Switch on the upper left of the teach pendant. In the Manual mode, the Robot can be moved using the jog keys on the keypad at the right of the pendant. The Repeat mode is a mode in which a program created using CL (Core Language) can repeatedly be executed.

displayed on the right side of the screen (indicated by the black rectangle in the Figure 6.14).

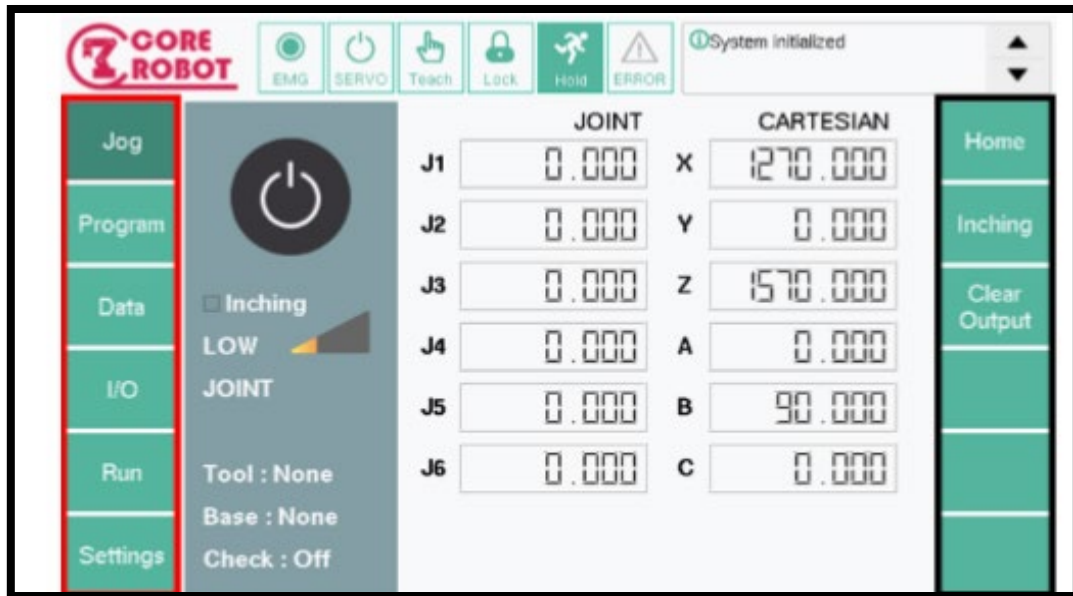


Figure 6.14 Main Menu and Sub Menu

The Main Menu items are:

- Jog: Check and change the current Robot position.
- Program: Program a defined motion for the Robot.
- Data: Check, store and edit data about the Robot position.
- I/O: View all I / O, including system I / O (this function is not used).
- Run: Run a saved program.
- Settings: Modify the settings of the Robot.

The Robot can be moved manually (called jogging) in Manual mode.

- Turn the Select switch to Manual mode.
- Holding the Teach Pendant in two hands, press and hold the Enable switch (at the rear of the Teach Pendant) with your left hand. The machine motion will stop if the Enable switch is not pressed.
- Use the right keypad as shown in Figure 6.15 of the Teach Pendant to manipulate the Robot, as follows.

Multiple button can be pressed on the keypad if is supposed to operate in various Axes simultaneously. However, pressing plus, minus buttons on the same axis will not work.

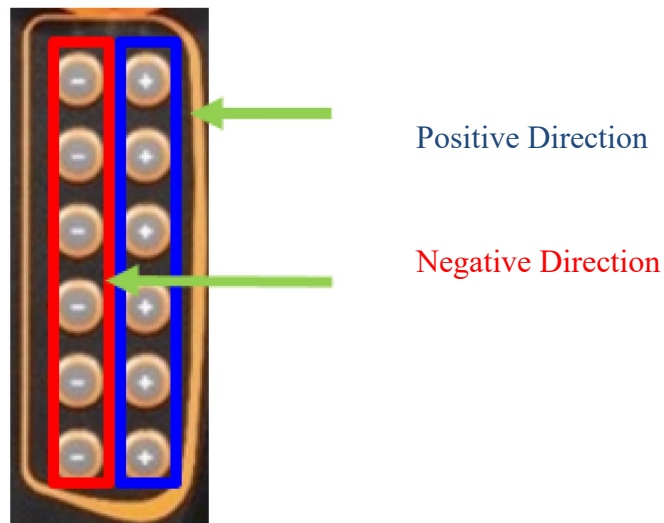


Figure 6.15 Jog Buttons

In order to move precisely, use inching mode to move the Robot with single pitch. Inching mode on jogging will not proceed serial motions. The inching mode can be activated via pressing inching button as shown in Figure 6.16. Configuring motion range on inching mode is like changing speed; up and down arrow keys will be used to change the range. Once pressed, LED colour on the top right corner will be changed from red to blue. This signal informs inching mode is currently operating.

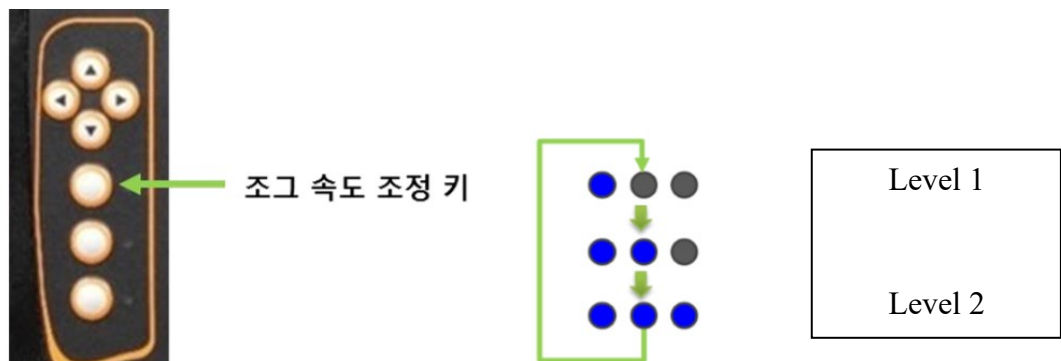


Figure 6.16 Inching Control

The speed of movement of the tool can be controlled by pressing the Up and Down arrows on the left side of the Teach Pendant (see following Figure 6.17). The selected speed is indicated by the three LED lights just beneath the Emergency Stop button.



Figure 6.17 Speed Control

The maximum speed of the Robot has been limited by the Administrator for safe operation.

In Repeat mode, a previously saved program can be executed as shown in Figure 6.18.

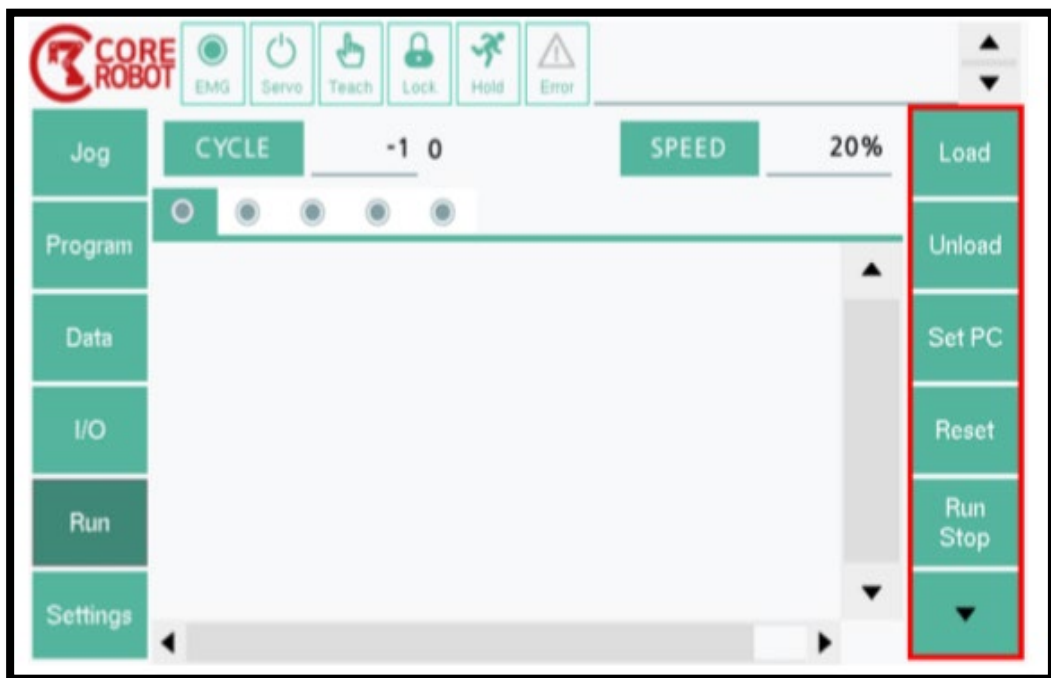


Figure 6.18 Run Menu

Following are the steps to run the program in Repeat mode.

- Turn the select switch to Repeat mode.
- Tap the Run menu button from the Main Menu.
- Load the program by tapping the Load button from the Sub Menu and selecting the required program.
- Tap on the “Speed” icon to adjust the speed – the speed is not set as part of the program.
- Tap on the “Cycle” icon to adjust the cycle number – this will set the number of times that the program will be executed; this should normally be set to 1; note that “-1” means an infinite cycle, i.e. the program will run indefinitely.
- The program will define the motion of the Robot head and will activate the hand-welder.
- Switch the Secondary Safety Switch to the “ON” position as shown in Figure 6.19:



Figure 6. 19 OFF Position and ON Position

- Operate the program by pressing the ‘Run Stop’ button on the Sub Menu to run the program.
- The Robot will operate the commands until the program has been completed.
- While the program is operating, the operation can be stopped by clicking the ‘Run Stop’ button if necessary.

6.6 Repeatability Test of Robot

Repeatability is usually the most important criterion for a Robot. ISO 9283 sets out a method whereby both accuracy and repeatability can be measured. Typically, a Robot is sent to a taught position several times and the error is measured at each return to the position after visiting 4 other positions. This machine repeatability test is conducted by a mechanical dial indicator with the least count of one micron and maximum movement is 1 millimetre. Once complete rotation complete 0.2mm of distance and its zero point can be set by rotating the black cover holder as shown in Figure 6.20. The Robot is programmed to touch six different places on the machine table using 'G' codes and finally come back to the original point. The repeatability is measure around ± 5 micron that is an acceptable limit because the machine VP requires the repeatability of no more than ± 0.1 mm to pass the machine for medical environment. This test is not one-time test. It must be conducted annually to make sure the wear and tear does not affect the repeatability.



Figure 6. 20 Repeatability test using dial indicator

6.7 Welding Test on Soft Material based Medical Devices

Ultrasonic welding is now widely used in different industries. This company is intending to weld thin plastic materials together. The welding has many parameters to adjust. Despite the parameterization the tools can penetrate the soft materials if too much energy or force are applied. In order to control, the exact press force is required to maintain the strong welds. These devices are tested using visual inspection in electron microscopic. A series of tests conducted by hit and trial method. The welding started at 0.5mm height from the machine base and observed that the material is totally melted, hence the tool passed through it. Continuously varying the parameters and height, provided the better results as shown in Figure 6.21.

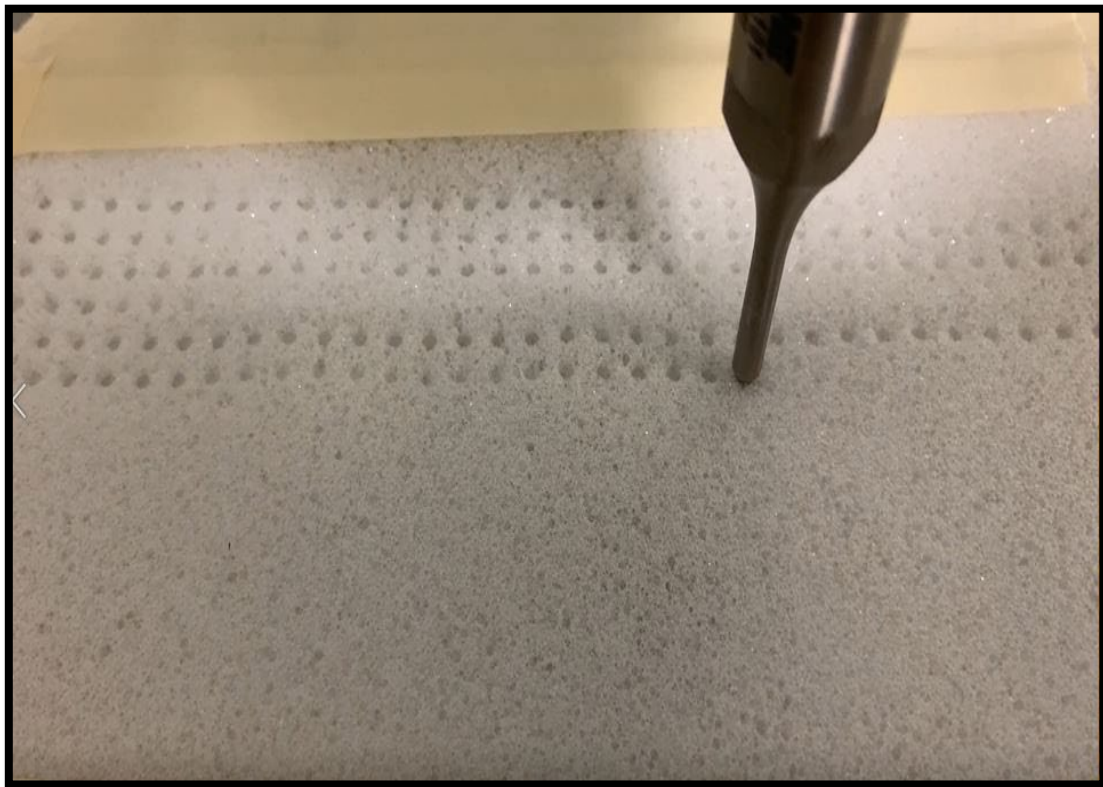


Figure 6. 21 Welding test of plastic materials.

6.8 Welding Test on Irregular Shapes by MV Algorithm

When surgery takes place on humans on the infected areas the shape requirements vary person to person and which part of the body is served. Therefore, the medical devices required to be welded accordingly. Many irregular shapes are placed on the machine to weld. The MV Algorithm is developed to take the size and position of the samples to calculate the trajectory of weld points same as defined in chapter 4.

6.9 Algorithm to Generate Different Bonding Pattern

The plastic materials can be welded together of different shapes and sizes. These devices are welded in different pattern. The pattern's spacings are achieved by the research and trials method. It can be regular, that are equally spaced by fixed numerical value in horizontal, vertical or diagonal direction. These types of patterns generations are very easy to achieve with the help of 'G' Codes. The codes can be generated by CAM (Computer Aided Manufacturing) software or by typing the program manually on the controller screen. The problem arises for the generation of irregular bonding patterns on specific shapes. It cannot be programmed manually, as it takes hours including human errors. Therefore, such Algorithm for the irregular bonding pattern is developed using MV, that can adjust the variation in the boundary of the device automatically. However, different regular and irregular bonding patterns are tested during the practice. These Algorithm is the intellectual property of PolyNovo and hence it is not included in thesis.

6.10 Summary

This chapter mainly comprises the design and development of AUWS in the medical device industry. This machine is constructed and tested under VPs of medical environment against specifications provided by PolyNovo Biomaterials. AUWS is integrated with the state-of-the-art DSP and FPGA based Robot Controller (Daincube). This controller is capable of using EtherCAT servo drives that results in precise motion control in Z-Axis to achieve the strong weld joints. The precision of Z-Axis is ± 5 micron that was validated in section 6.6 using dial indicator. The height controls the amount of pressure exerted on the material using metal tool, hence it was controlled during the practice. The second objective after the construction of AUWS, is accomplished by generating the different irregular bonding patterns on the surface of the material. The results were tested on the microscope and AUWS is being used by the PolyNovo R&D department to produce their prototype medical devices.

Chapter 7

Chapter # 7 Conclusion and Future Work

- Brief of the research study and meeting the aims.
- Focus on the development of Algorithm and the importance of prototype.
- MV System in industrial applications.
- Scope for future work.

7.1 Conclusion

The research is to reduce the manual handling in all over the world where humans do not feel safe to palletise large and heavy objects or continuously palletising all day long. This is also one of the causes to have back pains among those factory workers who have extreme lifting jobs and employers violate the OHS rules. The palletising by the joint Robots is very common practice and is already been used in the world as discussed in **Chapter 2**. Though unfortunately, problem arises when the architectural designers are compelled to develop more complex shape objects. These irregular polygons do not have a specific shape or size sometimes they have very sharp edges and perforation is more than 50% in such scenarios the Robots need to be smarter to deal with every shape to palletise otherwise the human labour will be used in such scenarios.

The research is contributing in the list of tasks that the Robots can perform. On many occasions the Robots are currently dealing with 3-D shapes and irregular polygons. However, their end effectors are not programable pneumatic based that turns on and off particular solenoids on the basis of information supplied by MV system. In this study an end effector model is developed that has several solenoids to control the vacuum suction. If a Robot tries to grasp an object that has perforation more than 50%. This will drop the overall pressure because it is mandatory that each vacuum suction cup is used to maintain the overall pressure. Otherwise, the object can drop during the palletising or might not able to pick in the first grasping. Therefore, a methodology is developed using MV system to find the spots to grasp the irregular perforated objects and palletise to and from the machines.

This thesis belongs to the field of Mechatronics, Automation and Robotics Engineering, which describes the MV system Algorithm design for the calculations of trajectories for the irregular polygonal objects, by employing disintegration methodology and amplifying the trajectory formation for seeking appropriate positions. These Algorithm are developed in **Chapter 3 and 4**. Section 4.4.1 to 4.4.7 has covered the seven stages step by step for the development of Algorithms, begins with the image acquisition till formulating the point-based trajectory. The cartesian coordinates developed in section 4.5.2 is the information of each spot on the irregular shape to grasp. These points are developed by avoiding the sharp edges and perforation.

The modelling and simulation are the key to develop a product. But simulation and calculations have limits and boundaries, most of the time it is observed that when the product is experienced the real environment. It behaves far different from the designing set points. Therefore, it is very important to develop a prototype to experience the real difficulties. Hence a prototype is developed in **Chapter 5** to validate the MV Algorithms developed. The development of prototype used the Robot Mitsubishi RM-501 (5-Axis Serial Robot). The control unit of the Robot is replaced by the new state of the art DSP controller F280049C because it was unable to communicate with the MV system. The controller is configured in MATLAB software to be used as a DC servo driver and integrated with CYTRON MDD10A board to operate the DC servo motors with incremental encoders. After the development of the board the Robot kinematics is tested with MACH3 software. The MACH3 software is used as a Robot Controller interface, the calibration and kinematics are tested and checked for accuracy and repeatability. Chapter 4 is the main input of the prototype because the Robot depends on the positional information supplied by the Algorithm developed by MATLAB if the positional information is slightly inaccurate. The Robot can go totally out of the way and that is why the external limit switches are installed as a secondary safety option.

MV system is the integration of several units and each of the unit should work in a loop and communicate each other in milliseconds time. The MV system is used in the prototype is a low-cost camera with appropriate pixels. MATLAB software is installed on a core i7 laptop and used it as a main control unit for the development of coding. The software requests the camera to take image after specific interval of time. The image taken by camera is stored in a designated folder and read by Algorithm. After that all the processing takes place in few minutes that includes the information about type and size of image, develop the end effector trajectory, and finally converts the positional information into 'G' codes. These 'G' codes are then further communicated to Robot RCU that turn the Robot movement on the designated position and activate the solenoids to grasp the object. This all system is fully automated and in a closed loop.

First test was to check the Robot accuracies and kinematics to make sure that it is working in tolerances. Afterwards the different irregular polygonal shapes are placed under the camera and the Robot moves on the designated trajectory points for the validation of the Algorithm.

Last but not the least, the opportunity to implement the findings in an industrial environment is achieved through APR Internship program. They offered a research internship for three months at PolyNovo Biomaterials situated at Port Melbourne for the development of AUWS as described in **Chapter 6**. PolyNovo is a manufacturer of novel medical devices based on proprietary biodegradable polymers. The company has processes involves bonding of sheets of material together via a series of point bonds across the sheets. This process was currently conducted manually leading to slow production of devices and of variable quality at the bond-points. Therefore, this research is conducted to develop a machine that is capable of generating the bonding pattern for medical devices. There are two very precise objectives achieved during the research project.

1. Development of AUWS
2. Generate the bonding pattern using MV

The machine was required to hold the bonding tool (which weighs less than 1 kg), lower it to the surface of the sheets, activate the control unit for a few seconds, raise the tool, then move it in the XY-Axes plane into different pattern. The machine is developed with the reproducibility of 0.1mm in the Z-Axis. So, that the tool is always in the same vertical position relative to the surface of the sheets to generate consistent bond points. The tolerance in the X-Axis and Y-Axis is also achieved under 0.1 mm. This machine allows the user to easily define both the pattern for the bond-points in the X/Y-Axes, and the position of the tool relative to the surface of the sheets. The machine is capable of producing the devices up to 75 x 40 cm in size. The machine is tested under VPs of medical environment against specifications provided by PolyNovo Biomaterials. The construction of the machine was successful and next stage is the automatically generation of the bonding patterns.

When surgery takes place on humans on the infected areas, the shape requirements changes person to person and which part of the body is served. Therefore, the medical devices required to be welded and cut into particular shapes. These shapes vary according to the wounds on the surface of the body. However, the plastic materials are welded together of different shapes, sizes and pattern. These bonding patterns can be regular, or irregular depends on application. The pattern's spacings are achieved by the research and trials method. It can be regular, that are equally spaced by fixed numerical value in

horizontal, vertical or diagonal direction. Algorithm for the irregular bonding pattern is developed using MV, that can adjust the variation in the boundary of the device automatically. Many irregular shapes are placed on the machine to weld. The MV Algorithm took the size and position of the samples to calculate the trajectory (or bonding pattern) of weld points. These bonding patterns are then tested to check the quality of weld joints. These weld joints are observed by microscope to make sure, that the tool is not penetrated the material and the quality of welding is not compromised. However, a variety of bonding patterns and shapes were tested during the practice. All the Algorithm developed during the testing is the intellectual property of PolyNovo and hence it is not included in thesis. This internship is successfully completed, and the machine is being used in the R&D lab of PolyNovo Biomaterial to develop the biodegradable medical devices.

MV is creating high impact in the manufacturing industries by reducing the labour cost and enhancing the productivity with quality. Now Robots are not bounded to do the repetitive tasks only. The MV system unleashed the Robots to achieve the rear tasks that might occur only once in the whole tenure of Robot life. Today's Robot can think, learn and take decisions to deal with multiple scenarios using artificial intelligence and machine learning. These all findings during this research places its emphasis on the industrial processes of different packaging and manufacturing domains. The most common applications are Medical, Pharmaceutical, Cabinet Manufacturer, Laser and Plasma Cutter etc.

7.2 Future Scope

MV integration into the Robo Machines is the thrust area of research especially in the developing countries. It provides ample opportunities to the researcher to explore many potential challenges in MV system and artificial intelligence to reduce the manual handling load from humans. The following are some of the opportunities that have been planned to investigate in our future research are as follows:

- The Algorithm can be further extended to work in the dust environment. When CNC wood cutting machine cuts the wood into pieces using an End mill carbide bit. It generates the chip of the wood on the top of the surface. Despite new machines are integrated with the vacuum dust collector that covers the tool from all side. The thick layer of dust stuck between the wood pieces and sometimes over the cutting slot. This dust creates problems in the image processing. When the MV system takes the images to analyse it becomes impossible to find the closed loops. An Algorithm can be developed to generate the unknown ends connection automatically by approximating the possibility of the shape. Otherwise, the system can be integrated by a small vacuum dust cleaner that can be controlled by the MV Algorithm to clear the doubted areas. Therefore, the MV can generate the right trajectory for palletising.
- Like manual handling in cabinet manufacturing, there are many other areas in the industry where OHS is abundant. Employers uses manual labour for lifting the heavy objects. Exploring these locations in the industries for their MV applications would be a good future work option.
- This MV system can be further improved by analysing low density plastic materials. These materials have irregular perforations and hence the algorithm can find the densities on the material and use the densest areas to build the strong weld joints.
- The welding quality of soft plastic material can be further improved by the integration of MV system from the bottom of the material. This will help to control the tool penetration by developing a closed loop system that will sense the pressure on the top of material and image processing from the other side to monitor the weld conditions during the welding procedure.

-
- This code developed in chapter 4 still has limitations, if the shape is more than 80% perforated or have long sharp corners, it cannot deal at this stage. This Algorithm needs to improve to the next stage to achieve the common goal to palletise any shape using Robots.
 - Algorithm is built for one shape at a time. The sheets use in the profile cutting are mostly rectangular in shape and then it cuts in several small shapes and sizes. This code needs further investigation to deal with such scenarios where the MV system has to develop the trajectory for more than one object at the same time.
 - The Robot end effectors can be upgraded to deal with more small shapes to deal with fragile and sharp edges. Currently it is set on 125mm having the vacuum cup nozzle of 25mm. If the object needs more smaller grasping, a new end effector will be required to develop having small centre to centre distances.
 - This can be further explored in Oxy, Plasma profile cutting industries. When oxy cuts the thick material, it produces slugs on the top and bottom surface of the material. The MV Algorithm can be further improved to absorb the variation of shapes and calculating the size of the object after cutting.
 - The Laser cutting process is very clean and does not create a lot slug like Oxy and Plasma cutting hence it uses very thin sheets to cut for sheet metal processing with very high perforation ratio. This algorithm can be improved to work with different materials. Currently, it is designed to work on white A4 page only.
 - Currently this Algorithm works on the CPU that takes few seconds to generate a single trajectory. This algorithm can be deployed on GPU and FPGA to improve the cycle time.
 - This Algorithm can be used in different scenarios for the generation of bonding patterns on irregular shapes that results in strong welding between the soft plastic materials.

References

- [1] Rigby, J., ‘Multiple intersections of diagonals of regular polygons’, *Geometriae Dedicata*, 9(2), 1980.
- [2] Nooijen, M., Velde, G. T. and Baerends, E. J., ‘Symmetric Numerical Integration Formulas for Regular Polygons’, *SIAM Journal on Numerical Analysis*, 27(1), 1990, pp.198-218.
- [3] Harutyunyan, H. and Ohanyan, V., ‘The chord length distribution function for regular polygons’, *Advances in Applied Probability*, 41(2), 2009, pp.358-366.
- [4] Khalid, Z. and Durrani, S., ‘Distance Distributions in Regular Polygons’, *IEEE Transactions on Vehicular Technology*, 62(5), 2013, pp. 2363-2368.
- [5] Bedaride, N. and Cassaigne, J., ‘Outer billiard outside regular polygons’, *Journal of the London Mathematical Society*, 84(2), 2011, pp. 303-324.
- [6] Jeong, I., ‘Outer billiards with contraction: regular polygons’, *Dynamical Systems*, 33(4), 2017, pp. 565-580.
- [7] Paunic, D. and Yiu, P., ‘Regular Polygons and the Golden Section’, *Forum Geometricorum*, Vol. 16, 2016, pp. 273–281.
- [8] Du, D., Hwang, F. and Weng, J., ‘Steiner minimal trees for regular polygons’, *Discrete and Computational Geometry*, 2(1), 1986, pp. 65-84.
- [9] Van der Blij, F., “Regular polygons in Euclidean space”, *Linear Algebra and its Applications*, 226-228, pp.345-352, 1995.
- [10] Garza-Hume, C. E. and Maricarmen, C., ‘Areas and Shapes of Planar Irregular Polygons’, *Forum Geometricorum*, Vol.18, 2018, pp. 17-36.
- [11] Albano, A. and Sapuppo, G., ‘Optimal Allocation of Two-Dimensional Irregular Shapes Using Heuristic Search Methods’, *IEEE Transactions on Systems, Man, and Cybernetics*, 10(5), 1980, pp. 242–248.
- [12] Heighway, E., ‘A mesh generator for automatically subdividing irregular polygons into quadrilaterals’, *IEEE Transactions on Magnetics*, 1983, pp. 2535-2538.

-
- [13] Martins, T. D. C. and Tsuzuki, M. S. G., ‘Rotational placement of irregular polygons over containers with fixed dimensions using simulated annealing and no-fit polygons’, *Journal of the Brazilian Society of Mechanical Sciences and Engineering*, 30(3), 2008.
- [14] Singh, S., Jha, A. and Kumar, S., ‘Upper bound analysis and experimental investigations of dynamic effects during sinter-forging of irregular polygonal preforms’, *Journal of Materials Processing Technology*, 194(1-3), 2007, pp. 134–144.
- [15] Moreau, L. et al., ‘Scattering of guided waves by flat-bottomed cavities with irregular shapes’, *Wave Motion*, 49(2), 2012, pp. 375–387.
- [16] Kasimatis, E., ‘Dissections of regular polygons into triangles of equal areas’, *Discrete and Computational Geometry*, 4(4), 1989, pp. 375-381.
- [17] Cureton, L. and Kuttler, J., ‘Eigenvalues of the Laplacian on Regular Polygons and Polygons Resulting from Their Dissection’, *Journal of Sound and Vibration*, 220(1), 1999, pp. 83–98.
- [18] Mousavi, S. E. and Sukumar, N., ‘Numerical integration of polynomials and discontinuous functions on irregular convex polygons and polyhedrons’, *Computational Mechanics*, 47(5), 2010, pp. 535–554.
- [19] Garza-Hume, C. E. and Maricarmen, C., ‘Areas and Shapes of Planar Irregular Polygons’, *Forum Geometricorum*, 2018.
- [20] Cleland, D., Cleland, A. and Earle, R., ‘Prediction of freezing and thawing times for multidimensional shapes by simple formulae part 2: irregular shapes’, *International Journal of Refrigeration*, 10(4), 1987, pp. 234–240.
- [21] Hifi, M. and Mhallah, R., ‘A hybrid Algorithm for the two-dimensional layout problem: the cases of regular and irregular shapes’, *International Transactions in Operational Research*, 10(3), 2003, pp. 195–216.
- [22] Park, J., Pasaogullari, U. and Bonville, L., ‘Wettability measurements of irregular shapes with Wilhelmy plate method’, *Applied Surface Science*, 427, 2018, pp. 273–280.

-
- [23] Lakner, M. and Plazl, I., 'The finite differences method for solving systems on irregular shapes', *Computers and Chemical Engineering*, 32(12), 2008, pp. 2891-2896.
- [24] Keneti, A. R. and Jafari, A., 'Determination of volume and centroid of irregular blocks by a simplex integration approach for use in discontinuous numerical methods', *Geomechanics and Geoengineering*, 3(1), 2008, pp. 79-84.
- [25] Tsukrov, I. and Novak, J., 'Effective elastic properties of solids with defects of irregular shapes', *International Journal of Solids and Structures*, 39(6), 2002, pp. 1539–1555.
- [26] Elfasakhany, A. and Bai, X. S., 'Numerical and experimental studies of irregular-shape biomass particle motions in turbulent flows', *Engineering Science and Technologies, an International Journal*, 22(1), 2019, pp. 249-265.
- [27] Fitzpatrick, R., 'Centre of Mass', *Institute for Fusion Studies, University of Texas at Austin*, 2006.
- [28] Maus, H. M., Seyfarth, A. and Grimmer, S., 'Combining forces and kinematics for calculating consistent COM trajectories', *Journal of Experimental Biology*, 2011, pp. 3511-3517.
- [29] Sang, D. M., 'A self-calibration technique for active vision systems', *IEEE Transactions on Robotics and Automation*, Vol.12(1), 1996.
- [30] Harada, K., 'Validating an object placement planner for Robotic pick and place tasks', *Robotics and Autonomous Systems*, Issue No 10, 2014, pp. 1436-1477.
- [31] Museros, L., Falomir, Z. and Velasco, F., '2D qualitative shape matching applied to ceramic mosaic assembly', *Journal of Intelligent Manufacturing*, 2012, pp. 1973-1983.
- [32] Singh, T., Dhaytadak, D., Kadam, P. and Sapkal, R. J., 'Object Sorting by Robotic Arm Using Image Processing', *International Research Journal of Engineering and Technology*, Vol. 03(04), 2016.

-
- [33] Skoglund, P. G. and Soderend, K., ‘Container Unloading using Robotized Palletising Master of Science Thesis Work’, *Department of Product and Production Development, Chalmers University of Technology*, 2012.
- [34] Dzitac, P. and Mazid, M. A., ‘An Efficient Control Configuration Development for a High-speed Robotic Palletising System’, *2008 IEEE Conference on Robotics, Automation and Mechatronics*, 2008.
- [35] Horak, K. and Zalud, L., ‘Image Processing on Raspberry Pi In MATLAB’, *International Journal of Signal Processing Systems*, Vol. 4, No. 6, 2016, pp. 494-498.
- [36] Xu, G. and Xian, Y., ‘A Fast Reassembly Methodology for Polygon Fragment’, *2009 International Conference on Computer Engineering and Technology*, 2009.
- [37] Meng, Y. and Zhuang, H., ‘Self-Calibration of Camera-Equipped Robot Manipulators’, *The International Journal of Robotics Research*, 20(11), 2001, pp. 909–921.
- [38] Vischer, P. and Clavel, R., ‘Kinematic calibration of the parallel Delta Robot’, *Robotica*, 16(2), 1998, pp. 207-218.
- [39] Siddiqu, F., Amiri, S., Minhas, U. I., Deng, T., Wood, R., Raffert, K. and Crookes, D., ‘FPGA-Based Processor Acceleration for Image Processing Application’, *Journal of Imaging*, vol 5, 2019.
- [40] Samet, R., Bay, O., Aydın, S., Tural, S. and Bayram, A., ‘Real-Time Image Processing Applications on Multicore CPUs and GPGPU’, *Proceedings of the International Conference on Parallel and Distributed Processing Techniques and Applications*, 2015, pp. 116-122.
- [41] Qasaimeh, M., Denolf, K., Lo, J., Vissers, K., Zambreno, J. and Jones, P., ‘Comparing Energy Efficiency of CPU, GPU and FPGA Implementations for Vision Kernels’, *The 15th IEEE International Conference on Embedded Software and Systems*, 2019.
- [42] Saegusa, T., Maruyama, T. and Yamaguch, Y., ‘How fast is an FPGA in image processing?’, *Field Programmable Logic and Applications*, 2008.

-
- [43] Reddy, B. N., Shanthala, S. and Vijaya Kumar, B. R., 'Performance Analysis of GPU V/S CPU for Image Processing Application', *International Journal for Research in Applied Science and Engineering Technology*, vol 5, 2017, pp. 437-443.
- [44] Asano, S., Maruyama, T. and Yamaguchi, Y., 'Performance Comparison of FPGA, GPU and CPU in Image Processing', *19th International Conference on Field Programmable Logic and Applications*, 2009.
- [45] Zlatano, N., 'CUDA and GPU Acceleration of Image Processing', *IEEE Computer Society*, 2016.
- [46] Allusse, Y., Horain, P., Agarwal, A. and Cindula, S., 'GpuCV: A GPU-accelerated framework for Image Processing and Computer Vision', lecture notes in Computer sciences, 2008, pp. 430-439.
- [47] Chouchene, M., Haythem, B., Ezahr, S. F. and Mohamed, A., 'Image Processing Application on Graphics processors', *International Journal of Image Processing*, vol 8, 2014, pp. 66-72.
- [48] Abramov, A., Kulvicius, T., Worgotter, F. and Dellek, B., 'Real-time image segmentation on a GPU', *Facing the Multicore Challenge*, vol 6310, 2011.
- [49] Horrigue, L., Ghodhbane, R., Saidani, T. and Atri, M., 'GPU Acceleration of Image Processing Algorithm Based on MATLAB CUDA', *International Journal of Computer Science and Network Securit*, vol 18, 2018, pp. 91-99.
- [50] Salvo, R. D. and Pino, C., 'Image and Video Processing on CUDA: State of the Art and Future Directions', *international conference on Mathematical Methods and Techniques in Engineering and Environmental Science*, 2011, pp. 60-66.
- [51] Eklund, A., Dufort, P., Forsberg, D. and LaConte, S., 'Medical Image Processing on the GPU: Past, Present and Future', *Medical Image Analysis*, 2013.
- [52] Giot, I. R. and Rodrigues E. S., 'Image processing Algorithm optimization with CUDA for Pure Data', *Pure Data Convention - Berlin 2011*.

-
- [53] Saxena, S., Sharma, S. and Sharma, N., ‘Study of Parallel Image Processing with the Implementation of vHGW Algorithm using CUDA on NVIDIA’S GPU Framework’, *Proceedings of the World Congress on Engineering*, vol I, 2017.
- [54] Holloway, J., Kannan, V., Zhang, Y., Chandler, D. and Sohon, S., ‘GPU Acceleration of the Most Apparent Distortion Image Quality Assessment Algorithm’, *Journal of Imaging*, vol 4, 2018.
- [55] Veeraraghavan, H., Masoud, O. and Papanikolopoulos, N., ‘Computer vision Algorithms’, *IEEE Transactions on Intelligent Transportation Systems*, vol. 4, 2003, pp. 78-89.
- [56] Mahamkali, N. and Vadivel, A., ‘OpenCV for Computer Vision Applications’, *National Conference on Big Data and Cloud Computing (NCBDC’15)*, 2015.
- [57] Abdullah, A., Palash, W. and Rahman, A., ‘Digital Image Processing Analysis using MATLAB’, *American Journal of Engineering Research (AJER)*, vol. 5, no. 12, 2016, pp. 143-147.
- [58] Sheikh, H. R., Bovik, A. C. and Veciana, G. D., ‘An information fidelity criterion for Image Quality Assessment using natural’, *IEEE Transactions on Image Processing*, vol. 14, 2005, pp. 2117-2128.
- [59] Emlyn, W. and Irene, L., ‘Lifelong Learners in Engineering Education – Students’ Perspectives’, *International Journal of Education and Information Technologies*, 2012, pp. 9-16.
- [60] Wren, C. R., Azarbayejani, A., Darrell, T. and Pentland, A., ‘Pfinder: real-time tracking of the human body’, *IEEE Trans. Pattern Anal. Machine Intell.*, vol. 19, 1997, pp. 780–785.
- [61] Okoro, O. I., Govender, P. and Chikuni, E., ‘A new User-Friendly Software for Teaching and Research in Engineering Education’, *The Pacific Journal of Science and Technology*, Vol. 7. No. 2, 2006, pp. 130-136
- [62] Barrade, P., ‘Simulation Tools for Power Electronics: Teaching and Research’, *SIMPLORER Workshop 2001 Chemnitz*, 2001. pp. 35-46.
- [63] Alexander, L., Anastasios, N. and Smith, K., ‘High-Speed Architectures for Morphological Image Processing’, *Nonlinear Image Processing*, 1990, pp. 141–156

-
- [64] Christe, S. A., 'An efficient FPGA implementation of MRI image', *International Journal of VLSICS*, vol. 2, 2011.
- [65] Mahalanobis, A., 'Network Video Image Processing for security, surveillance and situational Awareness', *SPIE 5440 Digital Wireless*, 2004.
- [66] Lawan, S. and Wamedo, CL., 'Image Recognition Using MATLAB SIMULINK', *International Journal of Computer Science, Engineering and Applications (IJCSEA)*, vol. 7, 2017.
- [67] Muhammad, Z., 'Image Enhancement by using Histogram Equalization Technique in MATLAB', *International Journal of Advanced Research in Computer Engineering and Technology (IJARCET)*, vol. 7, no. 2, 2019.
- [68] Aggarwal, H., 'A Comprehensive Review of Image Enhancement Technique', *Journal of Computing*, vol. 2, no. 3, 2010, pp. 08-11.
- [69] Sruthi, B. R., 'Vision Based Sign Language by Using MATLAB', *International Research Journal of Engineering and Technology (IRJET)*, vol. 5, no. 3, 2018.
- [70] Martyanov, A. S., 'Development of control Algorithms in MATLAB / SIMULINK', *International Conference on Industrial Engineering*, 2016.
- [71] Otani, Y., Hashiura, H. and Komiya, S., 'A Software Testing Tool with the Function to Restore the State at Program Execution of a Program under Test', *International Journal of Education and Information Technologies*, 2012, pp. 71-78.
- [72] Molenda, M., 'In Search of the Elusive ADDIE Model', *Performance improvement*, 42 (5), 2003, pp. 34–37.
- [73] Pong, P. K. T. and Bowden, R., 'An improved adaptive background mixture model for real-time tracking with shadow detection', in *Proc. 2nd Eur. Workshop Advanced Video Based Surveillance Systems*, 2001.
- [74] McKenna, S. J., Jabri, S., Duric, Z. and Wechsler, H., 'Tracking interacting people', in *Proc. 4th Int. Conf. Automatic Face and Gesture Recognition*, 2000, pp. 348–353.
- [75] Meyer, F. G. and Bouthemy, P., 'Region-based tracking using affine motion models in long image sequences', *Computer Vis. Graph. Image Proc.*, vol. 60, no. 2, 1994, pp. 119–140.

-
- [76] Ridder, C., Munkelt, O. and Kirchner, H., ‘Adaptive background estimation and foreground detection using Kalman filtering’, in *Proc. Int. Conf. Recent Advances Mechatronics*, 1995, pp. 193–199.
- [77] Alvares, A. J., Toquica, J. S., Lima, E. J. and Souza, M. H., ‘Retrofitting of ASEA IRB2-S6 industrial Robot using numeric control technologies based on LinuxCNC and MACH3-MATLAB’, *2017 IEEE International Conference on Robotics and Biomimetics (ROBIO) in 2017*.
- [78] Lord, W. and Hwang, I. H., ‘Dc servomotors - modeling and parameter determination’, *Industry Applications IEEE Transactions on* vol. IA-13 no. 3, 1977, pp. 234-243.
- [79] Schulz, R. A., ‘A frequency response method for determining the parameters of high-performance DC motors’, *IEEE Trans. Ind. Electron.* vol. IE-30 no. 1, 1983, pp. 39-42.
- [80] Weerasooriya, S. and El-Sharkawi, M. A., ‘Identification and control of a DC motor using back-propagation neural networks’, *IEEE Trans. Energy Conversion* vol. 6, 1991, pp. 663-669.
- [81] Hanamoto, T., Tanaka, Y., Karube, I., Mochizuki and, T. and Xu, Z., ‘ A parameter estimation method using block pulse functions for DC servo motor systems’, *Proceedings of the 1992 International Conference on Industrial Electronics, Control, Instrumentation, and Automation*, 1992.
- [82] Saab, S. S. and Kaed-Bey, R. A., ‘Parameter identification of a DC motor: An experimental approach’, *Proc. 8th IEEE Int. Conf. Electron. Circuits Syst.* vol. 2, 2001, pp. 981-984.
- [83] Hung, J., ‘Parameter estimation using sensitivity points: Tutorial and experiment’, *IEEE Trans. Ind. Electron.* vol. 48 no. 6, 2001, pp. 1043-1047.
- [84] Pothiya, S., Chanposri, S., Kamsawang, S. and Kinares, W., ‘Parameter Identification of a DC Motor Using Tabu Search’, *KKU Engineering Journal*. Vol. 30. No 3, 2003, pp. 173-188.
- [85] Dupuis, A., Ghribi, M. and Kaddouri, A., ‘Multiobjective genetic estimation of DC motor parameters and load torque’, *Proc. IEEE Int. Conf. Ind. Technol*, vol. 3, 2004, pp. 1511-1514.

-
- [86] Basilio, J. C. and Moreira, M. V., ‘State-space parameter identification in a second control laboratory’, *IEEE Trans. on Education*, 47, 2004, pp. 204–210.
- [87] Krneta, R., Antic, S. and Stojanovic, D., ‘Recursive least square method in parameters identification of DC motors models’, *Facta Universitatis*. 18, 2005, pp. 467–478.
- [88] Mamani, G., Becedas, J., Sira-Ramirez, H. and Feliu Batlle, V., ‘Open-loop algebraic identification method for DC motors’, in *Proceedings of the European Control Conference*, Kos, Greece, 2007.
- [89] Hadeif, M., Bourouina, A. and Mekideche, M. R., ‘Parameter identification of a DC motor via moments method’, *International Journal of Electrical and Power Engineering*, vol. 1, no. 2, 2008, pp. 210–214.
- [90] Mamani, G., Becedas, J. and Feliu Batlle, V., ‘On-line fast algebraic parameter and state estimation for a DC motor applied to adaptive 16 control’, in *Proceedings of the World Congress on Engineering*, London, UK, 2008.
- [91] Ruderman, M., Krettek, J., Hoffman, F., and Betran, T., ‘Optimal state space control of DC motor’, in *Proceedings of the 17th World Congress IFAC*, 2008, pp. 5796-5801.
- [92] Mamani, G., Becedas, J. and Batlle, V. F., ‘On-line fast algebraic parameter and state estimation for a DC motor applied to adaptive control’, in *Proc. World Congress on Engineering*, London, UK, 2008.
- [93] Hadeif, M. and Mekideche, M. R., ‘Parameter identification of a separately excited DC motor via inverse problem methodology’, in *Proceedings of the Ecologic Vehicles and Renewable Energies*, Monaco, France, 2009.
- [94] Arshad, S., Qamar, S., Jabbar, T. and Malik, A., ‘Parameter estimation of a DC motor using ordinary least squares and recursive least squares Algorithms’, in *Proc. 8th Intl. Conf. on Frontiers of Information Technology (FIT)*, 2010, pp. 21-23.
- [95] Wei, W., ‘DC motor identification using speed step responses’, *Proceedings of the 2010 American Control Conference*, USA, 2010.
- [96] Galijasevic, S., Masic, S., Smaka, S., Aksamovic, A. and Balic, D., ‘Parameter identification and digital control of speed of a permanent magnet DC motors’,

2011 XXIII International Symposium on Information, Communication and Automation Technologies, Sarajevo, 2011.

- [97] Garrido, R. and Miranda, R., ‘DC servomechanism parameter identification: A closed loop input error approach’, *ISA Transactions*, Volume 51, Issue 1, 2012, pp. 42-49.
- [98] Obeidat, M. A., Wang, L. Y. and Lin, F., ‘Real-Time Parameter Estimation of PMDC Motors Using Quantized Sensors’, *IEEE Transactions on Vehicular Technology*, Volume: 62, Issue: 7, 2013.
- [99] Mohamad, M. S. A., Yassin, I. M., Zabidi, A., Taib, M. N. and Adnan, R., ‘Comparison between PSO and OLS for NARX Parameter Estimation of a DC Motor’, *IEEE Symposium on Industrial Electronics and Applications*, Kuching, Malaysia, 2013.
- [100] Jamadi, M. and Bayat, F. M., ‘New Method for Accurate Parameter Estimation of Induction Motors Based on Artificial Bee Colony Algorithm,’ *arXiv 2014*, arXiv:1402.4423, 2014.
- [101] Adewusi, S., ‘Modeling and Parameter Estimation of a DC Motor Using Constraint Optimization Technique’, *IOSRJ. of Mechanical and Civil Engineering*, 13, 2016, pp. 46-56.
- [102] Karnavas, Y. L. and Chasiotis, I. D., ‘PMDc Coreless Micro-Motor Parameters Estimation through Grey Wolf Optimizer’, *IEEE conf. on Electrical Machines*, 2016, pp. 865 – 870.
- [103] Sankardoss, V. and Geethanjali, P., ‘PMDc Motor Parameter Estimation Using Bio-Inspired Optimization Algorithms’, in *IEEE Access*, 5, 2017, pp. 11244 – 11254.
- [104] Puangdownreong, D., Hlungnamtip, S., Thammarat, S. and Nawikavatan, A., ‘Application of Flower Pollination Algorithm to Parameter Identification of DC Motor Model’, in *5th International Electrical Engineering Congress*, 2017, pp. 1 – 4.
- [105] Nayak, N. and Sahu, S., ‘Parameter estimation of DC motor through whale optimization Algorithm’, *International Journal of Power Electronics and Drive Systems* 10(1):83, 2019.

Appendix 1: Authorship Declaration: Co-Authoring Publications

This thesis contains work that has been published and prepared for publication.

Details of the work:
Tabish M. H., Kalam A., Zayegh A., "Robot DC Servo Motor Parameters Estimation in a closed loop Using BAT Optimization Algorithm", <i>International Conference on Electrical, Communication and Computer Engineering (ICECCE)</i> , 2019.
Location in thesis:
Chapter 5
Student contribution to work:
This study is to design and develop a controller to find DC Servo motor parameters by real time step testing method in a closed loop and deploy them to develop an application specific controller that can be used with that Robot in real-time.
Student signature:

Appendix 2: Doctorate Industrial Research Internship

Australian Postgraduate Research Intern (APR. Intern) is Australia's only PhD internship program spanning all sectors, disciplines and universities. This internship was posted in first quarter of the last year and received the confirmation after the successful interview to join for three months at PolyNovo Biomaterials. This industrial placement was regarding the medical devices. PolyNovo was looking for some cost-effective solution to develop a bonding process for its proprietary soft plastic materials. The research is conducted on the Industrial Design Engineering of Automated Ultrasonic Welding System for soft materials. The machine in the Figure A.1 is developed in only three months period that includes mechanical design, organising materials from overseas, programming the Robot controller, parametrisation of AC Servos, integrating the ultrasonic welder, assemble the control panel, and research on the soft material weld quality. This project was successful, and it is now producing the prototype medical devices at PolyNovo Biomaterial R&D Lab. Following is the video link of the project:

<https://youtu.be/B8XaPU0zy0>



Figure A.1 Automated Ultrasonic Welding System 2019

Best International Project Award INNOTECH-2019 (KIET)

This project is showcased last year in the international project competition INNOTECH-2019 held by KIET Group of Institutions, Ghaziabad, India and won the best international project award.

Appendix 3: International Robotics Competition

NIARC

NIARC (National Instruments Autonomous Robotics Competition), this competition started in 2011, NIARC has grown from 10 teams to 20 teams in 2018 from 20 top universities throughout Australia, New Zealand, Singapore and Malaysia. Built around the theme “Fast Track to the Future”, the competition required team robots to complete tasks such as going through hazardous terrain, bumps, avoiding obstacles all while optimising performance to maximise efficiency with the objective of earning the most points. Our team has participated in NIARC-2018. Our team (VU Robots) developed the program in LabVIEW and tested on myRIO kit that was supplied by National Instruments. The Robot structure was made up of acrylic and small DC motors were used. Test run of the Robot for first milestone can be seen in the following video link:

<https://youtu.be/P6YY3zrE5Ys>

Unfortunately, the Robot broke down during the test for second milestone as shown in Figure A.2, the chassis was broken into pieces, and the repairing was not possible.

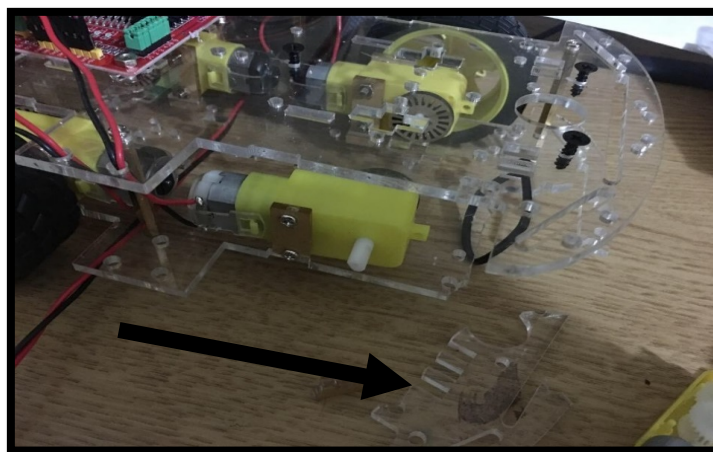


Figure A. 2 The Robot breakdown

To develop another Robot’s CAD model and fabrication was a challenging task and it was successfully completed within a month for passing the further milestones by the team efforts and unity. Figure A.3 demonstrates the CAD model using omni wheels while Figure A.4 is the working model of the Robot in Aluminium. Test run of the Robot for the next milestone can be seen in the following video link:

<https://youtu.be/T6Hvy4wHFFoo>

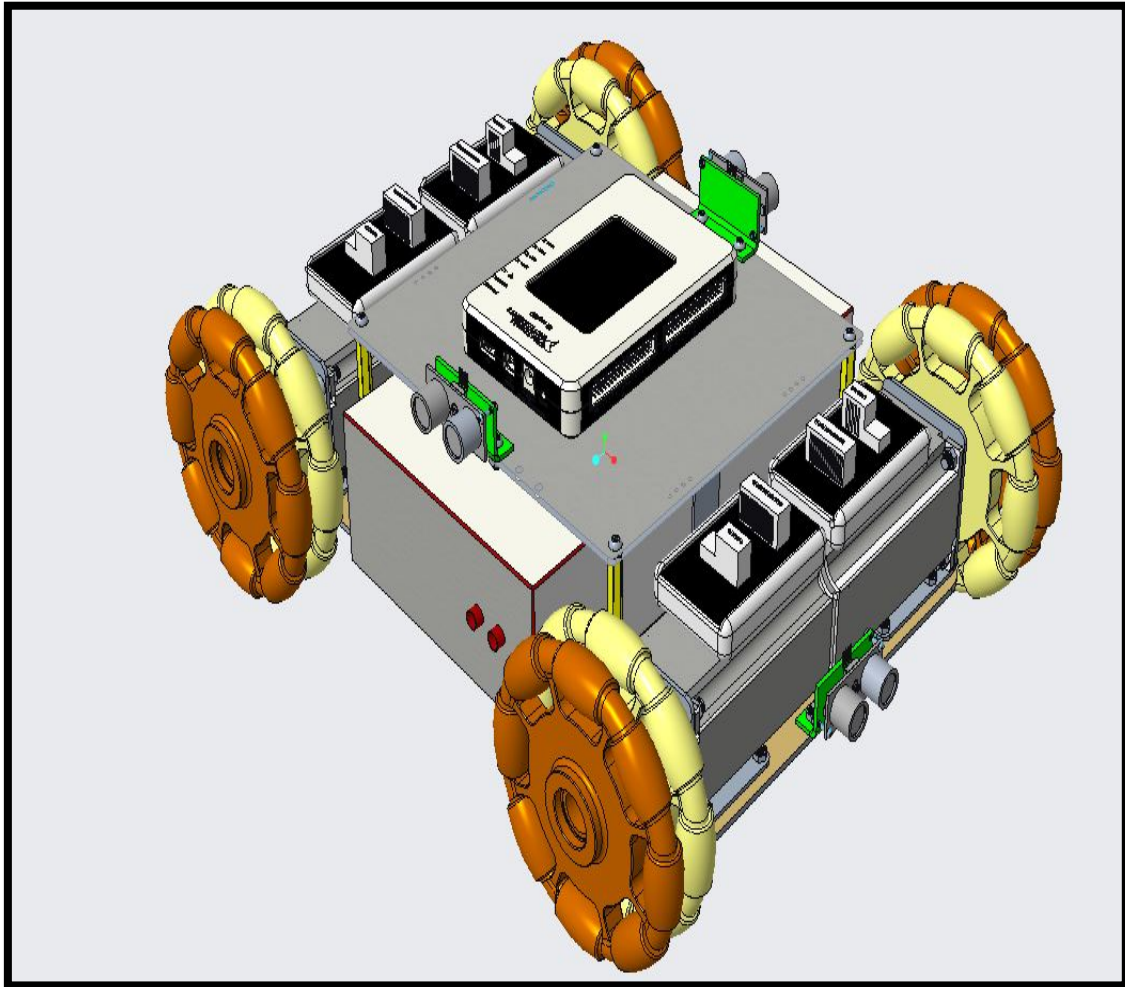


Figure A. 3 CAD Model of the Robot

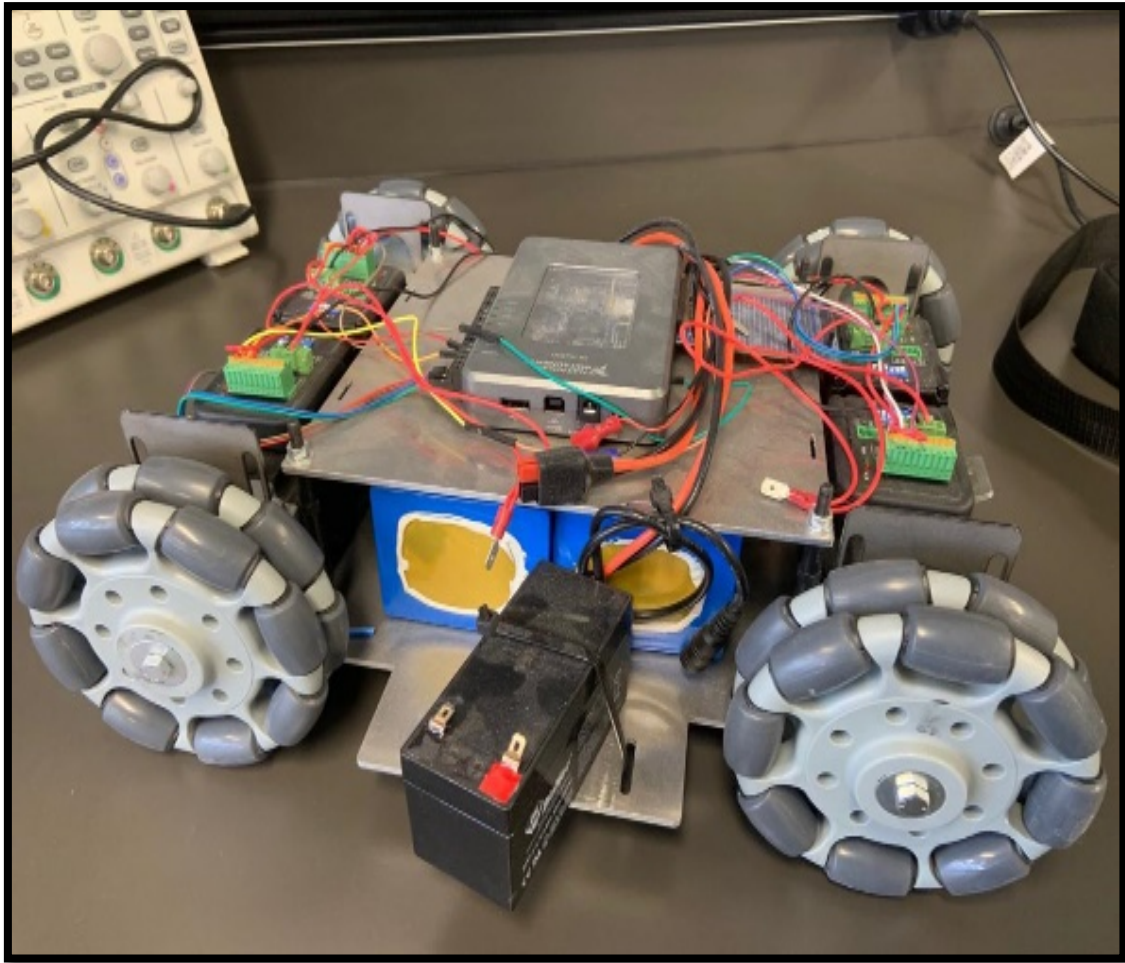


Figure A. 4 NIARC 2018 Robot, team (VU Robots)

Appendix 4: Articulated Robot based Research Project

Design and validate an application specific controller for the old Robots without retrofit the motors. Therefore, motors cannot be upgraded or replaced while the control circuitry was validated by new state of the art DSP controller. A test bench was also developed using one motor from each of three Robots as shown in Figure A.5.

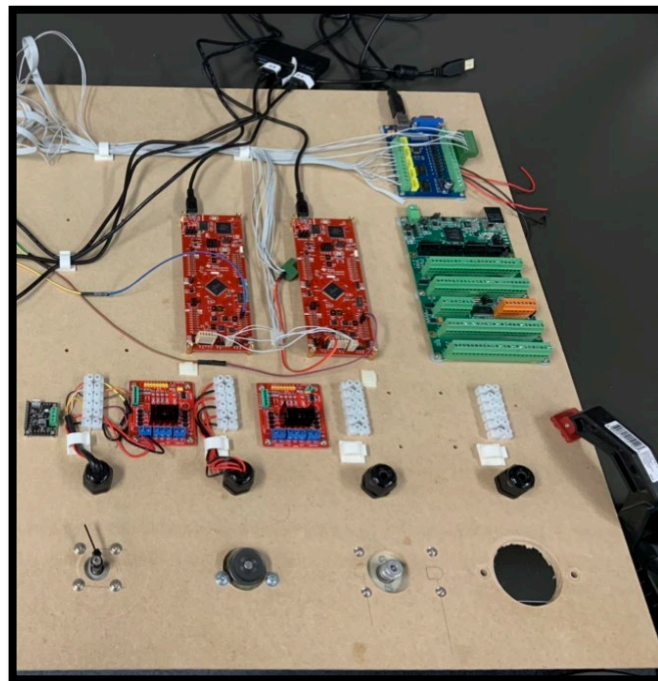


Figure A. 5 DC Motor Test Bench

Initially L298 was used to achieve maximum holding torque of the motor and later it was replaced by CYTRON driver. Different controllers were used that includes Pololu “JRK 21v3 USB Motor Controller with Feedback”. However, the position control loop in the controller could not reach the expectations. After that, MESA FPGA based “7I76ED STEP/IO Step and Dir Pulse I/O Card” was used. Despite, built-in servo control features, it comes with several limitations and hence it was also pulled out. Finally, “Piccolo DSP microcontroller TMS320”, validated the Algorithm by achieving the required holding torque and speed of the motor. Further, details about the programming, construction, validation and the smooth motion of the Robot Axes individual and simultaneously can be explored by the following video link:

<https://youtu.be/yhdJ3NJVVGs>